

August 27, 2015

**DETERMINISTIC, DELAY AND STOCHASTIC IN-HOST MODELS
FOR HUMAN MALARIA DYNAMICS**

**DOCTOR OF PHILOSOPHY
(MATHEMATICS)**

BY

ENOCK KOGA

AUGUST 2015

DETERMINISTIC, DELAY AND STOCHASTIC IN-HOST MODELS FOR HUMAN MALARIA DYNAMICS

Enock Koga

BSc.(Hon) (NUST,Zimbabwe), MSc. (Univ. of Zimbabwe)



Supervisor: Prof. Edward M. Lungu

BSc.(Univ. of Zambia), MSc (Bristol), Ph.D.(Bristol)

Thesis submitted in the fulfilment of the requirements for the award of the degree of

Doctor of Philosophy in Mathematics

at the University of Botswana

Approval

This thesis has been examined and approved as meeting the requirements for the fulfilment of the Doctor of Philosophy degree in Mathematics.

Supervisor.....

Date.....

External Examiner (i)

Date.....

External Examiner (ii).....

Date.....

Dean, School of Graduate Studies

Date.....

Declaration

I, **Enock Koga**, declare that this thesis is my work except where due reference is made and it has never been submitted for a degree at this or any other university or institution of higher learning.

Signature:

(*Enock Koga*)

Date:

Acknowledgements

I wish to extend my gratitude to the following organizations and individuals for making my studies, directly or indirectly, a success.

1. First and foremost, I would like to thank my supervisor, Professor E.M. Lungu for his undying love, support, encouragement and above all guidance with patience. Things went really bad during the course of my studies to the extent that I even wanted to withdraw from my studies but because of his fatherly approach to life, his advice and at times financial help, thus how far I have gone. May God bless you.
2. My beloved wife Marcelyne and our two lovely sons, Ryan and Russel for being there for me during the toughest moments of life. My dear wife, I really appreciate your encouragement that I continue to pursue my studies to the end. At least I did not disappoint anyone of you.
3. The Mathematics Department, University of Botswana for giving me the opportunity to do my studies under their institution.
4. Mathematics Department and Dean of Engineering and IT, University of Namibia

- for giving me an opportunity to visit my supervisor and for paying for my SAMSA conference fees and transport.
5. NUFU for partly funding my studies.
 6. AMMSI for partly funding my studies.
 7. SIMMONS FOUNDATION for partly funding my studies.
 8. SAMSA for providing opportunities and resources for me to present my work at their conferences.
 9. AIMS South Africa for financing my travel to South Africa for the June 2013 modelling clinic.
 10. Prof. F. Nyabadza, Dr M. Kgosimore, Dr E. Offen, Dr F. Chirove, Dr Mothebe, Mr E. Tyapa (Unam) and G. Hailundu (system admin. Unam) for their academic and moral support throughout my studies.

Dedication

To the almighty God for his guidance and protection during my studies, my dear wife
Marcelyne, my beloved boys, Ryan and Russel, my siblings and my late parents.

Contents

1	Introduction	2
1.1	Background	2
1.2	Statement of the problem	4
1.3	Methodology	5
1.4	Objectives	7
1.5	Significance	7
1.6	Scope	8
2	Literature Review	10
3	Inhost Malaria model with treatment	33
3.1	Introduction	33
3.1.1	Positivity of solutions	34
3.1.2	Analysis of the model	35
3.2	Model with treatment	41

3.3	Numerical simulations	42
4	Inhost transplacental malaria transmission with and without time delay	46
4.1	Introduction	46
4.2	Transplacental transmission model	50
4.3	Mathematical analysis for the model	52
4.3.1	Model without time delay, $\tau = 0$	52
4.4	Steady states	55
4.4.1	Parasite-free steady state	57
4.4.2	The infested steady states	58
4.4.3	Numerical Simulation: $\tau = 0$	64
4.5	Model with time delay, $\tau \neq 0$	68
4.5.1	Numerical Results: $\tau \neq 0$	73
5	A stochastic model for in-host malaria parasite infection of red blood cells	75
5.1	Introduction	75
5.2	Malaria in-host stochastic model	81
5.3	Existence of solutions for model (5.3) with (5.4)-(5.5)	83
5.4	The case of constant diffusion	88

5.5	Example 1: Malaria model with constant diffusion matrix	91
5.6	Example 2: Malaria model with linear diffusion matrix	94
5.7	Numerical simulations	98
5.8	Interpretation of patients data	98
6	Conclusions and Discussions	107
7	Appendices	123
7.1	Appendix	123
7.2	Matlab Codes	124

List of Figures

2.1	The graphs shows trends of WHO estimated cases of malaria in the WHO regions of the world.	11
2.2	Trends in the cause of death in children under 5 years of age	12
2.3	Trends in the cause of death in children under 5 years of age	12
2.4	Diagram of the malaria parasite's life cycle	14
3.1	Simulations of equation(3.1) showing the concentrations of (a) RBCs (b) IRBCs, and (c) parasites at different initial conditions over time for $R_0 > 1$ in the absence of treatment. For parameter values used, see table 3.1	43
3.2	Simulations of equation (3.12) showing the concentration of IRBCs for $\epsilon < \epsilon^*$ and $\epsilon > \epsilon^*$ using parameter values in table 3.1.	44
3.3	Simulations of equation (3.12) showing the parasite concentration for $\epsilon < \epsilon^*$ and $\epsilon > \epsilon^*$ using parameter values in table 3.1.	44

4.1	Trajectories of model (4.8)-(4.13) showing synchrony of the RBCs dynamics in the mother and foetus, in the absence of intervention under different initial conditions.	66
4.2	Trajectories of model (4.8)-(4.13) showing synchrony of the IRBCs dynamics in the mother and foetus, in the absence of intervention under different initial conditions	66
4.3	Trajectories of model (4.8)-(4.13) showing synchrony of the RBCs dynamics in the mother and foetus, in the absence of intervention under different initial conditions.	67
4.4	Simulations of equations (4.8) and (4.13) showing the IRBCs densities for (a) the mother and (b) foetus for different drug efficacy levels. For parameter values used, see table (4.1), with $\eta = 0.97$	67
4.5	Trajectories of model (4.1)-(4.6) showing the effects of time delay on the foetal IRBCs in the presence of treatment ($\epsilon_1 = 0.983$).	74
4.6	Trajectories of model (4.1)-(4.6) showing the effects of time delay on the foetal parasite population in the presence of treatment ($\epsilon_1 = 0.983$).	74
5.1	A deterministic ($\sigma_1 = 0$) and stochastic graph with linear diffusion coefficient ($\sigma_1 = 0.1$) for the RBCs density over time. Parameter values used: $\Lambda = 2.5 \times 10^9$, $\mu_r = 0.8$, $\beta = 2 \times 10^{-11.3}$, $\mu_i = 0.5$, $\mu_p = 0$, $r = 12$, with initial conditions $R(0) = 5 \times 10^9$, $R_i(0) = 10$, $P(0) = 2 \times 10^4$	98

5.2 A deterministic ($\sigma_1 = 0$) and stochastic graph with linear diffusion coefficient ($\sigma_1 = 0.1$) for the IRBCs density over time. Parameter values used: $\Lambda = 2.5 \times 10^9, \mu_r = 0.8, \beta = 2 \times 10^{-11.3}, \mu_i = 0.5, \mu_p = 0, r = 12$, with initial conditions $R(0) = 5 \times 10^9, R_i(0) = 10, P(0) = 2 \times 10^4$ 99

5.3 A deterministic ($\sigma_1 = 0$) and stochastic graph with linear diffusion coefficient ($\sigma_1 = 0.1$) for the parasite density over time. Parameter values used: $\Lambda = 2.5 \times 10^9, \mu_r = 0.8, \beta = 2 \times 10^{-11.3}, \mu_i = 0.5, \mu_p = 0, r = 12$, with initial conditions $R(0) = 5 \times 10^9, R_i(0) = 10, P(0) = 2 \times 10^4$ 99

5.4 Patient s-197 immune response explained by linear diffusion matrix. This describes an unstable parasite-present state 104

5.5 Patient’s immune response explained by a linear diffusion matrix. This describes symptomatic state which is followed by an asymptomatic state and again by a symptomatic state 104

5.6 Patient’s immune response explained by a constant diffusion matrix. This represents a stable parasite-present treatable state 105

5.7 Patient’s immune response explained by a constant diffusion matrix. This represents a stable parasite-present treatable state 105

5.8 Patient’s immune response explained by linear diffusion matrix. This shows an unstable asymptomatic parasite-present state which degraded into a symptomatic unstable parasite-present state 106

5.9 Patient’s immune response explained by linear diffusion matrix. This
represents an unstable parasite-present treatable state 106

List of Tables

3.1	Description of model parameters for system (3.1).	43
4.1	Description of model parameters for system (4.1-4.6)	63
4.2	Table showing the values of R_{0at} and R_{0ft} for different drug efficacy levels and for different drug permeability factor (η) for model (4.8)-(4.13)	64

Abstract

Malaria is one of the major public health hazards in the developing world in terms of infection, morbidity and mortality, with at least 300 million acute cases of malaria each year globally, resulting in more than a million deaths. The most vulnerable populations are pregnant women, their unborn babies and children under five years of age. Plasmodium falciparum, a parasite spread by the female anopheles mosquito, is the most common cause of malaria in humans and is responsible for almost all deaths associated with this case, followed by rare plasmodium vivax, popularly known for malaria relapse cases. In this thesis, we study the in-host dynamics of malaria (plasmodium falciparum and plasmodium vivax) based on the early work of Anderson *et al*'s inhost models. We begin our research by reviewing Anderson et al (1989)'s model and incorporate treatment to the model. A drug efficacy threshold ϵ approximately equal to 0.9952 for which the parasite is cleared from the host's blood was determined using numerical simulations.

We model the transplacental transmission of plasmodium falciparum (*P.falciparum*) malaria in pregnant mothers. A treatment model for the transplacental transmission of *P.falciparum* malaria in pregnant mothers with and without time delay was developed. The model is considered , first without delay and intervention and then

with treatment of the infected mother with Artemisinin-based combination therapies (ACTs) and injectable artesunate (AS). The model without delay, (4.8)-(4.13), is shown to possess three infected states, that is, an infected state where the erythrocytic infection in the host is active but latent in the foetus that is locally stable for $R_{0at} > 1$ and $R_{0ft} < 1$, a state where the erythrocytic infections are active in both the mother and the foetus which is locally stable for $R_{0at} > 1$ and $R_{0ft} > 1$, and lastly, a state where the erythrocytic infections are under control in the mother but active in the foetus which exist for for $R_{0at} < 1$ and $R_{0ft} > 1$. For the model incorporating treatment, the model reproduction numbers, R_{0ft} and R_{0at} are computed and numerical simulations carried out show that administering antimalarial drugs with a drug efficacy level of between 0.982 and 0.983, exclusively, will help in completely wiping out the malaria parasite in both the mother and foetus at an estimated placental drug transfer permeability factor of at least $\eta = 0.97$. For the model with delay, we investigate the effect of intracellular delay on the stability of the parasite present equilibrium state. A critical condition is given to ensure that the parasite-present steady state is asymptotically stable for all delays.

We also considers how the stability of the basic malaria model is altered by a Brownian diffusion structure. We first consider a model with constant diffusion matrix and show that for this diffusion structure, the revised Anderson et al model possesses two steady states, the parasite-free and parasite-present steady states whose stability is degraded by the diffusion term. This type of diffusion can be used to study infections whose states can switch from parasite-free to parasite-present and vice versa, such as *P.falciparum*. Secondly, we consider models with a variable diffusion matrix, and

find that models with this diffusion structure only possess parasite-present steady states and can be used to study infections which maintain unstable parasite-present states with relapse tendencies, like *P.vivax*.

Acronyms

ACTs-Arteminin -based Combination therapies

AS-Artesunate

RBCs-uninfected red blood cells

IRBCs-infected red blood cells

TNF α -Tumor Necrosis Factor-alpha

ITNs-Insecticide-treated nets

IPT-Intermittent preventive treatment

SMP-Safe motherhood programs

Chapter 1

Introduction

1.1 Background

The four malaria plasmodium species that can infect and be transmitted by humans are, Plasmodium Falciparum, Plasmodium vivax, Plasmodium ovale, and Plasmodium malariae. These parasites are transmitted to humans mainly via a bite of an infected female anopheles mosquito [1]. However, there are other ways in which the parasite can be transmitted namely, (i) a pregnant woman infected with malaria transmitting the infection to a foetus (congenital transmission), (ii) through transfusion of blood infected with malaria parasites to a healthy individual in need of blood, (iii) sharing of needles between an individual infected with the malaria parasites and a healthy individual and (iv) through organ transplant, although these transmission mechanisms are rare [2].

Globally, an estimated 3.3 billion people are at risk of being infected with malaria

according to the World Health Organization (WHO) report of 2011 [1]. This risk is greatest in sub-Saharan Africa, which contributes about 80% of reported clinical malaria cases and 90% of malaria related deaths [1]. Most of the deaths attributed to malaria in this region occur among pregnant women and children under the age of five.

Since the study on malaria transmission in 1911 by Sir Ronald Ross, several studies have been conducted on malaria transmission to ascertain the effectiveness of control, elimination and eradication programs. Malaria control programs are based on the assumption that if the human population is kept malaria-free through administration of prophylaxis and treatment drugs and vector control programs then herd immunity among humans can be achieved [5, 6] resulting in a parasite-free vector population as was the case for smallpox [7]. However, the last two decades have shown that the vector develops resistance to treatment drugs making malaria treatment less effective if it is implemented as a mono-therapy strategy. This in turn has exerted pressure on treatment drug development programs.

Regional malaria elimination programs conducted in the 1940's managed to eliminate malaria from Europe, North America and parts of Asia but proved to be ineffective in sub-Saharan Africa. The success of the elimination program in Western countries and parts of Asia gives hope to sub-Saharan Africa that elimination is possible if the right conditions prevail. Some parts of sub-Saharan Africa are endemic to conflicts, wars etc resulting from cultural and religious beliefs (or differences). The question is whether vector elimination on a continent which faces many logistical and economical

problems is achievable. Between 1950 and 1975 both treatment and vector control programs were used in sub-Saharan Africa as parasite elimination strategies with huge successes but drug resistant strains of the mosquito have eroded the successes. For now control appears to be the best option even though in the long run eradication should be the goal.

It has been shown that reducing transmission does not necessarily reduce the incidence of severe malaria cases and mortality [4]. Studies such as that by Trape and Rogier [5] led to studies on the immune response to parasite infection [10]. Anderson *et al* [10] have described the red blood cell-parasite dynamics that have been exploited by many subsequent studies [3, 8, 11, 23]. Our immunological study is a sequel to the deterministic studies by Anderson *et al* [10], Hoshen *et al* [3] and Macqueen *et al* [8].

1.2 Statement of the problem

The emerging and re-emerging diseases have led to a revived interest in infectious diseases. Mathematical models have become important tools in analyzing the spread and control of infectious diseases. In 1926 Kermack and Mckendrick published results from their mathematical models which established epidemic threshold results for an epidemic outbreak to occur [9]. Since then, mathematical epidemiology has grown exponentially and is being used to simplify the understanding of infection progression and to make projections on the long term dynamics of an infection.

Malaria is one such infection on which mathematical models have yielded tremendous results. The host's invasion by a malaria parasite and the chemo-effects of the anti-

malarial drugs on the parasite are very complex processes that require application of mathematical models.

1.3 Methodology

In this study, we use non-linear systems of ordinary differential equations to explain the progression of the malaria parasite within the human host, using the revised Anderson et al (1989) model. For the systems of equations, we calculate steady states such as parasite-free and parasite-present equilibria, and investigate their dynamic stability in terms of the basic reproduction number, R_0 . Biologically, threshold parameters are important to determine whether the parasite infection gets suppressed or persists within the host. Constant treatment parameters are used to evaluate the benefits of treatment on malaria infection as projected by the models in the numerical simulations. We then establish a threshold drug efficacy parameter for which the parasite level will be suppressed down to zero. For the case of transplacental transmission of malaria in pregnant mothers, we formulate a system of delay differential equations for the parasite interaction with the red blood cells of the mother as well as that of the foetus. We seek to gain insight into how transmission of the infection to the foetus can be prevented. We analyse the vertical transmission model under three scenarios:

1. no time delay and no treatment,
2. no time delay with treatment, and

3. time delay without treatment.

Under scenario 1, we determine the local and global stabilities of the parasite-free and parasite-present equilibria in both the mother and the foetus and determine threshold conditions under which the parasite fails to establish itself. Under scenario 2, treatment was also incorporated into the model and threshold drug efficacy level for the complete eradication of the parasite in both the mother and foetus was determined. For scenario 3, intracellular delay effect was investigated and a critical condition to ensure that the parasite-present steady state is asymptotically stable for all delays was established. Numerical simulations have been used to confirm our analytical results.

Lastly, we formulated a stochastic model based on the revised Anderson *et al* (1989)'s deterministic model. The stochastic model incorporates stochastic noises described by two different diffusion structures namely constant diffusion and linear diffusion. We prove the existence of solutions of the stochastic models and their biological feasibility. We then show how the asymptotic stability of the deterministic system is degraded by the constant diffusion and varying diffusion terms. Patients' data is then used to validate our model results.

At the end, we discuss the biological importance of our results and how these results can be used in the verification of existing public health policies, its contribution to the creation of new health policies or as an eye opener to the health policy advisors on alternative approaches to the analysis of parasite dynamics in humans.

1.4 Objectives

In contributing to the knowledge of Malaria infection within the host, this study seeks to understand the infection by addressing the following scenarios:

1. Reviewing the Anderson, May and Gupta's (1989) human host and malaria parasite interaction deterministic model and determine the threshold drug efficacy for reducing the parasitemia within the host to zero level.
2. To understand the host-parasite dynamics in pregnant mothers.
3. To underline the need for a shift of analysis, from deterministic to stochastic analysis of the within host parasite dynamics
4. To demonstrate the importance of understanding dynamical interactions, deterministic and stochastic dynamics and the associated non-linear relationships, in interpreting observed clinical patterns in the interactions of the malaria parasite with the host's immune system and within populations of hosts.

1.5 Significance

Malaria infection has been affected by various factors, among others, drug resistance, treatment defaults, climatic changes, changes in disposable incomes among nations and other socio-political factors such as wars. This study's focus is on addition of emphasis to the importance of treatment and drug efficacy in the case management of malaria. Since a lot is yet to be understood on the within host interactions of the red

blood cells (RBCs) and the malaria parasite in the most sensitive group of pregnant mothers and its effects on the foetus, this study will provide an insight on the probable transplacental transmission of malaria. It provides, as well, a strong foundation for the importance of stochastic modeling and analysis on the more accurate accountability of the parasite dynamics within the host. In addition to this, this study will contribute to the public health knowledge on malaria case management.

1.6 Scope

Chapter 1 of this thesis looks at the introduction, where the background information of Malaria epidemiology and immunology is given. The objectives, problem, significance and scope of the research are spelt out in this chapter. Chapter 2 gives the literature review which includes the history, global statistics of malaria morbidity and mortality and the previous studies on malaria epidemiology, and immunology. Chapter 2 will serve as a motivational ground that forms the foundation and order of this research. Chapter 3 provides an analysis of the pioneering study by Anderson et al (1989) and extends the ideas by incorporating the effects of treatment in the erythrocytic stage interaction between the malaria parasite and the host's red blood cells (RBCs). In Chapter 4, we extend the idea in Chapter 3 and focus on the erythrocytic stage of the malaria parasite-host interactions in pregnant mothers with intracellular delay. Experimental findings of White [21] and the genetic heterogeneity in host-parasite populations [10] gives birth to Chapter 5, which examines the Stochastic interaction of the erythrocytic stage malaria parasite and the host's red

blood cells. The thesis ends with Chapter 6, which gives conclusions and discussions on the major results obtained in the research.

Chapter 2

Literature Review

Malaria is an ancient disease. According to Francis Cox [12], the early Greeks, including Homer in about 8500 BC, Empedocles of Agrigento in about 550 BC and Hippocrates in about 400 BC, were well aware of the characteristic poor health, malarial fevers and enlarged spleens observed in individuals residing in marshy areas. Cox [12] further states that for over 2500 years, the idea that malaria fevers were caused by miasmas rising from swamps persisted and it is widely believed that the word 'malaria' comes from the Italian 'mal'aria' meaning spoiled air.

Studies only became possible after the discovery of the parasites themselves by Charles Luce Alphonse Laveran in 1888 and the incrimination of mosquitoes as the vectors, first for avian malaria by Ronald Ross in 1887 and then for human malaria by the Italian scientists between 1898 and 1900 [12].

Malaria is a vector-borne infectious disease caused by protozoan parasites of the genus *Plasmodium*, prevalent throughout sub-Saharan Africa, most parts of Latin America and Asia. Each year, there are approximately 300 million cases of malaria, killing

over one million people annually, the majority of whom are children in Sub-Saharan Africa [48].

Below (Figures 2.1,2.2, 2.3) are graphs drawn using the data from [14] showing the distribution of reported malaria cases and deaths according to the World Health Organization (WHO) statistics from the year 2000 to 2010. In areas of stable malaria

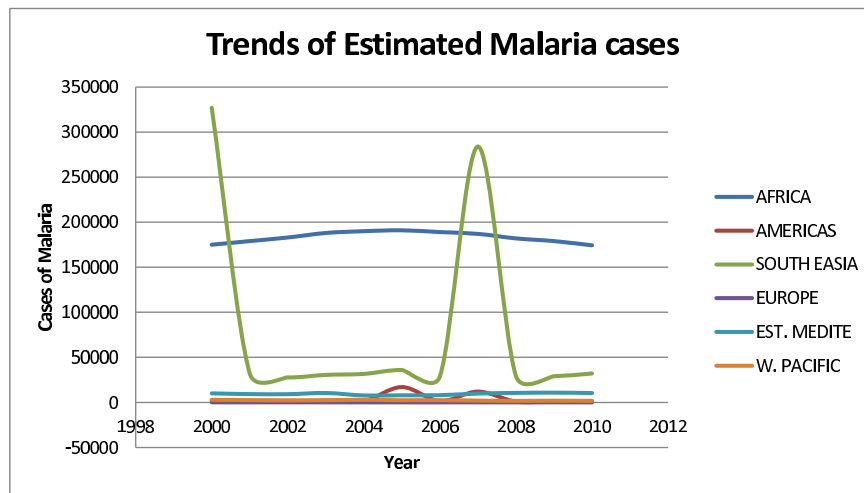


Figure 2.1: The graphs shows trends of WHO estimated cases of malaria in the WHO regions of the world.

transmission, very young children and pregnant women are the population groups at highest risk for malaria morbidity and mortality with most children experiencing their first malaria infections during the first year or two of life, when they have not yet acquired adequate clinical immunity [1].

Figure 2.1 show the trend of estimated malaria cases in the World Health Organization (WHO) regions of the world. Figure 2.2 show the estimated number of malaria deaths in children under 5 years of age. Figure 2.3 illustrate the dominance of malaria as the leading cause of death in children under the age of 5 in Africa compared to

other diseases like HIV-AIDS and Diarrhoea.

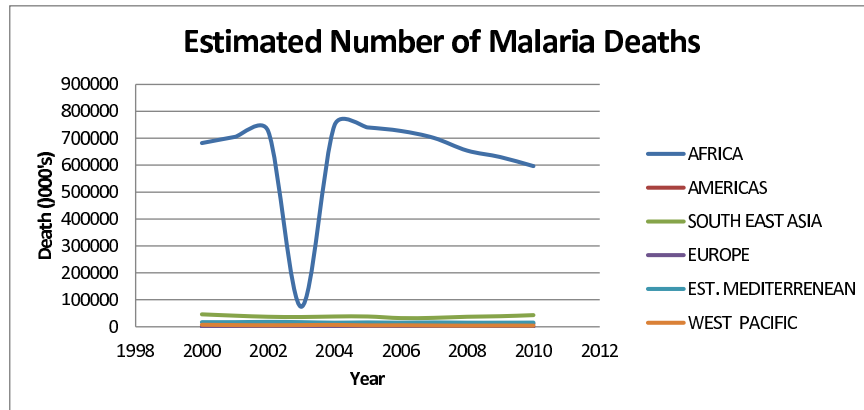


Figure 2.2: Trends in the cause of death in children under 5 years of age

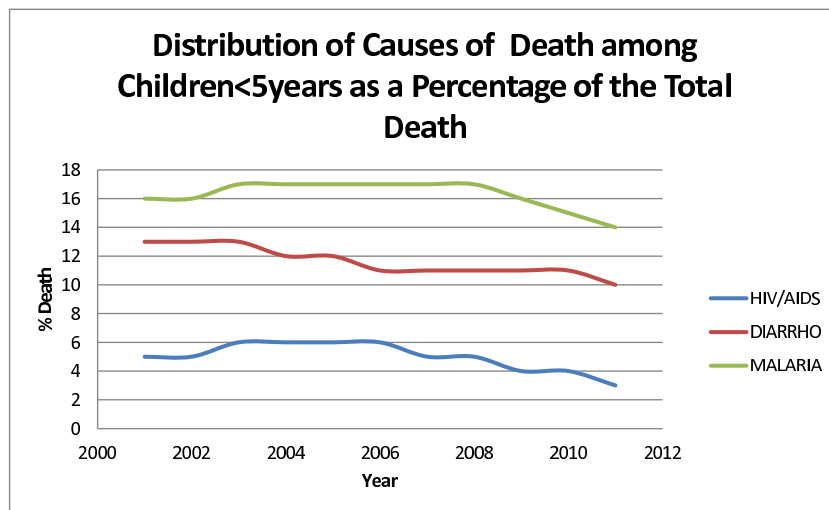


Figure 2.3: Trends in the cause of death in children under 5 years of age

Malaria parasites are transmitted to humans by female Anopheles mosquito bites and they multiply within red blood cells (gametocytes), causing symptoms of anemia (light headaches, shortness of breath, tachycardia, etc) as well as other general symptoms

such as fever, chills, nausea, flu-like illness, and in severe cases, coma and death [46].

The malaria parasite exhibits a complex life cycle. The mosquitoes are infected with the parasite as they feed on the blood of infected humans. In the mosquito's gut the gametocytes (male and female) from the infected person fuse to form ookinete that penetrate the gut lining and produce an oocyst in the gut wall. When the oocyst ruptures, it releases sporozoites that migrate through the mosquito's body to the salivary glands sporozoites. The mosquito then becomes infectious and will be ready to infect a new individual. Once within the humans the malaria undergoes two phases, an exoerythrocytic which involves maturation and development of the parasite (sporozoites) in the liver. These sporozoites infect hepatocytes and as a result the sporozoites multiplies in about 6-15 days. The parasites then replicate into thousands of merozoites within the hepatocytes causing the rupture of the host cells and release into the blood. With *Plasmodium vivax* (*P.vivax*) and *Plasmodium ovale* (*P.ovale*), the sprozoites may, sometimes, not immediately go into exoerythrocytic phase merozoites, but produce hypnozoites that lie dormant in the liver (for about 6-12 months to around 3 years) resulting in late relapses of malaria due to long incubation. In the erythrocytic phase, the merozoites multiply further asexually, in the red blood cells (RBCs), and burst the RBCs releasing the merozoites in the blood. Each burst is associated with a bout of fever [13, 15, 16, 17] (see Figure 2.4).

Repeated invasion of RBCs and the subsequent death of infected erythrocytes results in a depression in RBCs density in an infected person and a 50% or more reduction

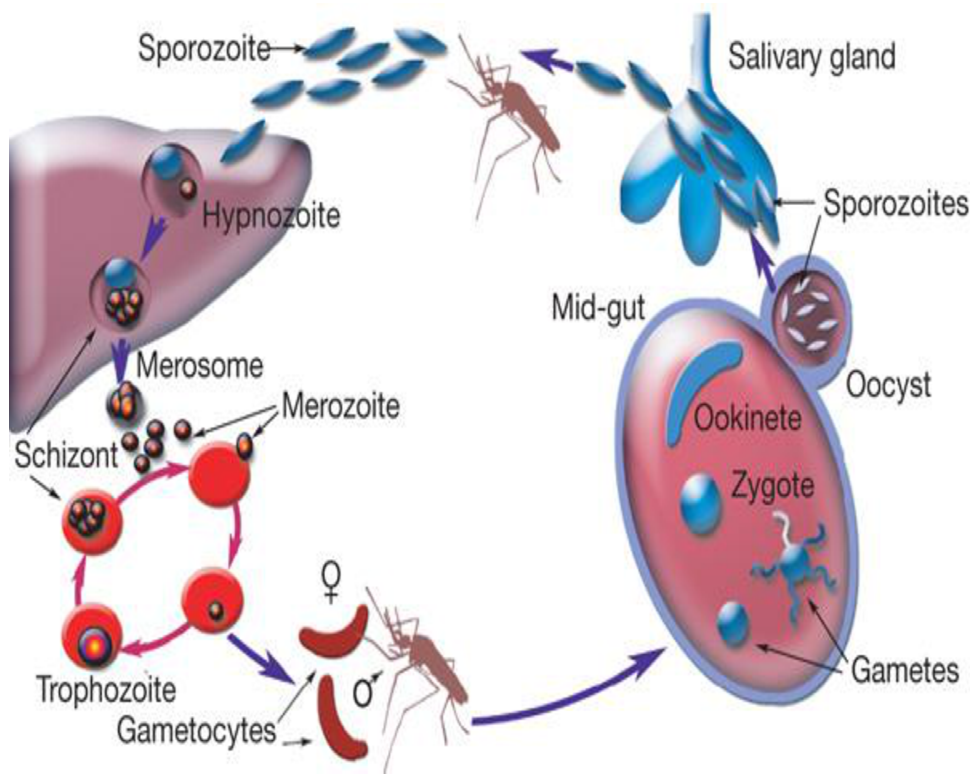


Figure 2.4: Diagram of the malaria parasite's life cycle

in the density may occur in severe cases of infection with further bursts and bouts of fever [10].

Although some vaccines are under development, no vaccine is currently available for malaria but preventive prophylactic drugs are usually taken continuously to reduce the risk of infection. Therapy drugs such as quinine or artemisinin derivatives, are available to treat already infected individuals. Rising mortality is linked to the growing incidence of chloroquine-resistant *Plasmodium falciparum* (*P. falciparum*) infections, the most lethal malaria strain [45, 48]. The promotion and use of insecticide-treated mosquito nets has become a leading strategy in malaria prevention and control [50]. On the sociopolitical and economic side, social, political, and economic changes, especially large scale uncontrolled population movements and ecological disturbances, all contribute to the worsening malaria problem. Environmental change brought about by development has created conditions suitable for malaria transmission, resulting in resurgence in regions where malaria had previously been under control [44].

Children who survive malaria may suffer long-term consequences of the infection, with repeated episodes of the fever and illness reducing appetite and restrict play, social interactions, and educational opportunities thereby contributing to poor development [44]. Malaria is said to be not just a disease associated with poverty, but is also a cause of poverty. Two key determinants of the economic costs of malaria are the direct costs of expenditure on prevention and treatment and the indirect costs of productive labour time lost due to malaria morbidity and mortality [44].

However, malaria case management remains a vital component of the malaria control strategies. This entails early diagnosis and prompt treatment with effective antimalar-

ial medicines. The World Health Organization (WHO) guidelines for the treatment of malaria [46], provide global evidence based recommendations on the case management of malaria, targeted mainly at policy-making at country level, providing a framework for the development of specific national treatment protocols that include local antimalarial drug resistance patterns and health service capacity in the country. Antimalarial treatment cures the infection as rapidly as possible, and also prevents progression to severe disease and morbidity associated with treatment failure. The proportion of infected mosquitoes in a locality is related to the number of infected and infectious humans in the area and, therefore, lowering the infectivity of the infected persons to mosquito vectors will contribute to reducing malaria transmission, and to eventually reducing the incidence and prevalence of the disease. Therefore, public health goal of treatment is to reduce the infectious reservoir and to prevent the emergence and spread of resistance to antimalarial medicines [46, 49].

Each year approximately 25 million African women become pregnant in malaria endemic areas. In malaria high transmission areas, some population groups are at considerable high risk of infection with *P. falciparum* and development of malaria morbidity or mortality than others and these include children under the age of five years and pregnant women [24].

Placental malaria (also known as umbilical cord parasitemia) is defined as the accumulation of Plasmodium-infected erythrocytes in the intervillous space in the placenta, causing histologic changes including leucocyte-induced damage to the trophoblastic basement membrane. It does not reflect the existence of peripheral infection over

a short period preceding the delivery or whether it is related to infection during pregnancy. The principal effects of malaria infection during pregnancy are associated with malaria-related anaemia in the mother and with the presence of parasites in the placenta. Malaria contributes significantly to perinatal disease burden in terms of pregnancy losses, prematurity due to pre-term labor and intra-uterine growth retardation. Pregnant women are at high risk of malaria infection because pregnancy causes a transient depression of cell mediated immunity. Age under 25 years and primiparity are both risk factors for developing placental malaria and moreover, the risk increases in the first and second trimester of pregnancy. Placental malaria is quite common during *Plasmodium falciparum* infections, but less common in *Plasmodium vivax* malaria infections. *Plasmodium falciparum* and *Plasmodium vivax* placental mixed-infection can occur and *P. vivax* placental malaria may lead to some adverse events as *P. falciparum* infection (see [24, 25, 31, 32, 33, 34, 35]).

Alterations of materno-fetal blood exchange are the basis of placental malaria. During infection, parasitized RBCs both from *P. falciparum* and *P. vivax* are sequestered within the placenta and may accumulate in intervillous spaces. Trophozoite and schizont form may also accumulate in the placenta. The presence of infected red blood cells (IRBCs) activates mononuclear cells which release chemokines to recruit additional phagocytic cells in the intervillous spaces. IRBCs, leukocyte infiltration, fibrin and hemozoin deposits contribute to increasing the thickness of the trophoblast basement membrane and to altering the intervillous and perivillous spaces, causing reduction of oxygen and nutrient transport to the fetus [25, 36].

Control of malaria during pregnancy depends on both preventing infection and clear-

ing parasitemia when it occurs. For decades the prophylaxis and treatment of malaria during pregnancy has relied on chloroquine. Resistance of *Plasmodium falciparum* to chloroquine and increasingly to sulfadoxine-pyrimethamine in Africa has resulted in the use of other antimalarials in pregnancy such as Artemisinin Combination Therapies (ACTs). However, in most areas of malaria transmission, highly effective prevention interventions are needed such as intermittent preventive treatment (IPT) and insecticide-treated nets (ITNs). IPT is based on the use of antimalaria drugs given in treatment doses at predefined intervals after quickening (around 18-20 weeks of pregnancy). The World Health Organization (WHO) recommends IPT with an effective, preferably one-dose, antimalarial drug to be provided in areas of stable transmission, as part of antenatal care, starting after quickening. ITNs reduce human-vector contact by physically excluding vector mosquitos, killing if they land on ITNs or repelling them, thereby driving them from the vicinity of sleepers [31].

There are few studies in humans on the pharmacokinetics, safety and efficacy of antimalarials in pregnancy because pregnant women are systematically excluded from clinical trials. The absence of adequate safety, especially in the first trimester, is an important obstacle to developing treatment strategies [37, 38, 39].

With few exceptions, most of drugs that are ingested by a pregnant woman during pregnancy can cross the placenta and reach the foetus via diffusion, facilitated diffusion, active transport and phagocytosis or pinocytosis. The drugs may pose potential danger to the foetus or newborn infant in view of their pharmacologic effects, side effects, or complications [74].

Artemisinin-based combination therapies (ACTs) and injectable artesunate (AS) are

currently recommended as the frontline antimalarial treatments for uncomplicated and severe malaria, respectively. Despite possessing excellent therapeutic activity and tolerability, neurotoxicity and embryotoxicity have been reported in cross-species animal models [75]. Studies in animals are very valuable in indicating possible risks in human from medicines. Artemisinin and its derivatives are considered safe and effective in pregnant women who have been treated with artemisinin compounds, including small doses in the first trimester [75] but according to a review by Dellicour *et al* [76] on the possible relationship between artemisinin compounds and adverse pregnancy outcomes, the authors concluded that current data are limited and the published studies do not have adequate power to rule out rare serious adverse events, even in second and third trimesters.

From documented publications and clinical data on malaria relapses, White [21] has suggested possible postulations regarding the basic biology and epidemiology of *P.vivax* relapse which need recognition and answers in order to adequately address seriously the control and elimination of malaria parasites.

P.vivax malaria, which is endemic to Asia, Ocenia and South America and in the horn of Africa, is a major cause of morbidity and an important contributor to early pregnancy loss and reduced birth weight which increases in infancy. *P.vivax* malaria is more difficult to eliminate than *P.falciparum* because of its tendency to relapse after resolution of the primary infection. *P.vivax* relapse is the recurrences of *P.vivax* malaria derived from persistent liver stages of the parasite (hypnozoites) and recrudescence is the recurrence of *P.vivax* malaria derived from persistence of the blood stage

infection. In endemic areas, relapse of vivax malaria is a major source of malaria transmission [21]. The factors which control *P.vivax* malaria stochastic episodes of relapse and determine their periodicity are not known, and the study by White [21] identifies some possible causes with a review of documented clinical data and publications. White [21] has traced the historical episodes of relapses as far as 1913. Early experimental work showed recurrences of vivax malaria commonly occurred many months after successful treatment of the primary infection.

Relapse arises after the 'awakening' of the hypnozoites and the subsequent intrahepatic schizogony followed by blood stage multiplication. From early data on relapse patterns from Korean vivax malaria and tropical frequent relapse *P.vivax*, White [21] noted that once the relapse had occurred (after a latency of 7-10 months), subsequent relapses would then usually occur with intervals of approximately 3 to 4 weeks following quinine or 6 to 8 weeks of chloroquine treatment. According to White [21], the data on artificial infection studies conducted in humans (17 USA volunteers were infected by a single mosquito bite with the Chesson strain of *P.vivax* and treated with chloroquine) and experimental primates suggested that even with a single infected mosquito bite some Chesson strain *P.vivax* infections relapse after intervals which were as long as a year after a series of regular 'short interval' relapse with non-constant periodicity. The review noted the initial inter-relapse intervals of Chesson strain *P.vivax* in volunteers and also *P.cynomolgi* in Rhesus monkeys being remarkably regular though with gradual lengthening in each successive relapse. White [21] explained this as the simultaneous activation of several hypnozoites that will shorten the relapse interval because the interval is measured until the progeny of most rapidly

growing parasites cause patent infection. For more activated genetically identical hypnozoites, relapse interval shortens than if one hypnozoite is activated. This is due to natural phenotypic variation amongst genetically identical organisms and it is the progeny of the earliest activated and most rapidly multiplying parasite that become patent first. From clinical data on US volunteer, the interval from inoculation to relapse (approximately 9 months later) shortening with increasing inocula was noted, that is, the more hypnozoites that are activated the shorter is the average interval between relapses. The review noted that, though in natural setting multiple genotypically distinct hypnozoites may be activated, in many occasions only one or two genotypes will be detected at clinical relapse. Hypnozoites, may as well, reach patency later, or asexual growth may be suppressed by fever, illness, immune response, and treatment such that they never reach patency. Larger doses of anti-malarials [21] resulted in longer intervals to relapse consistent with a concentration-dependent slowing of asexual rates and slowly eliminating anti-malarials delayed the onset of *P.vivax* relapse, and consequently reduced their frequency, though the overall number of relapses experienced did not appear to reduce. In trying to understand relapse, White [21] argues that artificial infections provided invaluable information but they differed from natural infections in several respects. Some of the differences are from the fact that infections were in non-immune adults whereas the burden of vivax disease in endemic areas have usually developed significant immunity to a broad range of local parasites which controls symptoms and reduce parasite densities. Artificial infections in the majority of volunteer studies carried out and in malaria therapy followed the bites of 5-10 infected anopheline mosquitoes selected for maximal infectivity, based on

salivary gland sporozoite loads in sibling mosquitoes and the timing of inoculation in malaria therapy and experimental studies, contrasts with the natural setting where anopheline mosquitoes display a wide range of infectivities depending on sporozoite age and other factors, White [21] argued. The study elaborates further that this observation resulted in reliable infections but did not bring out the important stochastic component of *P.vivax* epidemiology resulting from low sporozoite inocula in areas of low seasonal transmission. Also, the 'strains' of *P.vivax* used in the experiments were likely to have been of single genotype or very closely related interbreeding genotypes which were passed through a very large number of patients over many years, whereas in contrast multiple unrelated genotype infections are common in natural infections. In tracking the periodicity of relapse, White [21] noted, from the data on US volunteers who were infected with a Chasson strain of *P.vivax* that the number of relapses varied with the seven volunteers who were not reinfected having a median number of relapses of five (one of nine) following a single bite and 11 of the 39 relapses in this group (28 percent) occurred more than six months after the initial infection. The interval from one relapse to the next was similar but overall the inter-relapse intervals gradually lengthened; which proves that long-latency does occur with the tropical frequent relapse phenotype.

The importance to understand inhost malaria dynamics has led to the development of a vast of mathematical models. Anderson *et al* [10] demonstrated the importance of non-linear relationships in dynamical systems at a series of different interactions with the aim of stressing the importance of understanding dynamical interactions, interpreting observed patterns in the interactions of parasitic organisms with the

host's immune system and with populations of hosts. The study [10] focused on the transmission dynamics of parasitic organisms and control methods that influence the prevalence or intensity of infection. It examined the impact of mass vaccination and community based chemotherapy programmes, the relative merits of sporozoite and gametocyte targeted vaccines in infection prevention by malaria parasites and concomitant disease. The study [10] describes the complications introduced by genetic heterogeneity in host-parasite population interactions and the impact of selective pressures induced by the host's immune system or the application of chemotherapeutic agents on the transmission dynamics of heminth parasites. The study examined the interactions between malaria parasites and the host's immunological responses and in particular, investigated the impact of the immune differentiation to target merozoites and the infected erythrocytes during the erythrocytic stages of malaria.

The Anderson *et al* [10] model possesses a parasite-free and a parasite-present equilibrium states. The stability analysis showed that both parasite-free and parasite-present states are locally asymptotically stable but with exhibitions of periodic damped oscillations to equilibrium. In the same work, Anderson *et al* [10] explored the impact of immunological responses directed against merozoites and the impact of immunological responses directed against infected erythrocytes. The threshold condition for the immune system targeting merozoites was derived and in their conclusions it was noted that if the proliferation rate of specific lymphocytes is high enough, the derived threshold for the immune system reduces back to the threshold of the basic model. The work also suggested an extreme difficulty in the eradication of the parasite from the host by antibody-mediated attack against the free merozoites alone. The immune

response targeted against infected erythrocytes was found to be able to eliminate the parasite from the host after the initial 'epidemic' of infected cells, while the one targeted against merozoites is not.

Time delays of different types have been incorporated into biological models by many authors (for example [3],[80],[82]). Generally, delay differential equations exhibit more complicated dynamics than the ordinary differential equations since a time delay could cause a stable equilibrium to become unstable and cause fluctuations in populations. Calshaw and Ruan [80] incorporated a discrete time delay to the model on HIV infection of $CD4^+$ T cells, to describe the time between infection of a $CD4^+$ and the emission of viral particles on a cellular level. They showed that the infected steady state of the model is stable, independent of the size of the delay, meaning that delay can cause the $CD4^+$ T cells and HIV virus populations to fluctuate in the early stage of infection and converge to the infected state values in the long term.

In a similar work, Wang *et al* [82] developed and analysed an inhost viral model with cure of infected cells and humoral immunity. The study showed that time delay beyond some critical value may cause a stable endemic equilibrium point to be unstable.

In another study, Hoshen *et al* [3] reviewed Anderson *et al*'s basic model on the red blood cells and parasite interactions. In the study, Hoshen *et al* [3] argued that the mathematical model used in Anderson *et al* is highly nonlinear which makes analytical solutions difficult and thus dependent on guessing the parameters to fit experimental data and that synchronicity of malaria infections or periodicity of symptoms is not

accounted for by the model. The Hoshen *et al* [3] model explicitly introduced a parameter for the life-span of the infected red blood cells caused by macrophage attack on signaled erythrocytes or by protection against the re-invading merozoites (onset of host immunity) and introduced time delay in the dynamics.

These arguments led to proposing a system of linear delayed differential equations models and obtained solutions for the RBCs and IRBCs populations at any time as functions of the delay. Hoshen *et al* [3] compared the analytic results with clinical data and observed that the absence of a clear cyclical drop in parasitemia is a result of their model presenting the total parasitemia, while in vivo for human *P.falciparum*, only the circulating parasitemia, that is, ring stage parasites are measured. The work [3] also examined synchrony of parasites and wondered whether synchrony (rythmic fluctuations in the bloodstream parasitemia) would be expected from the asynchronous release of merozoites from the liver? Simulations in [3] were carried out under the assumption that parasites are released over the first half of the parasite cycle or over the whole cycle at uniform density with 16-fold multiplication rate per cycle and with no killing from the immune response. In the absence of immune clearance, periodic fluctuations in total parasitemia were observed but in the presence of the immune response at constant kill rate, large fluctuations in total parasitemia are observed. From these results, Hoshen *et al* [3] proposed that synchrony of parasites is genetic as a result of stochastic fluctuations in the individual periodicity of the parasite cycle. Chiyaka *et al* [18] developed a model based on Anderson *et al* by including the response of the immune system. Their model assumed five interaction species, the RBCs, IRBCs, merozoites, immune cells and antibodies. The authors [18] assumed

that i) the supply rate of RBCs from the bone marrow is accelerated by the presence of IRBCs, ii) production rate of merozoites is reduced by immune cells, and that iii) antibodies that block invasion of RBCs proliferate in the presence of merozoites. The model was analyzed and a globally stable parasite-free equilibrium was computed together with the intra-host basic reproductive number. Numerical simulations were used to confirm the existence and stability of the parasite-present equilibrium. Chiyaka *et al* [18] extended the immune response model by incorporating drug therapy. The effective reproductive number, which measures the number of secondary infections generated by a single parasitized RBC in an environment when antimalarial drugs are administered as a control strategy was computed, and the critical drug efficacy determined when the parasite can be cleared in the blood. Chiyaka *et al* [18]'s results show that without treatment the most effective part of the immune response in its mission to clear parasites is its ability to inhibit parasite growth in erythrocytes. They recommended that drugs specifically targeting infected red blood cells targeted and those targeting merozoites should be made available to make treatment more effective.

Yilong Li *et al* [19] looked at the blood stage dynamics of malaria in an infected host by incorporating the interactions of four populations, RBCs, IRBCs, malaria parasite and immune effectors with nonlinear bounded Michaelis-Menten-Monod functions describing how immune cells interact with the IRBCs and merozoites. That study [19], computed the model parasite-free equilibrium and showed that this state was globally stable but only established the local stability of the parasite-present equilibrium. The study [19] also shows conditions for the occurrence of Hopf bifurcation and

periodic solutions near the parasite-present equilibrium.

Friedman and Lungu [11] developed the immune response in-host model for malaria which involves the role of cytokines. That model [11] assumed a density dependent control mechanism for the parasite population. The basic model was then extended to include dual therapy namely $TNF\alpha$ externally injected and generic drug treatment that decreases the efficacy of extracellular parasites. In an attempt to measure the influence of the adaptive immune response, the model reproduction number, in an environment with treatment, was computed and sensitivity analysis to show the impact of the various parameters on the reproduction number was done. Their sensitivity results showed a highly positive correlation of the reproduction number to the intracellular parasite growth rate and a highly negative correlation to the natural death rate of IRBCs and the intracellular parasite related parameter (n). Numerical simulations showed the replication of extracellular parasites in the host to be fastest for the intracellular parasite for values of the parameter n in the range $8 \leq n < 15$. Particularly, $n = 8$ the parasite growth is fastest. The authors determined a threshold drug efficacy for which treatment with efficacy greater than the threshold, the parasite level in the blood stream will be reduced to zero. From their findings, Avner and Lungu [11] recommended dual therapy, of generic and cytokine based drugs, as the best strategy to follow to prevent parasites from developing resistance to malaria treatment drugs.

The accuracy of the results derived from existing deterministic in-host models was discussed in Saul [20]. Saul [20] suggests that mathematical models of in-host dynamics for malaria parasites by Anderson *et al* and researches may not be accurate and may

lead to significant over-estimates in parasite growth rates. In [20], the author argues that the assumptions in Anderson *et al*'s model that all red blood cell destruction in addition to the normal removal of old red cells, is due only to the rupture of IRBCs and, that the life of an infected red cell follows an exponential decay with an average span equal to the parasite growth cycle (48 hr for *P.falciparum*) contrasts with the essentially discontinuous process which occurs in nature. Saul [20] argues that, although it seems obvious that the rate at which merozoites are being released should be the number of merozoites times the rupture rate of schizonts, there is evidence of errors in this term. In this study, Saul [20] gave examples of the sources of error in the modelling process. He considered a situation where the number of RBCs will be nearly constant under initial conditions with experimental work showing that under these conditions nearly all merozoites invade and there is an exponential increase in parasitemia. He suggested that under these conditions the growth rate should be taken to be αr (Anderson *et al*). The study suggests an alternative strategy of describing in-host dynamics, not as a series of differential equations relying on rate constants, but as recursion equations that describe population at discrete times in terms of the multiplication factors which occurs between different stages and the probability of surviving from one time point to the next and the size of the population at a previous time which leads to computationally efficient deterministic and stochastic simulations of population dynamics and simpler analytical solutions for equilibrium situations. In response to Saul, Gravenor and Lloyd [22] argued that replacing the parameter for the number of merozoites produced (r) by each parasite at schizogony with $\ln(r) + 1$ does not address the true underlying problem with the model, that is, the use of the

constant rate α assumes an exponential and hence much more variable distribution. The authors suggested the addition of more age compartments to the intracellular parasite stage. n categories were introduced, that is, as a parasite matures, it passes through these categories in a sequence, with constant transition rates between categories. By so doing, the overall parasite life-span is described by a sum of many exponential distributions, which is considerably less variable than the single exponential distribution used in Anderson *et al* and Saul [20]. When Gravenor and Lloyd [22] compared their model results with that of Anderson *et al*, they noted that their model leads to equilibrium solutions that are identical to those obtained from their expanded model. They concluded that erythrocyte competition alone is insufficient to regulate parasitemia and that low parasitemias can potentially account for considerably more erythrocyte distribution than expected. The authors [22] pointed out that including age structures in the basic Anderson *et al*'s models has the benefit of addressing the key biological questions relevant to *P. falciparum* infection. However, they acknowledged the use of constant rates to describe life-span as an attractive starting point, though unrealistic in many biological systems.

Niger and Gumel [23] incorporated an n stage parasite life cycle, immune cells and antibodies in the Anderson *et al* (1989)'s basic model as suggested by Gravenor and Lloyd [22] in response to Saul [20]. The model [23] was shown to be biologically feasible. The model's parasite-free equilibrium and the basic reproduction numbers were computed. The local and global stability conditions for the parasite-free equilibrium were determined. As in Anderson *et al*, Niger and Gumel [23] included immune response to the n stage basic model. The parasite-free equilibrium and the immune

reproduction number for this extended model were computed and it was shown that the parasite-free equilibrium is globally stable when the corresponding reproduction number is less than unity. This stability criterion was confirmed by numerical simulations. In the study [23], the immune response n -staged model was further extended to incorporate potential imperfect malaria vaccines which block the transmission of infection, enhances an immune response, reduces the number of merozoites released per burst of an IRBC and enhances the production of antibodies. The model's parasite-free equilibrium and the corresponding vaccine reproduction number which depend on the n stages transition rates was computed. The parasite-free equilibrium was shown to be globally stable whenever the reproduction number was less than unity. The vaccine critical efficacy was computed and numerical simulations of the model revealed that an imperfect vaccine with efficacy of at least 87 percent can lead to the effective control of malaria in vivo. The authors pointed out that a malaria vaccine that decreases the total number of merozoites released per bursting IRBC reduces the concentration of IRBC in vivo and that a vaccine that reduces the immune response decreases the concentration of IRBC in vivo, and hence recommended for candidate vaccines that meet these conditions as the best strategy in the control of malaria.

In a study on stochastic perturbations, Aguirre Pablo [40] was interested in investigating the dynamics of a species subjected to a predation-driven Allee effect. Allee effect is a situation of a low density prey population that faces difficulties to grow and avoid extinction. The author considered two classes of stochastic models of predator-prey interaction with Allee effect on the prey. The first class incorporated an additive Allee effect in the prey growth rate and the second class incorporated multiplicative Allee

effect to the logistic growth rate in the prey population. In both models, it was shown that the models were well posed, and in the absence of random noise, all solutions are bounded. It was also shown that the models' solutions exist and are pathwise unique and have bounded moments. In response to his aim, Pablo [40] found that if both populations (predator and prey) have a low density, the trajectories of the stochastic system tend to be the same as that of the associated deterministic model and hence concluded that the time evolution of the species is increasingly governed by the Allee effect. By the additive and multiplicative Allee effect approach, the author also found that environmental randomness effect is stronger for higher population sizes.

In the study by Viet *et al* [41], the Volterra type predator-prey model with the Beddington-DeAngelis functional response, that is, a functional response that depends on both prey's and predator's densities and not only on prey's density under random fluctuations, was considered. The aim of the study was to study the existence, uniqueness and positivity of solutions of the modified Volterra model and to analyze the asymptotic properties of the stochastic predator-prey model in population dynamics with the intention of wanting to know the extinction rate of each species, the information vital for suitable policy in investment and for timely measures in protecting these species from the extinct disaster. The modified Volterra model solutions were shown to exist and to be locally unique for some time up to but not to explosion time of the model coefficients that are locally Lipschitz continuous. The model solutions were also shown to be global, using the localization technique. The study of asymptotic moments behaviour of stochastic models helps in gaining a deeper insight of the underlying process since most models have no explicit solu-

tions. In this study [41], the model was shown to have bounded moments. The long term behaviour of the solutions was studied when there is no noise (deterministic) and when there are stochastic perturbations and it was found that a relatively large stochastic perturbation can cause the extinction of the population which can serve as a warning for us to have a timely decision to protect species in our ecosystem.

Chapter 3

Inhost Malaria model with treatment

3.1 Introduction

Recently, there has been several studies [3, 11, 19, 20, 22] on in-host mathematical modeling of the dynamics of malaria infections. The starting point for all these studies is the study by Anderson *et al* [10] which models the blood-stage asexual cycle of the malaria parasite, which included the infection of erythrocytes (RBCs) by merozoites. The Anderson *et al* study models the malaria parasite infection of red blood cells using the following system of coupled deterministic differential equations:

$$\begin{aligned}\dot{R} &= \pi_a - \mu_r R - \beta_a RP \\ \dot{R}_i &= \beta_a RP - \alpha R_i \\ \dot{P} &= \alpha r R_i - \mu_p P - \beta_a RP\end{aligned}\tag{3.1}$$

where R denotes the uninfected red blood cell (RBC) concentration (per μl), R_i denotes the concentration of infected red blood cells (IRBC) and P represents the merozoite population. We assume that bone-marrow erythropoiesis is at a fixed rate π_a , and the normal decay of RBCs is a first-order process at a constant rate μ_r . Merozoites are released from bursting of the IRBCs at a rate α , with a multiplication rate of r per cycle. The merozoites population is reduced by invading fresh RBCs at a rate β_a , and due to natural death at a constant rate μ_p .

3.1.1 Positivity of solutions

We can show that the Anderson *et al* [10] model (3.1) is positively invariant, a necessary and sufficient condition for the model to be useful to study the infection dynamics.

Lemma 3.1.1 *Consider a system of differential inequalities*

$$\frac{dx_i}{dt} \geq A_i x_i + \sum_{j=1}^n B_{ij} x_j + \epsilon \quad (i = 1, \dots, n) \quad (3.2)$$

where

$$B_{ij} \geq 0, \quad \epsilon \geq 0.$$

If $x_i(0) \geq \epsilon$ for $i = 1, \dots, n$, then $x_i(t) \geq 0$ for all $t > 0$ and $1 \leq i \leq n$.

Proof Without loss of generality we may assume that $\epsilon > 0$, since the case $\epsilon = 0$ follows by approximating the system with a sequence $\epsilon = \epsilon_k$, $\epsilon_k \downarrow 0$.

Suppose the assertion $x_i(0) \geq \epsilon > 0$, for $1 \leq i \leq n$, is not true. Then there exists a

smallest number $t_0 > 0$, such that

$$x_i(t) > 0 \quad \text{for } 1 \leq i \leq n, \quad 0 \leq t < t_0$$

$$x_i(t_0) = 0 \quad \text{for at least one } i, \text{ say } i = i_0.$$

Then x_{i_0} is a decreasing function at $t = t_0$, so that

$$\frac{dx_{i_0}}{dt}(t_0) \leq 0.$$

From the differential inequality (3.2) for $x_{i_0}(t)$ we get

$$\frac{dx_{i_0}}{dt}(t_0) \geq \sum_{j=1}^n B_{ij}x_j(t_0) + \epsilon \geq \epsilon > 0$$

which is a contradiction. Hence, if $x_i(0) \geq \epsilon$ for $i = 1, \dots, n$ then $x_i(t) \geq 0$ for all $t > 0$ and $1 \leq i \leq n$.

3.1.2 Analysis of the model

Intra-host basic reproductive number and stability analysis

Following Molineaux and Dietz [42], we define the intra-host basic reproductive number R_0 as the number of secondary infected red blood cells (IRBCs) produced per primary infected red blood cell (IRBC) in a host at the beginning of infection. If $R_0 < 1$, then on average an IRBC produces less than one new IRBC and the infection cannot grow. However, if $R_0 > 1$, then on average each IRBC produces more than one new IRBC and the infection persists.

Following the next generation operator method (Diekman *et al* [43]; van den Driessche and Watmough [52]), the matrices F and V^{-1} for the system (3.1) are given by:

$$F = \begin{bmatrix} 0 & \frac{\beta_a \pi_a}{\mu_r} \\ 0 & 0 \end{bmatrix}, V^{-1} = \begin{bmatrix} \frac{1}{\alpha} & 0 \\ \frac{r\mu_r}{\mu_p\mu_r + \beta_a\pi} & \frac{\mu_r}{\mu_p\mu_r + \beta_a\pi_a} \end{bmatrix}. \quad (3.3)$$

The matrix FV^{-1} is called the next generation matrix [43] and the reproductive number R_0 , is the dominant eigenvalue of FV^{-1} .

For the model (3.1), this number is given by:

$$R_0 = \frac{r\beta_a\pi_a}{\mu_r\mu_p + \beta_a\pi_a}.$$

Model (3.1) has two steady states, the parasite-free steady state given by

$$E_0 = (R^*, R_i^*, P^*) = \left(\frac{\pi_a}{\mu_r}, 0, 0 \right)$$

and the parasite-present steady state given by

$$E_p = (R^{**}, R_i^{**}, P^{**}),$$

where

$$R^{**} = \frac{\mu_p}{(r-1)\beta_a}, \quad R_i^{**} = \frac{\pi_a\beta_a + \mu_r\mu_p}{\alpha(r-1)}(R_0 - 1), \quad P^{**} = \frac{\pi_a\beta_a + \mu_r\mu_p}{\mu_p\beta_a}(R_0 - 1)$$

which exists if and only if and only if $R_0 > 1$.

Local stability of parasite-free equilibrium

The Jacobian of (3.1) evaluated at the parasite-free equilibrium, E_0 , is

$$J_{E_0} = \begin{bmatrix} -\mu_r & 0 & -\frac{\beta_a\pi_a}{\mu_r} \\ 0 & -\alpha & \frac{\beta_a\pi_a}{\mu_r} \\ 0 & \alpha r & -\frac{\mu_p\mu_r + \beta_a\pi_a}{\mu_r} \end{bmatrix}. \quad (3.4)$$

For the parasite-free equilibrium to be locally stable, all the real parts of the eigenvalues of the characteristic equation $|J_{E_0} - \lambda I| = 0$, should be negative.

One of the eigenvalues of this characteristic equation is $\lambda_1 = -\mu_r$ and the other eigenvalues are obtained from

$$\lambda^2 + \left(\alpha + \mu_p + \frac{\beta_a \pi_a}{\mu_r}\right)\lambda + \frac{\alpha}{\mu_r}(\mu_r \mu_p + \beta_a \pi_a)(1 - R_0) = 0. \quad (3.5)$$

The roots of (3.5) have negative real parts if $1 - R_0 > 0$, that is, if and only if $R_0 < 1$.

We can summarize this as follows:

Theorem 3.1.2 *The parasite-free equilibrium is locally asymptotically stable if $R_0 < 1$ and unstable otherwise.*

Global stability of parasite-free equilibrium

The technique for proving the global stability by Carlos Castillo Chavez *et al* [53] is summarized in the following lemma:

Lemma 3.1.3 *If a system can be written in the form:*

$$\frac{d\mathbf{X}}{dt} = F(\mathbf{x}, Z) \quad \frac{d\mathbf{Z}}{dt} = G(\mathbf{x}, Z), \quad G(\mathbf{x}, \mathbf{0}), \quad (3.6)$$

where $\mathbf{X} \in \mathbf{R}^m$ denotes (its components) the number of uninfected individuals and $\mathbf{Z} \in \mathbf{R}^n$ denotes (its components) the number of infected individuals including latent, infectious, etc, and $\mathbf{U}_o = (\mathbf{x}^*, \mathbf{0})$ denotes the disease-free equilibrium of the system kin

question, and if the following conditions (H1) and (H2) below are met to guarantee local asymptotic stability

(H1) For $\frac{d\mathbf{X}}{dt} = F(X, 0)$, X^* is globally asymptotically stable (G.A.S)

(H2) $G(X, Z) = AZ - \hat{G}(X, Z) \geq 0$ for $(X, Z) \in \mathbf{D}$, where $A = D_Z G(X^*, 0)$ is an M-matrix (the off diagonal elements of A are non-negative) and \mathbf{D} is the region where the model makes biological sense,

then the fixed point $\mathbf{U}_o = (\mathbf{x}^*, \mathbf{0})$ is a globally asymptotically stable (g.a.s) equilibrium of the biological system provided that $R_o < 1$ (l.a.s) and that assumptions (H1) and (H2) are satisfied.

Theorem 3.1.4 *The disease-free equilibrium point E_o of system (3.1) is globally asymptotically stable (G.A.S) whenever $0 \leq R_o < 1$ and unstable otherwise.*

Proof Using lemma (3.1.3), system (3.1) can be expressed as follows:

$$X = (R(t)), \text{ and } Z = (R_i(t), P(t)). \quad (3.7)$$

From $A = D_Z G(X^*, 0)$, we have

$$A = \begin{bmatrix} -\alpha & \beta_a R^* \\ \alpha r & -(\mu_p + \beta_a R^*) \end{bmatrix}, \quad (3.8)$$

and from $G(X, Z) = AZ - \hat{G}(X, Z)$, we have

$$\hat{G}(X, Z) = \begin{bmatrix} \hat{G}_1 \\ \hat{G}_2 \end{bmatrix} = \begin{bmatrix} \beta_a P(R^* - R) \\ 0 \end{bmatrix} \geq 0 \quad (3.9)$$

since $R^* \geq R$.

Local Stability of parasite-present equilibrium

Theorem 3.1.5 *The parasite-present steady state $E_p = (R^{**}, R_i^{**}), P^{**}$ is locally asymptotically stable when $R_0 > 1$ and unstable otherwise.*

Proof From the Jacobian of model (3.1), evaluated at the parasite-present equilibrium, we obtain

$$J_{E_p} = \begin{bmatrix} -\mu_r - \beta_a P^{**} & 0 & -\beta_a R^{**} \\ \beta_a P^{**} & -\alpha & \beta_a R^{**} \\ -\beta_a P^{**} & \alpha r & -\mu_p - \beta_a R^{**} \end{bmatrix}, \quad (3.10)$$

and from the characteristic equation $|J_{E_p} - \lambda I| = 0$ we have

$$\lambda^3 + a_2 \lambda^2 + a_1 \lambda + a_0 = 0, \quad (3.11)$$

where

$$a_2 = \mu_r + \alpha + \mu_p + \beta_a P^{**} + \beta_a R^{**},$$

$$a_1 = \alpha(\mu_r + \mu_p) + \mu_p \mu_r + (\alpha + \mu_p) \beta_a P^{**} + (\mu_r - (r-1)\alpha) \beta_a R^{**} > 0$$

and

$$a_0 = \alpha(\pi_a \beta_a + \mu_p \mu_r)(R_0 - 1) > 0$$

since $R_0 > 1$.

Using the Routh-Hurwitz stability theorem with $n = 3$, the coefficients of the characteristic equation (3.11) are all positive when $R_0 > 1$. Hence all the eigenvalues of the Jacobian matrix (3.10) have negative real parts when $R_0 > 1$ and the parasite-present equilibrium point is locally asymptotically stable.

Theorem 3.1.6 *The parasite present equilibrium state E_p is globally asymptotically stable if*

1. $R_0 > 1$ and
2. $(1 - \frac{R}{R^{**}})$ and $(1 - \frac{P}{P^{**}})$ have the same sign.

Proof We define the nonlinear Lyapunov function

$$V = (R - R^{**} - R^{**} \ln R) + (R_i - R_i^{**} - R_i^{**} \ln R_i) + \frac{1}{r}(P - P^{**} - P^{**} \ln P)$$

The time derivative of V for $R_0 > 1$ reduces to

$$\begin{aligned} \dot{V} = \mu_r R^{**} \left(2 - \frac{R}{R^{**}} - \frac{R^{**}}{R} \right) + \beta_a R^{**} P^{**} \left(3 - \frac{R^{**}}{R} - \frac{R_i^{**} P^{**}}{R_i^{**} P} - \frac{R R_i^{**} P}{R^{**} R_i P^{**}} \right) - \\ \frac{\beta_a R^{**} P^{**}}{r} \left(1 - \frac{R}{R^{**}} \right) \left(1 - \frac{P}{P^{**}} \right). \end{aligned}$$

As the arithmetic mean exceeds the geometric mean (see [23]),

$$2 - \frac{R}{R^{**}} - \frac{R^{**}}{R} \leq 0, \quad 3 - \frac{R^{**}}{R} - \frac{R_i^{**} P^{**}}{R_i^{**} P} - \frac{R R_i^{**} P}{R^{**} R_i P^{**}} \leq 0.$$

Therefore, $\dot{V} < 0$.

3.2 Model with treatment

Antimalarial drugs taken prophylactically or during infection (blood schizonticide) concentrate particularly in parasitized erythrocytes. The drug diffuse into parasite lysosomal compartments and becomes protonated in the acidic environment within, so it can not pass out through the membrane. It raises the pH of lysosome, inhibiting the polymerase that converts toxic free haem to a harmless by-product. It prevents digestion of haemoglobin by parasites, reducing its supply of amino acids and therefore makes the parasite survival development difficult [18].

In this section we consider administering drugs that promote transmission blocking by replacing the parasite transmission rate β_a in model (3.1) by $(1 - \epsilon)\beta_a$, where ϵ is the drug efficacy, $0 \leq \epsilon \leq 1$, with $\epsilon = 0$ meaning the drug is totally ineffective and $\epsilon = 1$, the drug is 100% effective [11]. The model (3.1) becomes:

$$\begin{aligned}\dot{R} &= \pi_a - \mu_r R - (1 - \epsilon)\beta_a RP \\ \dot{R}_i &= (1 - \epsilon)\beta_a RP - \alpha R_i \\ \dot{P} &= \alpha r R_i - \mu_p P - (1 - \epsilon)\beta_a RP\end{aligned}\tag{3.12}$$

with an associated reproduction number

$$R_\epsilon = \frac{(1 - \epsilon)r\beta_a\pi_a}{\mu_r\mu_p + (1 - \epsilon)\beta_a\pi_a}.$$

Note that if $\epsilon = 1$, $R_\epsilon = 0$ meaning that the parasite clears in the host's blood stream and if $\epsilon = 0$, $R_\epsilon = R_0$.

Critical Drug Efficacy

Solving for ϵ from the expression for $R_\epsilon = 1$ gives

$$\epsilon^* = 1 - \frac{\mu_r \mu_p}{(r-1)\beta_a \pi_a},$$

and for the parameter values given in Table 3.1, $\epsilon^* = 0.9952$.

Lemma 3.2.1 *The treatment reproductive threshold $R_\epsilon < 1$ whenever $\epsilon > \epsilon^*$.*

If the malarial drug efficacy is greater than ϵ^* , the parasite is cleared from the blood, that is, $R_\epsilon < 1$. The results for $\epsilon > \epsilon^*$ are illustrated numerically below.

3.3 Numerical simulations

Using parameter values in Table 3.1, we have numerical simulations giving rise to Figure 3.1 showing trajectories of the RBCs, IRBCs and parasite populations at any time $t > 0$ for different initial conditions. Irrespective of where we start from, the trajectories converge to the same values in the long-run, demonstrating stability of the equilibrium points.

Figure 3.2 shows the concentration of IRBCs when the drug efficacy is less and greater than the critical drug efficacy of 0.9532. For $\epsilon < \epsilon^*$, we have the parasite persistence in the blood stream whereas $\epsilon > \epsilon^*$, the parasite will be cleared from the blood stream. The figures below show the concentrations of RBCs, IRBCs and parasites at different drug efficacy levels. Numerical simulations (see Figures 3.2 and 3.3) have shown that

Table 3.1: Description of model parameters for system (3.1).

Parameter	Definition	Value	Ref.
π_a	Prod. rate of RBCs from the bone-marrow (<i>cell/mil.day</i>)	2.5×10^9	[11]
μ_r	Natural death rate of uninfected RBCs (<i>perday</i>)	0.8	[18]
β_a	Rate of infection (<i>ml/cell.day</i>)	$2 \times 10^{-11.3}$	[11]
α	Bursting rate of IRBCs (<i>perday</i>)	0.5	[11]
μ_p	Natural death rate of parasites (<i>perday</i>)	0.022	[11]
r	Num. of merozoites released per bursting IRBC (<i>perday</i>)	16	[11]

as the drug efficacy level increases to $\epsilon = 0.954$, with $R_\epsilon =$ reaching 0.98, the parasite will be wiped out completely from the blood stream though a question might still remain on the practical attainability of such an efficacy level.

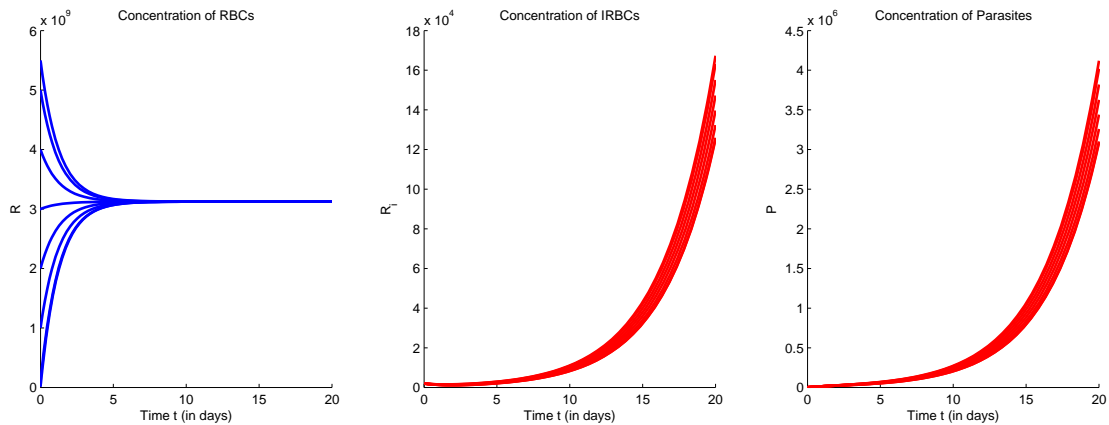


Figure 3.1: Simulations of equation(3.1) showing the concentrations of (a) RBCs (b) IRBCs, and (c) parasites at different initial conditions over time for $R_0 > 1$ in the absence of treatment. For parameter values used, see table 3.1

This model (3.12) does not present all manifestations of malaria. For example, White

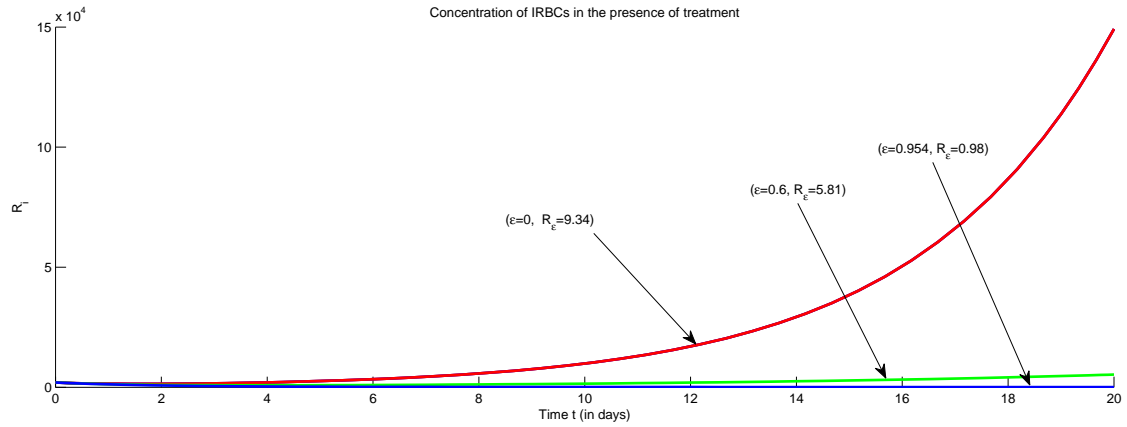


Figure 3.2: Simulations of equation (3.12) showing the concentration of IRBCs for $\epsilon < \epsilon^*$ and $\epsilon > \epsilon^*$ using parameter values in table 3.1.

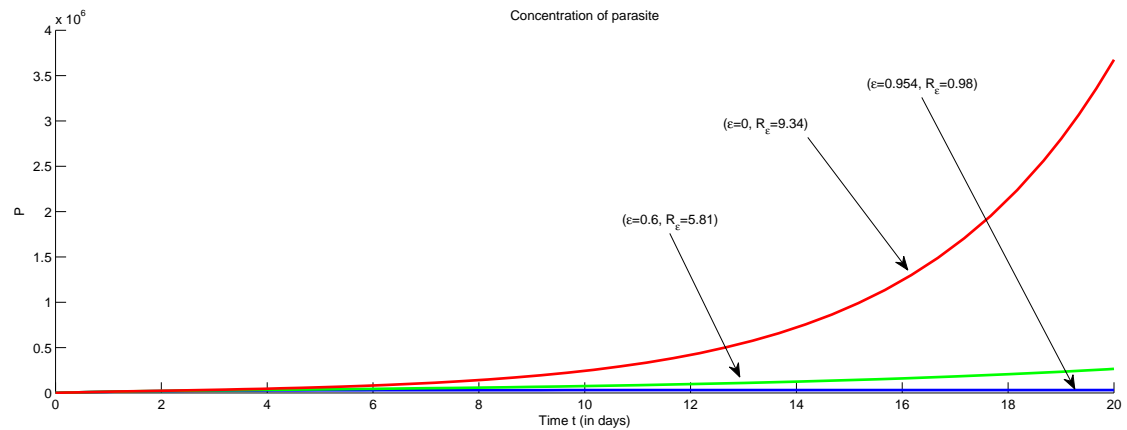


Figure 3.3: Simulations of equation (3.12) showing the parasite concentration for $\epsilon < \epsilon^*$ and $\epsilon > \epsilon^*$ using parameter values in table 3.1.

[21] has reviewed a clinical study for patients infected with vivax malaria. This review revealed various manifestations of malaria infections which can not be described by a simple model of Anderson *et al* [10].

Chapter 4

Inhost transplacental malaria transmission with and without time delay

4.1 Introduction

Pregnant women experience an increased risk of *Plasmodium falciparum* infection during pregnancy than non-pregnant women because of weakened immunity. This increased risk contributes significantly to perinatal disease burden in terms of pregnancy loss, prematurity due to preterm labor, and intrauterine growth retardation [27]. The direct burden of neonatal malaria infection in terms of prevalence is not well-described in malaria endemic areas, and reported estimates vary widely from 0% to 33% [29]. Epidemiological studies estimate 125 million pregnancies are at risk

of malaria infection every year within an estimate of 32 million women who become pregnant every year in malaria endemic sub-Saharan Africa countries [1, 28]. According to the World Health Organization (WHO), malaria accounts for over 10,000 maternal and 200,000 neonatal deaths per year [1].

Symptoms of malaria infection can appear in new born babies 24 hours after birth. However, the disease may be seen in a day-old infant or appear after weeks to months [26, 29]. Evidence of occurrence and characteristics of congenital malaria in endemic areas is summarized by the following clinical case reports that will form the basis of our mathematical model: The first case report of congenital malaria is that of a mother who delivered identical male twins through spontaneous delivery. The mother and one of the twins tested positive for malaria parasites on the day of delivery. The second twin tested positive for malaria parasites on the second day after delivery [60]. Even though the mother had taken all the recommended doses of sulfadoxine/pyrimethamine for intermittent preventive treatment for malaria, she still developed the infection immediately after delivery. The infection remained active in both the mother and the foetus even though it was not detected. The question is whether the malaria parasites had developed resistance to the preventive drugs that were administered or whether the drug concentration that diffused to the foetuses was too weak to clear the infections. The second case report is that of a woman who lived in Europe but visited a malaria endemic area for a short period in 2008 [59]. She returned to a malaria-free Europe and became pregnant one year after her short visit to a malaria endemic area. She gave birth to a female infant. 22 days after birth

the infant developed fever and a wrong clinical diagnosis of neonatal sepsis was made and treatment with antibiotics was started. However, twenty-four hours after the infants's admission an accidental examination of the infant's peripheral blood revealed a diagnosis of vivax malaria. The mother's history revealed that she had been treated for malaria during her short visit to the malaria endemic area. The mother was then re-evaluated in view of the infant's diagnosis but tested negative for malaria parasite [59]. The third case report is that of an infant who tested positive for plasmodium vivax immediately after birth but the mother tested negative for malaria parasite.

Ou édraogo et al [24] have found evidence of infection with Plasmodium falciparum in about 1.4% of new born babies in Burkina Faso. However, the majority of mothers who tested positive for Plasmodium falciparum during pregnancy went on to deliver normal healthy babies [24]. There is clear evidence [26] that the interaction between HIV-1 and malaria in pregnancy causes more peripheral and placental parasitemia and that placental HIV-1 is increased in women with placental malaria. The association between the two infections can potentially have disastrous effects. Therefore, any interaction between these infections will have a significant public health effect in sub-Saharan Africa, even if the statistical effect is modest.

Based on these clinical case reports, we want to formulate a mathematical model that mimics the four clinical case reports presented in [24, 59].

Malaria endemic areas with high HIV prevalence are susceptible to increasing congenital malaria prevalence. This study aims to investigate vertically transmitted malaria from the placenta of a pregnant mother to her foetus (congenital malaria). Some of

the children who survive malaria infection are known to suffer long-term consequences such as repeated episodes of the illness which affect their educational opportunities and contribute to poor development[24, 44].

Alterations of maternal-fetal blood exchange is the source of congenital malaria. During the pregnant mother's malaria infection, parasitized RBCs can accumulate in the intervillous spaces of the placenta and infiltrate the placenta barrier to initiate malaria infection in the foetus [25, 36]. New malaria infection or malaria relapse during pregnancy can pose substantial risks to the mother and foetus.

Treatment of uncomplicated malaria in pregnancy is a balance between potential foetal adverse effects from drug toxicity and improved clinical status with clearance of the parasite [30]. Although safe and effective in reducing mortality from severe malaria in adults and children older than 2 years of age, data on the safety and efficacy of intravenous artesunate in infants are limited, with scant data on its use in neonates [1, 29]. While chemotherapy in pregnancy appears efficacious, a major question remains-which drugs are safest for both the mother and foetus and in what quantities?

Therefore, understanding how malaria specifically affects pregnant women and whether the drug has a deleterious effect on the development of the embryo is crucial [25, 36]. Despite the public health hazard caused by placental malaria, few studies have also addressed the impact of time delay on pregnancy outcome and the health of new born babies in sub-saharan Africa.

This chapter examines the vertical transmission mechanism of *Plasmodium falciparum* malaria and is structured as follows. Section 4.1 is the introduction, Section 4.2 examines the inhost transplacental transmission model of malaria in pregnant mothers with and without time delay in the presence of intervention. Section 4.3 presents the mathematical and numerical analysis for the models without delay. Section 4.4 presents the mathematical analysis for the model with time delay.

4.2 Transplacental transmission model

We formulate a model that includes malaria infection of the primary host, the mother, followed by malaria infection of the secondary host, the foetus, due to failure of the mother's immune system to detect and reject infected red blood cells crossing the umbilical (transplacental) cord to enter the foetus blood system. We assume that the infection in the mother is described by the Anderson et al (1989) [10] model given by:

$$\dot{R}(t) = \Pi_a - \mu_r R(t) - \beta_a(1 - \epsilon_1)R(t)P(t) \quad (4.1)$$

$$\dot{R}_i(t) = \beta_a(1 - \epsilon_1)R(t)P(t) - (\alpha + \delta(u(t_b - t_a)))R_i(t) \quad (4.2)$$

$$\dot{P}(t) = \alpha r R_i(t) - \mu_p P(t) - \beta_a(1 - \epsilon_1)R(t)P(t), \quad (4.3)$$

where the parameter α in [10] is replaced by $\alpha + \delta(u(t_b - t_a))$ where δ is the constant transplacental transmission rate, $u(t_b - t_a)$ is the unit step function and $t_a \leq t \leq t_b$ is the assumed period of transfer of malaria infection from mother to foetus. The terms in equations (4.1)-(4.3) have the same meaning as in Anderson et al [10] except for the term $\delta(u(t_b - t_a))R_i$ which represents the infected red blood cells from the primary host that avoid immune detection in the umbilical cord and enter the blood stream of

the foetus. For the asexual stage in the foetus, we incorporate intracellular discrete time delay between the infection of the mother and the initiation of the infection in the foetus. The asexual stages within the foetus are described by the following system of delay differential equations:

$$\dot{R}_f(t) = \Pi_f - \mu_f R_f(t) - \beta_f(\delta)(1 - \epsilon_2)R_f(t)P_f(t - \tau) \quad (4.4)$$

$$\dot{R}_{if}(t) = \beta_f(\delta)(1 - \epsilon_2)R_f(t)P_f(t - \tau) - \alpha_f R_{if}(t) \quad (4.5)$$

$$\dot{P}_f(t) = \alpha_f r R_{if}(t) + \delta(u(t_b - t_a))r R_i(t) - \mu_{pf} P_f(t - \tau) - \beta_f(\delta)(1 - \epsilon_2)R_f(t)P_f(t - \tau) \quad (4.6)$$

under the initial conditions

$$R(0) = R_0, \quad R_i(0) = R_{i0}, \quad P(0) = P_0, \quad R_f(0) = R_{f0}$$

$$R_{if}(\theta) = R_{0if}, \quad P_f(\theta) = P_{0f}, \quad \theta \in [-\tau, 0].$$

The parameters in equations (4.4)-(4.6) have the following meaning: ϵ_i , $i = 1, 2$ denote drug efficacy in the mother (ϵ_1) and foetus (ϵ_2), Π_f represents constant replenishment rate in the foetus, μ_f is constant normal decay rate for healthy red blood cells in the foetus, and $\beta_f(\delta)$ is the infection coefficient in the foetus, which depends on the transmission rate δ of infected red blood cells from mother to foetus, and $\tau > 0$ represents the length of the delay. We shall illustrate the problem of congenital malaria infection with a very simple function $\beta(\delta)_f$ given by:

$$\beta_f(\delta) = \begin{cases} 0, & \text{if } \delta = 0 \\ k\delta, & \text{if } \delta \neq 0. \end{cases} \quad (4.7)$$

Normally, transmission of the infection from mother to the foetus is a random event and should be represented by more realistic functions of the jump type. But our main

interest is to demonstrate how this type of infection occurs and to make recommendations on the levels of drug efficacy and drug permeability factor in the primary host that would stop the infection transferring to the foetus.

The assumed infection dynamics within the foetus ((4.4)-(4.6)) are similar to those in the host, except that there is intracellular time delay in the parasite dynamics.

4.3 Mathematical analysis for the model

4.3.1 Model without time delay, $\tau = 0$

We consider a scenario where an expectant mother infected with malaria is treated with a malaria drug of efficacy ϵ_1 , which passively diffuses to the foetus at a constant efficacy $\epsilon_2 = \eta\epsilon_1$, where $0 < \eta < 1$ is the transplacental drug permeability factor. The assumption $\epsilon_2 < \epsilon_1$ is supported by a study [75] which has shown that for either bolus administration of drug or continuous administration of drug peak maternal concentrations of drug are higher than foetal peak concentrations except during the drug elimination phase. In this study, we have assume that the chemo-dynamic effects of the drug is constant in both the mother and the foetus. The model (4.8)-(4.13) investigates possible efficacy levels of malarial drugs that must be administered to the mother to ensure a parasite free state in the foetus.

First, we make an assumption that the malaria infection in the foetus begins at the same time as the infection in the mother, that is, $\tau = 0$. The model (4.1)-(4.6)

becomes:

$$R = \Pi_a - \mu_r R - \hat{\beta}_a RP, \quad (4.8)$$

$$\dot{R}_i = \hat{\beta}_a RP - (\alpha + \hat{\delta})R_i, \quad (4.9)$$

$$\dot{P} = \alpha r R_i - \mu_p P - \hat{\beta}_a RP, \quad (4.10)$$

$$\dot{R}_f = \Pi_f - \mu_f R_f - \hat{\beta}_f(\delta)R_f P_f, \quad (4.11)$$

$$\dot{R}_{if} = \hat{\beta}_f(\delta)R_f P_f - \alpha_f R_{if}, \quad (4.12)$$

$$\dot{P}_f = \alpha_f r R_{if} + \hat{\delta} r R_i - \mu_{pf} P_f - \hat{\beta}_f(\delta)R_f P_f, \quad (4.13)$$

where $\hat{\beta}_a = (1 - \epsilon_1)\beta_a$, $\hat{\beta}_f = (1 - \epsilon_2)\beta_f$ and $\hat{\delta} = \delta u(t_b - t_a)$.

Positivity of solutions

We denote by R_+^6 the set of points $x_t = (x_1, \dots, x_6)$ with positive coordinates and consider the system (4.8)-(4.13) with initial values $x^0 = (x_1^0, \dots, x_6^0)$.

Using lemma (3.1.1) in Chapter 3, and for the state variables in our model, we take

$$R(0) \geq 0, R_i(0) \geq 0, P(0) \geq 0$$

$$R_f(0) \geq 0, R_{if}(\theta) \geq 0, P_f(\theta) \geq 0, \theta \in [-\tau, 0].$$

From Lemma (3.1.1) we conclude that

$$R(t) \geq 0, R_i(t) \geq 0, P(t) \geq 0$$

$$R_f(t) \geq 0, R_{if}(t) \geq 0, P_f(t) \geq 0.$$

Thus, the region defined by $\Omega = \{(R, R_i, P, R_f, R_{if}, P_f) \in \mathfrak{R}_+^6\}$ is immunologically and mathematically well posed and we can use it to study congenital malaria infection.

The model reproduction number

The reproduction number is obtained by the Watmough and Van Driesche [52] technique. We obtain two reproduction numbers one for the infection in the mother (primary infection) and the other for the infection in the foetus (secondary infection) given by

$$\begin{aligned}
R_{0a} &= \frac{r\alpha\Pi_a\beta_a}{(\alpha + \delta u(t_b - t_a))(\Pi_a\beta_a + \mu_p\mu_r)}, & R_{0f} &= \frac{r\Pi_f\beta_f(\delta)}{\Pi_f\beta_f(\delta) + \mu_f\mu_{pf}}, \\
R_{0at} &= \frac{r\alpha\Pi_a\beta_a(1 - \epsilon_1)}{(\alpha + \delta u(t_b - t_a))(\Pi_a\beta_a(1 - \epsilon_1) + \mu_p\mu_r)} \\
&= \frac{r\alpha\Pi_a\beta_a}{(\alpha + \delta u(t_b - t_a))(\Pi_a\beta_a + \mu_p\mu_r)} (1 - \epsilon_1) \left(1 - \frac{\Pi_a\beta_a\epsilon_1}{\Pi_a\beta_a + \mu_p\mu_r}\right)^{-1} \\
&= R_{0a} \left(1 - \left(1 - \frac{\Pi_a\beta_a}{\Pi_a\beta_a + \mu_p\mu_r}\right)\epsilon_1 + O(\epsilon_1^2)\right) \\
&< R_{0a}, \\
R_{0ft} &= \frac{r\Pi_f\beta_f(\delta)(1 - \epsilon_2)}{(\Pi_f\beta_f(\delta)(1 - \epsilon_2) + \mu_f\mu_{pf})} \\
&\leq R_{0f} \left(1 - \left(1 - \frac{\Pi_f\beta_f(\delta)}{\Pi_f\beta_f(\delta) + \mu_f\mu_{pf}}\right)\epsilon_2 + O(\epsilon_2^2)\right) \\
&< R_{0f},
\end{aligned}$$

where R_{0a} and R_{0f} are the pre-treatment reproduction numbers in the mother and foetus, respectively. R_{0at} and R_{0ft} are the reproduction numbers when treatment is administered.

4.4 Steady states

The model (4.8)-(4.13) has two steady states, the infection-free, x_0 , and an infected steady state, x , given by

$$x_0 = \left(\frac{\Pi_a}{\mu_r}, 0, 0, \frac{\Pi_f}{\mu_f}, 0, 0 \right) \quad (4.14)$$

and

$$x = (R^{**}, R_i^{**}, P^{**}, R_f^{**}, R_{if}^{**}, P_f^{**}), \quad (4.15)$$

where

$$\begin{aligned} R^{**} &= \frac{\mu_p(\alpha + \hat{\delta})}{\hat{\beta}_a(\alpha(r-1) - \hat{\delta})}, & R_i^{**} &= \frac{\alpha r \hat{\beta}_a \Pi_a (R_{0at} - 1)}{(\alpha + \hat{\delta})(\alpha(r-1) - \delta\hat{\delta})R_{0at}} \\ P^{**} &= \frac{\alpha r \hat{\beta}_a \Pi_a (R_{0at} - 1)}{(\alpha + \hat{\delta})\mu_p R_{0at}}, & R_f^{**} &= \frac{\Pi_f - \alpha_f R_{if}^{**}}{\mu_f}, & P_f^{**} &= \frac{\alpha_f R_{if}^{**}}{\hat{\beta}_f R_f^{**}}. \end{aligned}$$

R_{if}^{**} is the positive root of the quadratic equation

$$AR_{if}^{**2} + BR_{if}^{**} + C = 0 \quad (4.16)$$

where

$$\begin{aligned} A &= \hat{\beta}_f \alpha_f^2 (r-1) > 0, \\ B &= \alpha_f (\mu_{pf} \mu_f + \Pi_f \hat{\beta}_f) (1 - R_{0ft}) + \alpha_f \hat{\delta} r \hat{\beta}_f R_i^{**} \\ C &= -\frac{\hat{\delta} \alpha r^2 \hat{\beta}_f \Pi_f \hat{\beta}_a \Pi_a (R_{0at} - 1)}{(\alpha + \hat{\delta})(\alpha(r-1) - \hat{\delta})R_{0at}} < 0. \end{aligned}$$

We shall show below that the steady state (4.15) can either be one where the host is actively infected but the foetus is latently infected or one where both host and foetus

are actively infected or one where the infection clears in the mother but remains in the foetus. We describe these infections in the foetus in the following cases:

Case 1:

$$(R_f^{**}, R_{if}^{**}, P_f^{**}) = \left(\frac{\Pi_f - \alpha_f R_{if}}{\mu_f}, \frac{-B + \sqrt{B^2 - 4AC}}{2A}, \frac{\alpha_f R_{if}}{\hat{\beta}_f R_f} \right). \quad (4.17)$$

when $R_{0at} > 1$ and $R_{0ft} < 1$.

In this case, the infection remains latent in the foetus. Eventually, this infection will clear as the mechanism that maintained it ended at birth.

Case 2: Malaria infections in newly born babies have been reported [33]. The cause of these infections has been a subject of contention [26]. Some studies have reported these as new infections. This study is presenting a model that assumes that such infections result from congenital infections. To illustrate this, we consider the case when the number of infected red blood cells breaching the placental barrier successfully replicate and initiate the erythrocytic cycle in the foetus. We obtain the following infected steady state for the foetus:

$$(R_f^{**}, R_{if}^{**}, P_f^{**}) = \left(\frac{\Pi_f - \alpha_f R_{if}}{\mu_f}, \frac{-B + \sqrt{B^2 - 4AC}}{2A}, \frac{\alpha_f R_{if}}{\hat{\beta}_f R_f} \right). \quad (4.18)$$

when $R_{0at} > 1$ and $R_{0ft} > 1$.

Note that treatment with a perfect drug reduces both foetal infected steady states (4.17) and (4.18) to a parasite-free state.

Case 3:

$$(R_f^{**}, R_{if}^{**}, P_f^{**}) = \left(\frac{\Pi_f - \alpha_f R_{if}}{\mu_f}, \frac{-B \pm \sqrt{B^2 - 4AC}}{2A}, \frac{\alpha_f R_{if}}{\hat{\beta}_f R_f} \right). \quad (4.19)$$

when $R_{0at} < 1$ and $R_{0ft} > 1$.

In this case the infection clears in the mother but remains active in the foetus [24].

Note that A, B and C used in cases 1, 2 and 3 are the coefficients of (4.16).

4.4.1 Parasite-free steady state

We begin by proving the stability of the parasite-free steady state:

Theorem 4.4.1 *The parasite-free equilibrium state is locally stable if $R_{0ft} < 1$ and $R_{0at} < 1$.*

We have shown in Appendix that all the eigenvalues of (4.8)-(4.13) have negative real parts if $R_{0ft} < 1$ and $R_{0at} < 1$.

Theorem 4.4.2 *The parasite-free steady state (4.14) is globally asymptotically stable if $R_{0at} < 1$. and $R_{0ft} < 1$.*

Proof We define the Lyapunov function V in terms of the infected states only as follows:

$$V = aR_i + \frac{1}{r}P + bR_{if} + \frac{1}{r}P_f,$$

where a and b are constants to be determined. Differentiating gives

$$\dot{V} = a\dot{R}_i + \frac{1}{r}\dot{P} + b\dot{R}_{if} + \frac{1}{r}\dot{P}_f$$

$$\begin{aligned}
&= a\beta_a RP - a(\alpha + \hat{\delta})R_i + \alpha R_i - \frac{\mu_p}{r}P - \frac{1}{r}\hat{\beta}_a RP \\
&+ b\hat{\beta}_f R_f P_f - b\alpha_f R_{if} + \alpha_f R_{if} + \hat{\delta}R_i - \frac{\mu_{pf}}{r}P_f - \frac{1}{r}\beta_f R_f P_f. \quad (4.20)
\end{aligned}$$

Letting linear terms in R_i and R_{if} go to zero gives $a = 1, b = 1$. Hence, we have

$$\begin{aligned}
\dot{V} &= \beta_a RP - \frac{\mu_p}{r}P - \frac{1}{r}\beta_a RP \\
&+ \beta_f R_f P_f - \frac{\mu_{pf}}{r}P_f - \frac{1}{r}\beta_f R_f P_f \\
&= \left[\beta_a R - \left(\frac{\mu_p}{r} + \frac{\beta_a}{r}R \right) \right] P + \left[\beta_f R_f - \left(\frac{\mu_{pf}}{r} + \frac{\beta_f}{r}R_f \right) \right] P_f \\
&\leq \left[\beta_a R^* - \left(\frac{\mu_p}{r} + \frac{\beta_a}{r}R^* \right) \right] P + \left[\beta_f R_f^* - \left(\frac{\mu_{pf}}{r} + \frac{\beta_f}{r}R_f^* \right) \right] P_f \\
&= -\frac{(\mu_p \mu_r + \beta_a \Pi_a)}{r \mu_r} (1 - R_{0at}) P - \frac{\mu_{pf} \mu_f + \beta_f \Pi_f}{r \mu_f} (1 - R_{0ft}) P_f \\
&< 0 \quad \text{if and only if } R_{0at} < 1 \text{ and } R_{0ft} < 1.
\end{aligned}$$

4.4.2 The infested steady states

The system (4.8)-(4.13) possesses three infected steady states. There are three possible scenarios. First, we consider a steady state where the erythrocytic infection in the host is active but latent in the foetus (x_l), secondly, a state where the erythrocytic infections are active in both the mother and the foetus (x_e) and thirdly, a state where the erythrocytic infections are clear in the mother but remain active in the foetus (x_T). From (4.8)-(4.13), x_l and x_e are given by:

For latency in the foetus, we obtain:

$$x_l = \left(R^{**}, R_i^{**}, P^{**}, \frac{\Pi_f - \alpha_f R_{if}}{\mu_f}, \frac{-B + \sqrt{B^2 - 4AC}}{2A}, \frac{\alpha_f R_{if}}{\hat{\beta}_f R_f} \right),$$

when $R_{0at} > 1$ and $R_{0ft} < 1$.

For active infection in both host and foetus, we have:

$$x_e = (R^{**}, R_i^{**}, P^{**}, R_f^{**}, R_{if}^{**}, P_f^{**})$$

where

$$\begin{aligned} R^{**} &= \frac{\mu_p(\alpha + \delta)}{\hat{\beta}_a(\alpha(r-1) - \delta)}, & R_i^{**} &= \frac{\alpha r \hat{\beta}_a \Pi_a (R_{0at} - 1)}{(\alpha + \delta)(\alpha(r-1) - \delta) R_{0at}}, \\ P^{**} &= \frac{\alpha r \hat{\beta}_a \Pi_a (R_{0at} - 1)}{(\alpha + \delta) \mu_p R_{0at}}, & R_f^{**} &= \frac{\Pi_f - \alpha_f R_{if}}{\mu_f}, \\ R_{if}^{**} &= \frac{-B + \sqrt{B^2 - 4AC}}{2A}, & P_f^{**} &= \frac{\alpha_f R_{if}}{\hat{\beta}_f R_f} \end{aligned}$$

with $R_{0at} > 1$ and $R_{0ft} > 1$, and for the erythrocytic infections under control in the mother but active in the foetus we have:

$$x_T = (R^{**}, R_i^{**}, P^{**}, R_f^{**}, R_{if}^{**}, P_f^{**})$$

where

$$\begin{aligned} R^{**} &= \frac{\mu_p(\alpha + \delta)}{\hat{\beta}_a(\alpha(r-1) - \delta)}, & R_i^{**} &= \frac{\alpha r \hat{\beta}_a \Pi_a (R_{0at} - 1)}{(\alpha + \delta)(\alpha(r-1) - \delta) R_{0at}}, \\ P^{**} &= \frac{\alpha r \hat{\beta}_a \Pi_a (R_{0at} - 1)}{(\alpha + \delta) \mu_p R_{0at}}, & R_f^{**} &= \frac{\Pi_f - \alpha_f R_{if}}{\mu_f}, \\ R_{if}^{**} &= \frac{-B \pm \sqrt{B^2 - 4AC}}{2A}, & P_f^{**} &= \frac{\alpha_f R_{if}}{\hat{\beta}_f R_f} \end{aligned}$$

when $R_{0at} < 1$ and $R_{0ft} > 1$.

In general, the Jacobian matrix of the system (4.8)-(4.13) at an infected steady state x

$$\text{is given by: } J_x = \begin{pmatrix} -\mu_r - \hat{\beta}_a P^{**} & 0 & -\hat{\beta}_a R^{**} & 0 & 0 & 0 \\ \hat{\beta}_a P^{**} & -(\alpha + \hat{\delta}) & \hat{\beta}_a R^{**} & 0 & 0 & 0 \\ -\hat{\beta}_a P^{**} & \alpha r & -(\mu_p + \hat{\beta}_a R^{**}) & 0 & 0 & 0 \\ 0 & 0 & 0 & -(\mu_f + \hat{\beta}_f P_f) & 0 & -\hat{\beta}_f(\delta)R_f \\ 0 & 0 & 0 & \hat{\beta}_f P_f & -\alpha_f & \hat{\beta}_f(\delta)R_f \\ 0 & \hat{\delta}r & 0 & 0 & \alpha_f r & -(\mu_{pf} + \hat{\beta}_f R_f) \end{pmatrix}.$$

Solving $|J_x - \lambda I| = 0$ yields two distinct characteristic equations given by:

For the host:

$$\lambda^3 + A_2\lambda^2 + A_1\lambda + A_0 = 0, \quad (4.21)$$

and for the foetus:

$$\lambda^3 + (a_{11} + a_{33})\lambda^2 + (a_{22} + a_{44})\lambda + a_{55} = 0, \quad (4.22)$$

where

$$\begin{aligned}
A_2 &= \alpha + \hat{\delta} + \mu_p + \mu_r + \hat{\beta}_a(R^{**} + P^{**}), \\
&= (\alpha + \delta) + \mu_p + \mu_r + \frac{\alpha r \mu_p}{(\alpha(r-1) - \delta)} + \frac{r \alpha \hat{\beta}_a \prod_a}{(\alpha + \delta) \mu_p R_{0at}^2} (R_{0at} - 1) \\
&> 0 \quad \text{for } R_{0at} > 1.
\end{aligned}$$

$$\begin{aligned}
A_1 &= (\alpha + \delta)(\mu_r + \mu_p) + \mu_r \mu_p + (\mu_r + \delta) \hat{\beta}_a R^{**} + (\alpha + \delta + \mu_p) \hat{\beta}_a P^{**} - \alpha(r-1) \hat{\beta}_a R^{**} \\
&= \mu_r \mu_p \left(\frac{\alpha r}{\alpha(r-1) - \hat{\delta}} \right) + (\alpha + \hat{\delta}) \mu_r + (\mu_p + \alpha + \hat{\delta}) \hat{\beta}_a P^{**} \\
&> 0 \quad \text{for } R_{0at} > 1.
\end{aligned}$$

$$\begin{aligned}
A_0 &= (\alpha + \delta) \mu_r \mu_p + \delta \mu_r \hat{\beta}_a R^{**} + (\alpha + \delta) \mu_p \hat{\beta}_a P^{**} - \alpha(r-1) \mu_r \hat{\beta}_a R^{**} + (\alpha + \delta) \beta_a^2 R^{**} P^{**} \\
&= (\alpha + \delta) \mu_p \left(\frac{\alpha r}{\alpha(r-1) - \delta} \right) P^{**} > 0 \quad \text{for } R_{0at} > 1.
\end{aligned}$$

$$\begin{aligned}
A_1 A_2 &= \left((\alpha + \delta) \mu_p \left(\frac{\alpha r}{\alpha(r-1) - \delta} \right) P^{**} + \text{positive terms} \right) \\
&> (\alpha + \delta) \mu_p \left(\frac{\alpha r}{\alpha(r-1) - \delta} \right) P^{**} = A_0.
\end{aligned}$$

Remark 4.4.1 *The parasite-present steady state is stable in the host for $R_{0at} > 1$.*

Next, we investigate the nature of stability in the foetus under the scenarios (4.17), (4.18) and (4.19) above.

The coefficients in the equation (4.22) for any infected steady state x are given by:

$$a_{11} = \alpha_f + \mu_f + \hat{\beta}_f P_f^{**},$$

$$a_{22} = \alpha_f (\mu_f + \hat{\beta}_f P_f^{**}),$$

$$a_{33} = \mu_{pf} + \hat{\beta}_f R_f^{**},$$

$$\begin{aligned}
a_{44} &= \alpha_f \mu_{p_f} + \mu_{p_f} \mu_f + \mu_{p_f} \hat{\beta}_f P_f^{**} + \hat{\beta}_f^2 R_f^{**} P_f^{**} - \alpha_f (r-1) \beta_f R_f^{**}, \\
a_{55} &= \alpha_f \mu_f \mu_{p_f} - \mu_f \alpha_f (r-1) \hat{\beta}_f R_f^{**} + \alpha_f \mu_{p_f} \hat{\beta}_f P_f^{**} + \alpha_f \hat{\beta}_f^2 R_f^{**} P_f^{**}. \quad (4.23)
\end{aligned}$$

At x_l , the coefficients (4.23) become:

$$\begin{aligned}
a_{55} &= \alpha_f \mu_f \mu_{p_f} + \mu_f (\alpha_f + r \alpha_f) \hat{\beta}_f R_f^{**} > 0 \\
a_{11} + a_{33} &= \alpha_f + \mu_f + \mu_{p_f} + \hat{\beta}_f R_f^{**} > 0 \\
a_{22} + a_{44} &= \alpha_f \mu_f + \alpha_f \mu_{p_f} + \mu_{p_f} + \mu_f (\alpha_f + \mu_f r \alpha_f) \hat{\beta}_f R_f^{**} > 0 \\
(a_{11} + a_{33})(a_{22} + a_{44}) &= \left(\alpha_f \mu_f \mu_{p_f} + \mu_f (\alpha_f + r \alpha_f) \hat{\beta}_f R_f^{**} + \text{Positive terms} \right) \\
&> \left(\alpha_f \mu_f \mu_{p_f} + \mu_f (\alpha_f + r \alpha_f) \hat{\beta}_f R_f^{**} \right) = a_{55}.
\end{aligned}$$

By the Routh-Hurwitz stability criterion, we conclude that the latently infected steady state x_l is stable if $R_{0at} > 1$, that is, whenever the steady state in the host is stable.

Similarly, at x_e , the coefficients (4.23) become:

$$\begin{aligned}
a_{11} + a_{33} &= \alpha_f + \mu_f + \mu_{p_f} + \hat{\beta}_f P_f^{**} + \hat{\beta}_f R_f > 0 \\
a_{22} + a_{44} &= \alpha_f \left(\mu_f + \hat{\beta}_f P_f^{**} \right) + \mu_{p_f} (\alpha_f + \mu_f) + \mu_{p_f} \hat{\beta}_f P_f^{**} \\
&+ (\alpha_f + \mu_f + r \alpha_f) \hat{\beta}_f R_f^{**} > 0 \\
a_{55} &= \alpha_f \mu_f \mu_{p_f} + \mu_f (\alpha_f + r \alpha_f) \hat{\beta}_f R_f^{**} + \alpha_f \mu_{p_f} \hat{\beta}_f P_f^{**} > 0 \\
(a_{11} + a_{33})(a_{22} + a_{44}) &= \left(\alpha_f \mu_f \mu_{p_f} + \mu_f (\alpha_f + r \alpha_f) \hat{\beta}_f R_f^{**} + \alpha_f \mu_{p_f} \hat{\beta}_f P_f^{**} + \text{Positive terms} \right) \\
&= a_{55} + \text{Positive terms} > a_{55}.
\end{aligned}$$

By the Routh-Hurwitz stability criterion, the solutions of (4.22) have negative real parts. Hence, the steady state x_e is stable for $R_{0at} > 1$ and $R_{0ft} > 1$.

Remark 4.4.2 *For a mother infected with the malaria parasite, either the foetus is latently infected or it is actively infected. For a latently infected foetus the disease prognosis is good as the infection clears after the baby is born. An actively infected foetus may progress to clinical malaria shortly after birth.*

Table 4.1: Description of model parameters for system (4.1-4.6)

Parameter	Definition (Note: *est. means estimate.)	Value	Ref.
π_a	Prod. rate of RBCs from bone-marrow of mother (<i>cell/mil.day</i>)	2.5×10^9	[11]
π_f	Prod. rate of RBCs from bone-marrow of the foetus (<i>cell/mil.day</i>)	2.5×10^9	<i>est.</i>
μ_r	Nat. death rate of mother's RBCs (<i>perday</i>)	0.8	[18]
β_a	Rate of infection (<i>ml/cell.day</i>) in mother	$2 \times 10^{-11.3}$	[11]
α	Bursting rate of mother's IRBCs (<i>perday</i>)	0.5	[11]
α_f	Bursting rate of foetus's IRBCs (<i>perday</i>)	0.5	<i>est.</i>
μ_p	Nat. death rate of parasites (<i>perday</i>) in mother	0.022.0	[11]
μ_{pf}	Nat. death rate of parasites (<i>perday</i>) in foetus	0.022	<i>est.</i>
r	Num. of meroz. released per bursting IRBC (<i>perday</i>)	16	[11]
δ	transplacental transmission rate	1	<i>est.</i>
k	constant	$2 \times 10^{-11.3}$	<i>est.</i>

4.4.3 Numerical Simulation: $\tau = 0$

Synchronicity of parasite spread and control, in both the mother and foetus, are numerically analyzed. Figures 4.1, 4.2 and 4.3 shows the RBCs, IRBCs and parasite synchrony, respectively, in the mother and foetus (a case where $\epsilon_1 = \epsilon_2 = 0$) for different initial conditions. RBCs densities in both the mother and foetus are decreasing over time as the parasite load increases, cases that results in fever, and in severe cases , anemia in the mother, and reduced growth or even foetal death in the womb. These figures also demonstrates the asymptotic stability of the pre-treatment parasite-present equilibrium of model (4.8)-(4.13) under various initial conditions. Figure 4.4 demonstrates the benefit on the foetus parasite load by administering antimalarial treatment on the mother. The simulations shows that by administering an antimalarial drug with a drug efficacy level between 0.982 and 0.983, exclusively, can eradicate completely, the malaria parasite in both the mother and foetus at a gestation period that allows the minimum placental permiability of at least $\eta = 0.97$ (see Table 4.2).

Table 4.2: Table showing the values of R_{0at} and R_{0ft} for different drug efficacy levels and for different drug permiability factor (η) for model (4.8)-(4.13)

(ϵ_1)	$\eta = 0.6$	$\eta = 0.8$	$\eta = 0.97$
0	$(R_{0at}, R_{0ft}) = (3.13, 9.39)$	$(3.13, 9.39)$	$(3.13, 9.40)$
0.95	$(R_{0at}, R_{0ft}) = (0.35, 6.07)$	$(0.35, 4.07)$	$(0.35, 1.61)$
0.983	$(R_{0at}, R_{0ft}) = (0.13, 5.89)$	$(0.13, 3.73)$	$(0.13, 0.99)$

Because the thickness of the placental barrier differs at different stages of gestation in

humans, where after 16 weeks of gestation, there is a reduction in the thickness of the barrier because of the partial disappearance of the cytotrophoblast layer which results in higher permeability in the term placenta compared with preterm placenta [78, 79], we give results of R_{0at} and R_{0ft} for drug efficacy levels $\epsilon_1 = 0, 0.95$ and $\epsilon_1 = 0.983$, under different possible placental drug transfer permeability factor η (see Table 4.2).

From table (4.2), we see that giving antimalarial drugs to a pregnant mother with a drug efficacy of about 0.95 at any stage in pregnancy, though it will help in reducing the foetal parasite load, it might not possibly help in eradicating the malaria parasite in the mother, and hence, a foetal re-infection might, as well, occur later.

From Table (4.2), administering a drug with efficacy level $0.982 < \epsilon_1 < 0.983$ will help wipe-out the malaria parasite in both the mother and foetus at a gestation stage of least $\eta = 0.97$.

Note that if the drug concentration transmitted to the foetus is reduced significantly, the foetus could be born with the malaria infection which could manifest itself within the first few weeks after birth. On the other hand, if the drug concentration is too strong it could lead to pregnancy complications and possibly to abortion.

For $\delta \neq 0$, this model assumes that the infected red blood cells are always transmitted to the foetus which is not always true. A stochastic approach would be preferred when the transmission from mother to child is stochastic.

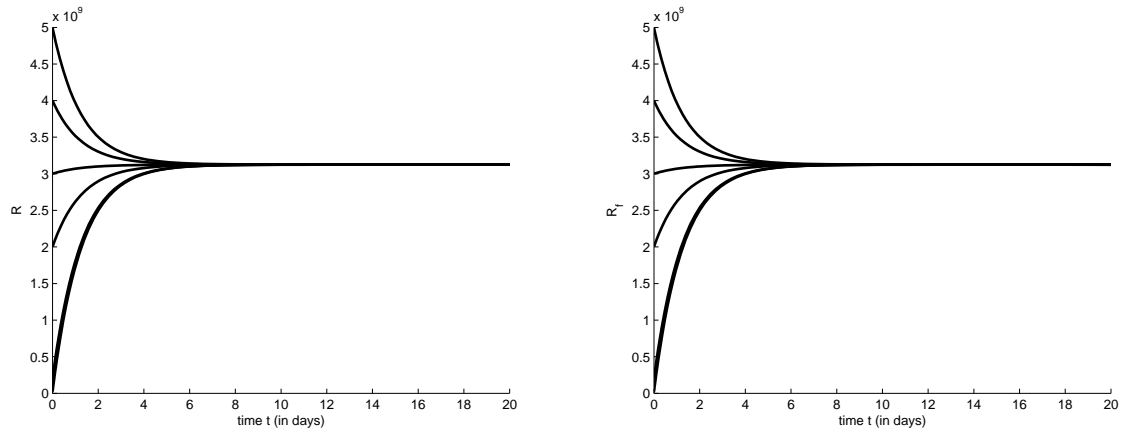


Figure 4.1: Trajectories of model (4.8)-(4.13) showing synchrony of the RBCs dynamics in the mother and foetus, in the absence of intervention under different initial conditions.

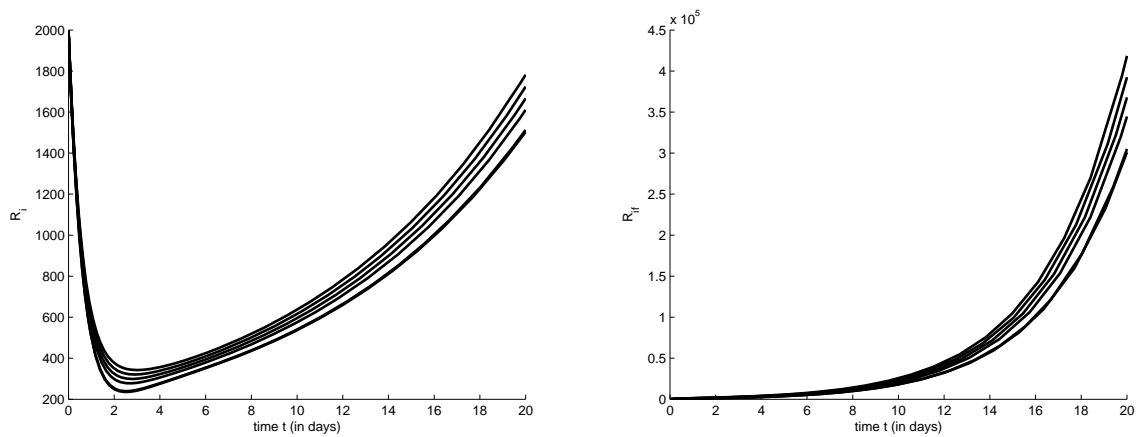


Figure 4.2: Trajectories of model (4.8)-(4.13) showing synchrony of the IRBCs dynamics in the mother and foetus, in the absence of intervention under different initial conditions

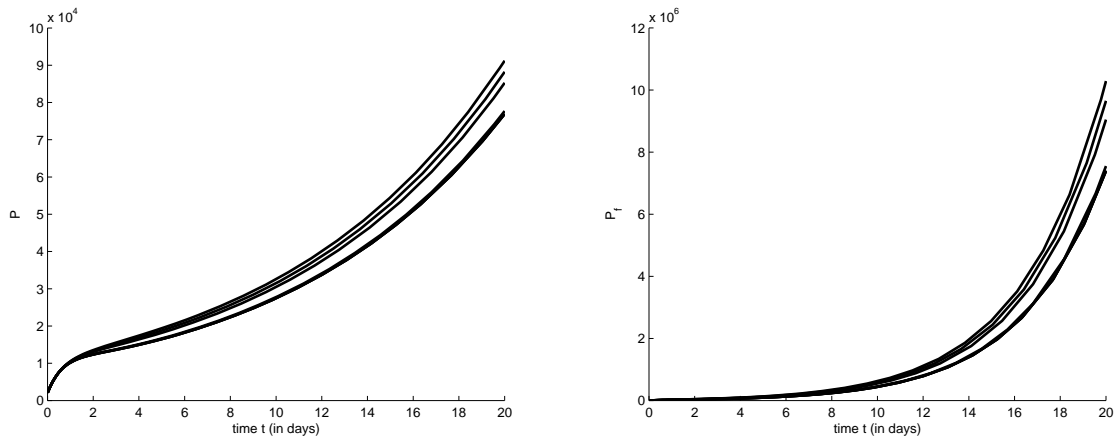


Figure 4.3: Trajectories of model (4.8)-(4.13) showing synchrony of the RBCs dynamics in the mother and foetus, in the absence of intervention under different initial conditions.

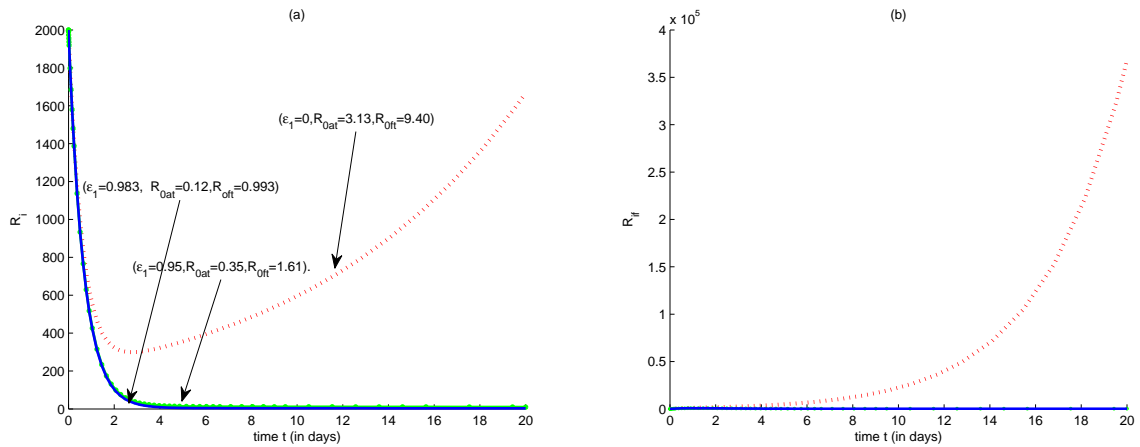


Figure 4.4: Simulations of equations (4.8) and (4.13) showing the IRBCs densities for (a) the mother and (b) foetus for different drug efficacy levels. For parameter values used, see table (4.1), with $\eta = 0.97$.

4.5 Model with time delay, $\tau \neq 0$

To study the stability of the steady states x , we define

$$x_1(t) = R(t) - R^{**}, x_2(t) = R_i(t) - R_i^{**}, x_3(t) = P(t) - P^{**}, x_4(t) = R_f(t) - R_f^{**},$$

$$x_5(t) = R_{if}(t) - R_{if}^{**}, x_6(t) = P_f(t) - P_f^{**}.$$

Then the linearized system of (4.1)-(4.6) at x is given by

$$\frac{dx_1(t)}{dt} = -\mu_r x_1(t) - \hat{\beta}_a P^{**} x_1(t) - \hat{\beta}_a R^{**} x_3(t) \quad (4.24)$$

$$\frac{dx_2(t)}{dt} = \hat{\beta}_a P^{**} x_1(t) + \hat{\beta}_a R^{**} x_3(t) - (\alpha + \delta) x_2(t) \quad (4.25)$$

$$\frac{dx_3(t)}{dt} = \alpha r x_2(t) - \mu_p x_3(t) - \hat{\beta}_a P^{**} x_1(t) - \hat{\beta}_a R^{**} x_3(t) \quad (4.26)$$

$$\frac{dx_4(t)}{dt} = -\mu_f x_4(t) - \hat{\beta}_f(\delta) P_f^{**} x_4(t) - \hat{\beta}_f(\delta) R_f^{**} x_6(t - \tau) \quad (4.27)$$

$$\frac{dx_5(t)}{dt} = \hat{\beta}_f(\delta) P_f^{**} x_4(t) + \hat{\beta}_f(\delta) R_f^{**} x_6(t - \tau) + \delta x_2(t) - \alpha_f x_5(t) \quad (4.28)$$

$$\frac{dx_6(t)}{dt} = \alpha_f r x_5(t) + \delta r x_2(t) - \mu_{pf} x_6(t - \tau) - \hat{\beta}_f P_f^{**} x_4(t) - \hat{\beta}_f(\delta) R_f^{**} x_6(t - \tau) \quad (4.29)$$

We then write system 4.24-4.29 in matrix form as follows:

$$\frac{d}{dt} \begin{pmatrix} x_1(t) \\ x_2(t) \\ x_3(t) \\ x_4(t) \\ x_5(t) \\ x_6(t) \end{pmatrix} = A_1 \begin{pmatrix} x_1(t) \\ x_2(t) \\ x_3(t) \\ x_4(t) \\ x_5(t) \\ x_6(t) \end{pmatrix} + A_2 \begin{pmatrix} x_1(t - \tau) \\ x_2(t - \tau) \\ x_3(t - \tau) \\ x_4(t - \tau) \\ x_5(t - \tau) \\ x_6(t - \tau) \end{pmatrix}$$

where

$$A_1 = \begin{pmatrix} -\mu_r - \beta_a P^{**} & 0 & -\beta_a R^{**} & 0 & 0 & 0 \\ \beta_a P^{**} & -(\alpha + \delta) & \beta_a R^{**} & 0 & 0 & 0 \\ -\beta_a P^{**} & \alpha r & -\mu_p - \beta_a R^{**} & 0 & 0 & 0 \\ 0 & 0 & 0 & -\mu_f - \beta_f(\delta)P_f^{**} & 0 & 0 \\ 0 & \delta & 0 & \beta_f(\delta)P_f^{**} & -\alpha_f & 0 \\ 0 & \delta r & 0 & -\beta_f(\delta)P_f^{**} & \alpha_f r & 0 \end{pmatrix}$$

and

$$A_2 = \begin{pmatrix} 0 & 0 & 0 & 0 & 0 & 0 \\ 0 & 0 & 0 & 0 & 0 & 0 \\ 0 & 0 & 0 & 0 & 0 & 0 \\ 0 & 0 & 0 & 0 & 0 & -\beta_f(\delta)R_f^{**} \\ 0 & 0 & 0 & 0 & 0 & \beta_f(\delta)R_f^{**} \\ 0 & 0 & 0 & 0 & 0 & -\mu_{pf} - \beta_f(\delta)R_f^{**} \end{pmatrix}.$$

The characteristic equation of system (4.24)-(4.29) is given by

$$|\lambda I - A_1 - A_2 e^{-\lambda\tau}| = 0,$$

that is, two characteristic equations of order three

$$\lambda^3 + a_2 \lambda^2 + a_1 \lambda + a_0 = 0, \quad (4.30)$$

and

$$f(\lambda) + g(\lambda)e^{-\lambda\tau} = 0, \quad (4.31)$$

with

$$a_2 = \alpha + \delta + \mu_p + \hat{\beta}_a R^{**} + \mu_r + \hat{\beta}_a P^{**} > 0$$

$$\begin{aligned}
a_1 &= (\alpha + \delta)\mu_r + (\alpha + \delta)\hat{\beta}_a P^{**} + \mu_r\mu_p + \mu_r\hat{\beta}_a R^{**} + \mu_p\hat{\beta}_a P^{**} \\
&- \hat{\beta}_a R^{**}(\alpha_f r - (\alpha + \delta)) + (\alpha + \delta)\mu_p, \quad a_0 = (\mu_r + \hat{\beta}_a P^{**})[\mu_p(\alpha + \delta) - \hat{\beta}_a R^{**}(\alpha_f r - (\alpha + \delta))] + \\
&\hat{\beta}_a P^{**}\hat{\beta}_a R^{**}(\alpha r - (\alpha + \delta)), \text{ and :}
\end{aligned}$$

$$f(\lambda) = \lambda^3 + a_{11}\lambda^2 + a_{22}\lambda, \quad (4.32)$$

$$g(\lambda) = a_{33}\lambda^2 + a_{44}\lambda + a_{55}, \quad (4.33)$$

where

$$a_{11} = (\mu_f + \hat{\beta}_f P_f^{**} + \alpha_f), \quad a_{22} = \alpha_f(\mu_f + \hat{\beta}_f P_f^{**}), \quad a_{33} = (\mu_{pf} + \hat{\beta}_f R_f^{**}),$$

$$a_{44} = [\mu_f\mu_{pf} + \mu_f\hat{\beta}_f R_f^{**} + \mu_{pf}\hat{\beta}_f P_f^{**} + \alpha_f\mu_{pf} - \alpha_f(r-1)\hat{\beta}_f R_f^{**}],$$

$$a_{55} = \alpha_f\mu_{pf}(\mu_f + \hat{\beta}_f R_f^{**}) - \mu_f\alpha_f(r-1)\hat{\beta}_f R_f^{**} + \alpha_f\hat{\beta}_f^2 R_f^{**} P_f^{**}.$$

Let $\lambda = i\omega$ and substitute it into (4.31). On separating the real and imaginary parts gives:

$$\omega^3 + a_{22}\omega = (a_{55} - a_{33}\omega^2) \sin(\omega\tau) - a_{44}\omega \cos(\omega\tau), \quad (4.34)$$

$$a_{11}\omega^2 = (a_{55} - a_{33}\omega^2) \cos(\omega\tau) + a_{44}\omega \sin(\omega\tau). \quad (4.35)$$

Squaring on both sides of 4.34 and 4.35 and adding yield

$$\omega^6 + (a_{11}^2 - 2a_{22} - a_{33}^2)\omega^4 + (a_{22}^2 - a_{44}^2 + 2a_{33}a_{55})\omega^2 - a_{55}^2 = 0. \quad (4.36)$$

Letting $x = \omega^2$, $\alpha = a_{11}^2 - 2a_{22} - a_{33}^2$, $\beta = a_{22}^2 - a_{44}^2 + 2a_{33}a_{55}$, $\gamma = a_{55}^2$,

equation (4.36) reduces to

$$G(x) = x^3 + \alpha x^2 + \beta x - \gamma = 0. \quad (4.37)$$

For the parameter values given in Table 4.1 with $\epsilon_1 = 0$, $\alpha = 292.18$, $\beta = 72.83$ and $\gamma = 0.034$ and since $\gamma > 0$, then $G(0) = -\gamma < 0$ and $\lim_{x \rightarrow \infty} G(x) = \infty$, implying that (4.37) has at least one positive root, say x_0 . Consequently, (4.36) has at least one positive root, denoted by ω_0 and it follows that (4.36) and hence (4.37) has a positive root ω_0 implying that (4.31) has a pair of purely imaginary roots $\pm i\omega_0$.

Let $\lambda(\tau) = \eta(\tau) + i\omega(\tau)$ be the eigenvalue of (4.31) such that $\eta(\tau_0) = 0, \omega(\tau_0) = \omega_0$.

From (4.34) and (4.35),

$$\tau_j = \frac{1}{\omega_0} \arccos \left[\frac{a_{11}\omega_0^2(a_{55} - a_{33}\omega_0^2) - a_{44}\omega_0(a_{22}\omega_0 - \omega_0^3)}{(a_{55} - a_{33}\omega_0^2)^2 + a_{44}^2\omega_0^2} \right] + \frac{2\pi j}{\omega_0}, j = 0, 1, 2, \dots$$

and $\tau_0 = \min \{\tau_j, j = 0, 1, 2, \dots\}$.

Theorem 4.5.1 $G'(\omega_0^2)$ and $Re[\frac{d\lambda}{d\tau}]_{\tau=\tau_0}^{-1}$ have the same sign.

Proof Calculating the derivative of (4.31) with (4.32) and (4.33) with respect to τ ,

we get

$$\frac{d\lambda}{d\tau} (f'(\lambda) + g'(\lambda)e^{-\lambda\tau} - g(\lambda)e^{-\lambda\tau}\tau) = g(\lambda)e^{-\lambda\tau}\lambda.$$

$$\begin{aligned} \left[\frac{d\lambda}{d\tau} \right]_{\tau=\tau_0}^{-1} &= \frac{f'(\lambda) + g'(\lambda)e^{-\lambda\tau}}{\lambda g(\lambda)e^{-\lambda\tau}} - \frac{\tau}{\lambda} \\ &= \frac{f'(i\omega_0) + g'(i\omega_0)e^{-i\omega_0\tau}}{i\omega_0 g(i\omega_0)e^{-i\omega_0\tau}} - \frac{\tau}{i\omega_0}. \end{aligned}$$

Therefore,

$$Re\left[\frac{d\lambda}{d\tau}\right]_{\tau=\tau_0}^{-1} = Re\left[\frac{f'(i\omega_0) + g'(i\omega_0)e^{-i\omega_0\tau}}{i\omega_0 g(i\omega_0)e^{-i\omega_0\tau}}\right]$$

Using 4.31,

$$\begin{aligned}
Re\left[\frac{d\lambda}{d\tau}\right]_{\tau=\tau_0}^{-1} &= Re\left[\frac{f'(i\omega_0)}{i\omega_0(-f(i\omega_0))} + \frac{g'(i\omega_0)}{i\omega_0g(i\omega_0)}\right] \\
&= Re\left[\frac{1}{i\omega_0} \left\{ \frac{f'(i\omega_0)}{i\omega_0(-f(i\omega_0))} + \frac{g'(i\omega_0)}{i\omega_0g(i\omega_0)} \right\}\right] \\
&= Re\left[\frac{1}{i\omega_0} \left\{ \frac{-f'(i\omega_0)\bar{f}(i\omega_0)}{f(i\omega_0)\bar{f}(i\omega_0)} + \frac{g'(i\omega_0)\bar{g}(i\omega_0)}{g(i\omega_0)\bar{g}(i\omega_0)} \right\}\right] \\
&= Re\left[\frac{1}{i\omega_0} \left\{ \frac{-f'(i\omega_0)\bar{f}(i\omega_0) + g'(i\omega_0)\bar{g}(i\omega_0)}{|f(i\omega_0)|^2} \right\}\right].
\end{aligned}$$

The

$$sign(Re\left[\frac{d\lambda}{d\tau}\right]_{\tau=\tau_0}^{-1}) = sign(Im(-f'(i\omega_0)\bar{f}(i\omega_0) + g'(i\omega_0)\bar{g}(i\omega_0))).$$

With some calculations,

$$\begin{aligned}
&Im(-f'(i\omega_0)\bar{f}(i\omega_0) + g'(i\omega_0)\bar{g}(i\omega_0)) \\
&= 3\omega_0^5 + 2(a_{11}^2 - 2a_{22} - a_{33}^2)\omega_0^3 + (a_{22}^2 - a_{44}^2 + 2a_{33}a_{55})\omega_0.
\end{aligned}$$

Therefore,

$$\frac{d}{d\tau}Re(\lambda(i\omega_0)) = \frac{d}{d\tau}\eta(\tau)|_{\tau=\tau_0} > 0.$$

By continuity, the real part of $\lambda(\tau)$ becomes positive when $\tau > \tau_0$ and the steady state x becomes unstable. Moreover, a Hopf bifurcation occurs when τ passes through the critical value τ_0 [80].

This analysis can be summarized in a theorem as follows.

Theorem 4.5.2 *Since*

$$A_2 > 0, A_1 > 0, A_0 > 0, A_1A_2 > A_0,$$

$$a_{11} + a_{33} > 0, a_{22} + a_{44} > 0, a_{55} > 0, (a_{11} + a_{33})(a_{22} + a_{44}) > a_{55}$$

for the characteristic equations (4.21)-(4.22) then the parasite-infested state x_e of the delay model (4.1)-(4.6), is locally asymptotically stable when $\tau < \tau_0$ and unstable when $\tau > \tau_0$, where

$$\tau_0 = \frac{1}{\omega_0} \arccos \left[\frac{a_{11}\omega_0^2(a_{55} - a_{33}\omega_0^2) - a_{44}\omega_0(a_{22}\omega_0 - \omega_0^3)}{(a_{55} - a_{33}\omega_0^2)^2 + a_{44}^2\omega_0^2} \right].$$

When $\tau = \tau_0$, we expect a Hopf bifurcation to occur, that is, we expect a family of periodic solutions to bifurcate from x_e as τ passes through the critical value τ_0 . However, for the parameter values given in table with drug efficacy $\epsilon_1 = 0.983$, model (4.1)-(4.6) does not seem to exhibit such bifurcations.

4.5.1 Numerical Results: $\tau \neq 0$

We conduct numerical simulations to show the effect of intracellular delay on the qualitative behaviour of the pre-treatment foetal RBCs (see Figure 4.5), and the foetal RBCs in the presence of treatment (see Figure 4.6)

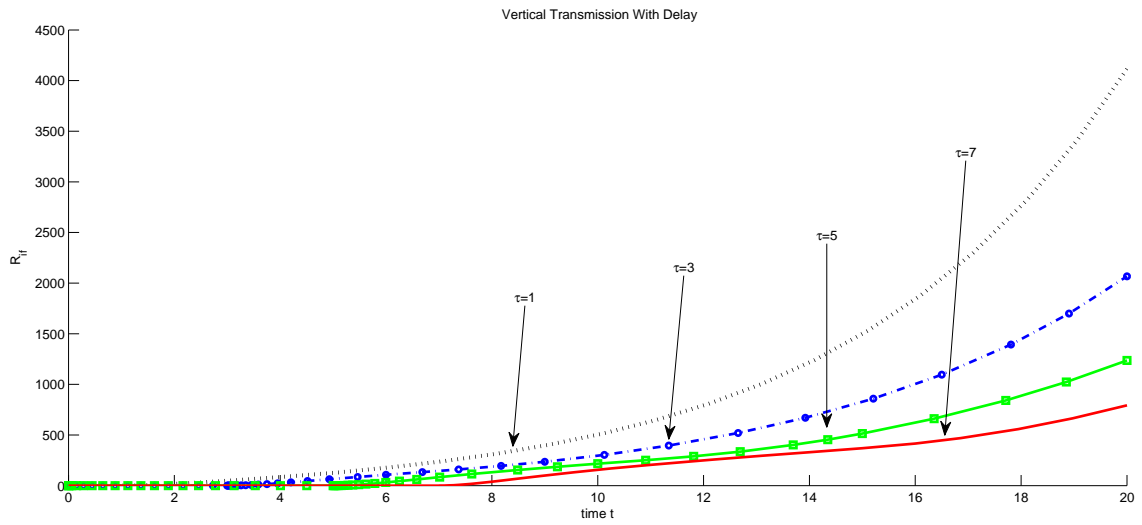


Figure 4.5: Trajectories of model (4.1)-(4.6) showing the effects of time delay on the foetal IRBCs in the presence of treatment ($\epsilon_1 = 0.983$).

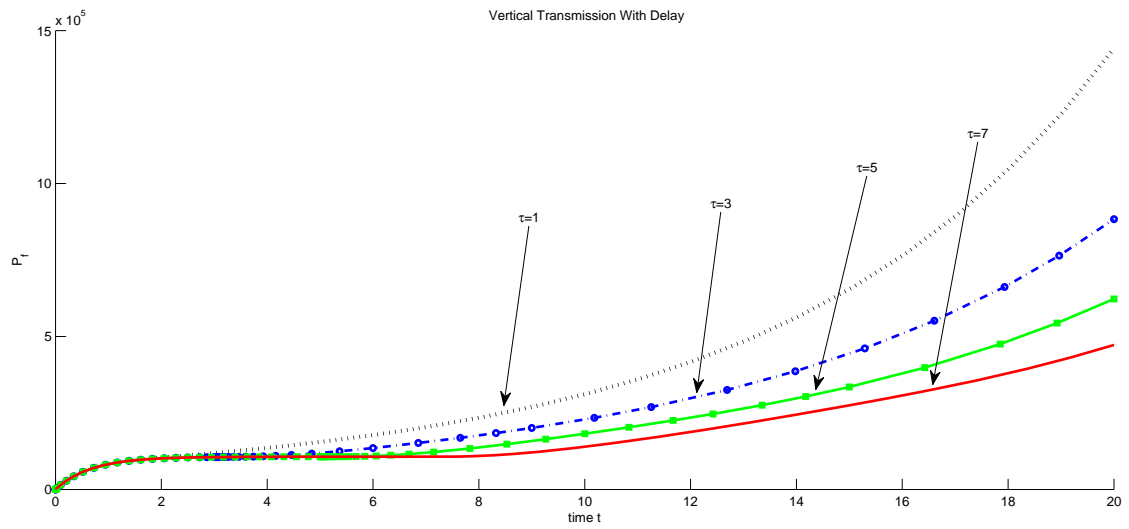


Figure 4.6: Trajectories of model (4.1)-(4.6) showing the effects of time delay on the foetal parasite population in the presence of treatment ($\epsilon_1 = 0.983$).

Chapter 5

A stochastic model for in-host malaria parasite infection of red blood cells

5.1 Introduction

Malaria is a disease caused when plasmodium parasites, injected into the human host by an anopheles mosquito during a blood meal, start a vicious cycle of destroying the host's red blood cells. About 40% of the world population lives in malaria endemic areas. Malaria has become one of the major killers of people living with AIDS.

Of the four known species of plasmodium that can infect and be transmitted by humans, plasmodium falciparum and plasmodium vivax are responsible for the majority of infections and deaths in sub-Saharan Africa [71], while plasmodium ovale and plas-

modium malariae are known generally to cause a milder form of malaria that is rarely fatal. These four species of plasmodium exhibit different patterns of disease development. For example, *P.vivax* and *P.ovale* infections are characterized by a cyclical occurrence of fever every two days while *P.malariae* and *P.falciparum* fevers may occur every three days for *P.malariae* and 36-48 hours, or a less pronounced and almost continuous fever, for *P.falciparum* [61].

The four plasmodium species are also known to possess different recovery characteristics [21]. *P.vivax* infections, for example, are characterized by relapses of malaria arising from persistent liver stages of the parasite [21]. Even this species may exhibit different characteristics depending on geographical location. A review by White [21] quantifies the relapse period for tropical *P.vivax* to be three-week intervals if the infection is treated using fast acting anti-malaria drugs, whereas in temperate regions and parts of the sub-tropics, *P.vivax* infections exhibit longer latency periods between illness and relapse. Relapse may also occur in *P.ovale* [21] but it rarely occurs in *P.malariae* and *P.falciparum* infections [8]. In sub-Saharan Africa most infected individuals are co-infected with *P.vivax* and *P.falciparum* [21]. Because *P.vivax* has the tendency to relapse after the primary infection, it has become difficult to determine whether a patient has a new *P.falciparum* infection or a relapse of a previous *P.vivax* infection. This makes it harder to decide whether to treat the patient with the same regimen if it is a new infection or a new regimen if the infection is a relapse. For this reason, it is important to understand infection characteristics of the plasmodium malaria parasites. Because the malaria parasite has two of its life stages

within the human host, the liver and the red blood stages, understanding the parasite characteristics within each stage can provide insights into treatment strategies and, in particular, to decide whether one drug for both stages should be continued as a treatment strategy.

Several studies [8, 23, 67], describing human malaria pathogenesis, have demonstrated various aspects of parasite infection characteristics. In some of these and other studies [3, 8], malaria is characterized by shortened life expectancy of the red blood cells from 120 days when they are removed naturally by phagocytosis to about 2 days when they are infected with plasmodium parasites. A study by McQueen and McKenzie [8] has concluded that some plasmodium species that infect humans are restricted to infecting particular age classes of red blood cells and that this strategy has a profound effect on the course of the infection.

We reproduce the basic model of in-host malaria proposed by Anderson *et al* presented in Chapter 3

$$\begin{aligned}
 \dot{R} &= \Lambda - \mu_r R - \beta R P_e, \\
 \dot{R}_i &= \beta R P_e - \mu_i R_i, \\
 \dot{P}_e &= r \mu_i R_i - \mu_{pe} P_e - \beta R P_e,
 \end{aligned}
 \tag{5.1}$$

where R represents susceptible red blood cells, R_i represents infected red blood cells (IRBC), and P_e are extracellular parasites, with model parameters defined as follows:

- Λ : Constant source of red blood cells (*cell/ml.day*)
- μ_r : Natural death rate of red blood cells (*day⁻¹*)
- β : Infection rate (*ml/cell.day*)
- μ_i : Death rate of infected red blood cells (*day⁻¹*)
- r : Number of parasites released (*8 – 32percell*)
- μ_{pe} : Natural death rate of extracellular parasites (*day⁻¹*).

This model was the starting point of various studies [3, 8, 11, 23, 67] in their investigation of various parasite characteristics. These studies have shown that the disease always posses a parasite-free equilibrium, E_0 , which is stable if $R_0 < 1$. If $R_0 > 1$, then E_0 becomes unstable and progresses into an endemic equilibrium or parasite-present state, E_1 , whose stability conditions have been derived in various studies [3, 11, 23].

However, in reality, the immunologic system of any individual is affected by immunological noises which we define as the state of the host prior to infection with the malaria parasite. This 'noise' is particularly present when the individual has been already infected with other diseases, such as schistosomiasis or sickle-cell. Globally, over one billion humans are at risk of contracting schistosomiasis (Bilharzia), a disease caused by parasitic worms. Approximately 80% of the 200 million individuals infected with schistosomiasis live in sub-Sahara Africa. Schistosome worms reside in

the mesenteric veins where they feed on red blood cells. If not treated, this condition can cause anemia, decreased resistance to other diseases and liver damage resulting in liver malfunction [69]. In sub-Saharan Africa, the annual mortality from this infection is estimated to be 280,000. Sickle-cell is another common disease throughout much of sub-Saharan Africa. Sickle-cells are deformed red blood cells with decreased flexibility, a condition which causes them to break down as they pass through capillaries and veins. This disease affects up to 3% of newly born and affects approximately 275,000 individuals in sub-Saharan Africa each year. The disease causes anaemia and if left untreated can be fatal. Clinically, a significant number of individuals in sub-Saharan Africa are co-infected with malaria, schistosomiasis and sickle-cell [21]. In such individuals, malaria is more severe as anaemia sets in faster. Moreover, decreased resistance to other diseases in such patients complicates the treatment of malaria [69].

Hence, although the deterministic approach (model (5.1)), describes the basic transmission behavior of infectious in-host malaria disease, it cannot accurately represent the various species of Plasmodium because such models do not incorporate the effects of a fluctuating environment within the host. The parameters, Λ , β , μ_r , μ_i , μ_{pe} , exhibit continuous oscillations around some average value (the deterministic value) but do not attain fixed values. For this reason, some authors [58, 64, 65] have studied epidemic dynamics with parameter perturbations. In this Chapter, we use a stochastic approach to study the dynamics of in-host malaria when the model parameters are oscillating due to a changing environment within the host. We show that this approach better describes various plasmodium infection characteristics than the de-

terministic approach.

The structure of this chapter is as follows:

In section 5.2 we consider a stochastic extension of the malaria model (5.1) with linear diffusion matrix (see (5.3) with (5.4)-(5.5)) and in Section 5.4 we consider the same model but with constant diffusion matrix. Existence and uniqueness are proved in Section 5.3, but our main interest is to study the dynamic behavior of the solution near stable points of the deterministic system (5.1).

In Section 5.4 we consider a general stochastic system with constant diffusion matrix and an asymptotically stable state y^s of the corresponding deterministic system. We then estimate the degree to which the stability of y^s is "degraded" by the constant diffusion matrix of the stochastic system. This result applies directly to the malaria model of Section 5.4.

The situation is quite different for the malaria model of Section 5.2 with linear diffusion matrix. After making a change of variables which transforms the system into a stochastic system with constant diffusion matrix, we find that the only steady state is the parasite-present state, which turns out to be unstable. Thus, a linear diffusion matrix introduces a much higher instability into the original deterministic system than a constant diffusion matrix. This phenomena probably applies to many other disease models.

In the last section we explain how our two stochastic models exhibit a wide range of infectivity characteristics extracted from patient data. We then summarize the novel

approach of this chapter in the context of personalized medicine.

5.2 Malaria in-host stochastic model

We first revise model (5.1) by replacing μ_i in the model (5.1) by $\mu_i + \gamma$ where γ represents the rate at which parasites are released from rupturing infected red blood cells and μ_i represents the rate at which latently infected red blood cells die naturally.

Next, we introduce randomness in the revised model by replacing the parameters μ_r, μ_i , and μ_{pe} by $\mu_r \rightarrow \mu_1 + \sigma_1 \dot{B}_1$, $\mu_i \rightarrow \mu_2 + \sigma_2 \dot{B}_2$, and $\mu_{pe} \rightarrow \mu_3 + \sigma_3 \dot{B}_3$, where the μ_j 's are positive constants and $B_j = B_{t,j} (j = 1, 2, 3)$ are independent standard Brownian motions with initial position $B_{0,j}(0) = 0$, and variance 1 and the σ_j are non-zero parameters. The stochastic system is given by:

$$\begin{aligned} dR &= (\Lambda - \mu_1 R - \beta R P_e) dt - \sigma_1 R dB_{t,1}, \\ dR_i &= (\beta R P_e - (\mu_2 + \gamma) R_i) dt - \sigma_2 R_i dB_{t,2}, \\ dP_e &= (r\gamma R_i - \mu_3 P_e - \beta R P_e) dt - \sigma_3 P_e dB_{t,3}. \end{aligned} \tag{5.2}$$

For simplicity of notation, we set $x_t = (x_1(t), x_2(t), x_3(t)) = (R(t), R_i(t), P_e(t))$, and write the system (5.2) in matrix form

$$dx_t = f(x_t) dt + \sigma(x_t) dB_t, \tag{5.3}$$

where

$$f(x_t) = \begin{pmatrix} \Lambda - \mu_1 x_1 - \beta x_1 x_3 \\ \beta x_1 x_3 - (\mu_2 + \gamma) x_2 \\ r\gamma x_2 - \mu_3 x_3 - \beta x_1 x_3 \end{pmatrix}, \quad (5.4)$$

$$\sigma(x_t) = \begin{pmatrix} \sigma_1 x_1 & 0 & 0 \\ 0 & \sigma_2 x_2 & 0 \\ 0 & 0 & \sigma_3 x_3 \end{pmatrix}, \quad (5.5)$$

and dB_t is the vector column of the $B_{t,j}$.

Remark 5.2.1 Note that by choosing the parameter of the death rate of red blood cells to be $\mu_1 + \sigma_1 \dot{B}_1$, we allow it to take negative values since Brownian motion takes arbitrarily large negative and positive values in any small time interval. However, the probability that this random death rate becomes negative is negligible if σ_1 is small compared to μ_1 . Thus, in the sense of probability, we can accept the death rate $\mu_1 + \sigma_1 \dot{B}_1$ as a small random perturbation about μ_1 . The same remark applies to the death rates of R_i and P_e . However, we shall need to prove that the solutions of the model (5.3) with positive initial components will have positive components for all $t > 0$. Later on, we shall consider the stability of the steady states x^s of the system (5.3). We shall then adopt the same probabilistic point of view, namely, instead of considering individual paths of $x_t - x^s$, we shall evaluate the expectation of $|x_t - x^s|^2$.

Remark 5.2.2 In Section 5.3, we shall prove that the system (5.3) with drift and diffusion matrices given by (5.4) and (5.5), respectively, has a unique solution with positive components for any initial state with positive components. In Section 5.4,

we consider a stochastic system (5.21) with constant diffusion matrix α , and study the behavior of solutions near a stable steady point of (5.20). Both models (5.3) with (5.4)-(5.5) and (5.21) with $h(y)$ being the vector $f(y)$ of the malaria model (5.3) can be used to study various aspects of malaria dynamics as will be explained in sections 5.5, 5.6 and the concluding section.

5.3 Existence of solutions for model (5.3) with (5.4)-(5.5)

We denote by R_+^3 the set of points $x_t = (x_1, x_2, x_3)$ in R^3 with positive coordinates and consider the system (5.3) with initial values

$$x^0 = (x_1^0, x_2^0, x_3^0) \in R_+^3. \quad (5.6)$$

In this Section, we prove the following theorem:

Theorem 5.3.1 The system (5.3) with any initial value (5.6) has a unique solution $x_t \in R_+^3$ for all $t > 0$, and

$$E |x_t|^2 \leq C e^{\alpha t} \quad \text{for } t > 0,$$

where C and α are constants.

For technical reasons, we modify the system (5.3) by replacing in $f(x_t)$ the nonlinear term $\beta x_1 x_3$ by the linearly bounded term $\beta g_\epsilon(x_1)g_\epsilon(x_3)$ where

$$g_\epsilon(s) = \begin{cases} 0 & \text{if } s < 0 \\ s & \text{if } 0 < s < \frac{1}{\epsilon} \\ \frac{1}{\epsilon} & \text{if } s > \frac{1}{\epsilon}, \end{cases} \quad (5.7)$$

where ϵ is an arbitrarily small positive number. We denote the modified $f(x_t)$ by $f^\epsilon(x_t)$ and consider the stochastic system

$$dx_t^\epsilon = f^\epsilon(x_t^\epsilon) dt + \sigma(x_t^\epsilon) dB_t. \quad (5.8)$$

Clearly

$$|f_\epsilon^\epsilon(x) - f_\epsilon^\epsilon(\bar{x})| \leq K_\epsilon |x - \bar{x}|, \quad (5.9)$$

$$|\sigma(x) - \sigma(\bar{x})| \leq K |x - \bar{x}| \quad (5.10)$$

for all $x, \bar{x} \in R^3$, where K_ϵ, K are constants. Hence, by Theorem 1.1 in [[62], Chapter 5], for any initial value $x^0 \in R_+^3$ there exists a unique solution x_t^ϵ of (5.8) with $x_0^\epsilon = x^0$.

We denote by τ_ϵ the exit time of x_t^ϵ from the domain

$$R_+^3 \cap \left\{ \max_{1 \leq i \leq 3} x_i < \frac{1}{\epsilon} \right\},$$

and we may assume that this domain contains the initial point x^0 . We want to prove that the system (5.8) possesses a nonnegative solution for $t > 0$, more precisely:

Lemma 5.3.2 For any $T > 0$ the solution x_t^ϵ remains in R_+^3 for all $t < T \wedge \tau_\epsilon$, that is, the components $x_{t,i}^\epsilon$ of x_t^ϵ satisfy:

$$x_{t,i}^\epsilon > 0 \text{ if } t < T \wedge \tau_\epsilon \text{ for } i = 1, 2, 3;$$

furthermore, the probability that $\tau_\epsilon < T$ is smaller than $C_0 T \epsilon$ where C_0 is a constant independent of ϵ .

Proof We introduce a Lyapunov-type function

$$V(x_1, x_2, x_3) = \sum_{i=1}^3 (x_i - k_i \log x_i) \quad (5.11)$$

where k_i are positive constants, and consider the differential of $V(x_t^\epsilon)$ for $t < T \wedge \tau_\epsilon$.

Since $f^\epsilon(x_t^\epsilon) = f(x_t^\epsilon)$ if $t < T \wedge \tau_\epsilon$, x_t^ϵ satisfies the system (5.3) for $t < T \wedge \tau_\epsilon$. Hence,

$$dV = \sum_{i=1}^3 \left\{ \left(1 - \frac{k_i}{x_i}\right) + \frac{k_i}{2x_i^2} (dx_i)^2 \right\} \quad (5.12)$$

$$\begin{aligned} &= \left(\Lambda - \mu_1 x_1 + \frac{k_1}{2} \sigma_1^2 - \frac{k_1}{2x_1} \Lambda + k_1 \mu_1 + k_1 \beta x_3 - \mu_2 x_2 + \frac{k_2}{2} \sigma_2^2 \right. \\ &\quad - k_2 \frac{x_1 x_3}{x_2} + k_2 (\mu_2 + \gamma) - \mu_3 x_3 - \beta x_1 x_3 \\ &\quad \left. + \frac{k_3}{2} \sigma_3^2 - r \gamma k_3 \frac{x_2}{x_3} + \mu_2 k_3 + \beta k_3 x_1 \right) dt - \sum_{i=1}^3 \sigma_i (x_i - k_i) dB_i. \end{aligned} \quad (5.13)$$

We choose $k_3 = \mu_1/\beta$, $k_1 = \mu_3/\beta$, so that the linear terms in x_1 and x_3 become equal to zero. The differential of $V(x_t)$ can then be written as

$$dV \leq LV - \sum_{i=1}^3 \sigma_i (x_i - k_i) dB_i \quad (5.14)$$

where

$$M = \Lambda + k_1 \mu_1 + k_2 (\mu_2 + \gamma) + \mu_2 k_3 + \frac{k_1}{2} \sigma_1^2 + \frac{k_2}{2} \sigma_2^2 + \frac{k_3}{2} \sigma_3^2, \quad (5.15)$$

$$LV = M dt - \left(\frac{k_1}{2} \Lambda + \mu_2 x_2 + k_2 \frac{x_1 x_3}{x_2} + \beta x_1 x_3 + r \gamma k_3 \frac{x_2}{x_3} \right) dt, \quad (5.16)$$

and the sum in the parenthesis of (5.16) is positive since the x_i 's are positive when $t < T \wedge \tau_\epsilon$.

Integrating (5.14), we obtain

$$\begin{aligned} \int_0^{T \wedge \tau_\epsilon} dV(X(t)) &\leq \int_0^{T \wedge \tau_\epsilon} M dt \\ &- \int_0^{T \wedge \tau_\epsilon} \sum_{j=1}^3 (x_j - k_j) \sigma_j dB_j, \end{aligned}$$

and taking the expectation, we get a bound independent of ϵ ,

$$E [V(x_{T \wedge \tau_\epsilon}^\epsilon)] \leq V(x^0) + MT. \quad (5.17)$$

If a path $x_t^\epsilon(\omega)$ is such that it exits R_+^3 at $T \wedge \tau_\epsilon$, then by (5.11) V becomes $+\infty$ at the exit point. In view of (5.17), the probability of this occurrence is zero. We conclude that x_t^ϵ does not exit R_+^3 , so that all its components are strictly positive for $t \leq T \wedge \tau_\epsilon$.

On the other hand, x_t^ϵ may exit the set

$$S_\epsilon = \left\{ \max_{1 \leq i \leq 3} x_i < \frac{1}{\epsilon} \right\},$$

but in view of (5.17) and the form of $V(x)$, the probability, P , of this event is less than $C_0 T \epsilon$, where C_0 is a constant independent of x^0 if x^0 remains in a fixed bounded set, that is

$$P(\tau_\epsilon < T) \leq C_0 T \epsilon. \quad (5.18)$$

This completes the proof of Lemma 5.3.2. Next, we prove Theorem 5.3.3, that is,

Theorem 5.3.3 The system (5.3) with any initial value (5.6) has a unique solution $x_t \in R_+^3$ for all $t > 0$, and

$$E |x_t|^2 \leq C e^{\alpha t} \quad \text{for } t > 0,$$

where C and α are constants.

Proof Set

$$y_t = x_{t,1}^\epsilon + 2x_{t,2}^\epsilon + x_{t,3}^\epsilon,$$

and recall, by Lemma 5.3.2, that $x_{t,i}^\epsilon > 0$ for $t < T \wedge \tau_\epsilon$. Clearly,

$$dy_{t \wedge \tau_\epsilon} = (\Lambda + Ay_{t \wedge \tau_\epsilon}) dt + \sum_{i=1}^3 \sigma_i x_{t \wedge \tau_\epsilon, i}^\epsilon dB_{t \wedge \tau_\epsilon, i},$$

where A is a constant vector. By using the relations

$$dy^2 = 2ydy + \frac{1}{2}(dy)^2,$$

$$E \left[\int_0^{t \wedge \tau_\epsilon} h_{t,i} dB_i(t) \bullet \int_0^{t \wedge \tau_\epsilon} h_{t,j} dB_{t,j} \right] = \delta_{ij} \int_0^{t \wedge \tau_\epsilon} h_{t,j}^2 dt,$$

we find that the function

$$\psi(t) = E |y_{t \wedge \tau_\epsilon}|^2$$

satisfies an inequality of the form

$$\psi(t) \leq C_1 + C_2 \int_0^t \psi(s) ds \quad \text{for all } t < T \tag{5.19}$$

where C_i are positive constants. Hence

$$\psi(t) \leq C e^{\alpha t} \quad \text{for } t < T,$$

which implies that

$$E |x_{t \wedge \tau_\epsilon}|^2 \leq C e^{\alpha t}$$

for some positive constants α and C . We now write the system (5.3) in integrated form and take $\epsilon \rightarrow 0$. Using (5.18), we can then show by a standard argument that $x_t = \lim x_t^\epsilon$ exists for a sequence $\epsilon \rightarrow 0$ and it is a solution of (5.3) subject to (5.6). Uniqueness of the solution follows from Theorem 2.1 in [Friedman, Chap. 5].

5.4 The case of constant diffusion

In this section we consider a dynamical system

$$\frac{dy}{dt} = h(y) \tag{5.20}$$

and a corresponding stochastic system

$$dy_t = h(y_t)dt + \alpha dB_t \tag{5.21}$$

where B_t is a 3-D column vector of independent Brownian motions with $B_0 = 0$ and variance 1, and

$$\alpha = \begin{pmatrix} \alpha_1 & 0 & 0 \\ 0 & \alpha_2 & 0 \\ 0 & 0 & \alpha_3 \end{pmatrix}, \quad \alpha_j \neq 0 \text{ for } j = 1, 2, 3. \tag{5.22}$$

If $h(y)$ is uniformly Lipschitz continuous, then there exists a unique solution of (5.21) for any initial values. Let

$$y^s = (y_1^s, y_2^s, y_3^s)$$

be any asymptotically stable steady point of (5.20). We wish to study to what extent y^s is also a stable point for the stochastic system (5.21). Clearly

$$h(y^s) = 0 \quad (5.23)$$

and

$$(y - y^s)J_s(y - y^s) \leq -\frac{1}{2}\mu |y - y^s|^2 \quad (5.24)$$

where J_s is the Jacobian matrix whose elements are computed at any point in some small ball $B_\delta(y^s)$ with radius δ and center y^s , and μ is a positive constant. We denote by τ_{y_0} the exit time of y_t from $B_\delta(y^s)$. In the sequel, we shall need to compute $E[t \wedge \tau_{y_0}]$. To do that we first note that the probability $P(\tau_{y_0} > T)$ can be computed as follows [[62], page 92]: Let Ψ_T denote the solution of the parabolic system

$$\begin{aligned} \frac{\partial \Psi}{\partial t} + h(y) \cdot \nabla_y \Psi + \frac{1}{2} \alpha^2 \nabla_y^2 \Psi &= 0 \quad \text{in } B_\delta(y^s) \times (0, T), \\ \Psi &= 0 \quad \text{on } \partial B_\delta(y^s) \times (0, T), \end{aligned} \quad (5.25)$$

$$\Psi = 1 \quad \text{on } B_\delta(y^s) \times \{t = T\}. \quad (5.26)$$

Then [[62], page 84]

$$P(\tau_{y_0} > T) = \Psi_T(y_0, 0) \quad \text{for any } y_0 \in B_\delta(y^s). \quad (5.27)$$

Next, we write

$$E[t \wedge \tau_{y_0}] = tP(\tau_{y_0} > t) + E[(\tau_{y_0} < t)\chi]$$

where χ is characteristic function of the set $\{\tau_y < t\}$. Then

$$E[(\tau_{y_0} < t)\chi] = \lim_{n \rightarrow \infty} \sum_{i=1}^{n-1} \frac{ti}{n} P\left[\frac{ti}{n} < \tau_{y_0} < \frac{t(i+1)}{n}\right]$$

$$\begin{aligned}
&= \lim_{n \rightarrow \infty} \sum_{i=1}^{n-1} \frac{ti}{n} \left\{ P \left(\tau_{y_0} > \frac{ti}{n} \right) - P \left(\tau_{y_0} > \frac{t(i+1)}{n} \right) \right\} \\
&= \lim_{n \rightarrow \infty} \sum_{i=1}^{n-1} \left[\frac{t(i+1)}{n} - \frac{ti}{n} \right] P \left(\tau_{y_0} > \frac{ti}{n} \right) - tP(\tau_{y_0} > t) \\
&= \int_0^t \Psi_u(y_0, 0) du - tP(\tau_{y_0} > t),
\end{aligned}$$

by (5.27). Hence

$$E[t \wedge \tau_{y_0}] = \int_0^t \Psi_u(y_0, 0) du. \quad (5.28)$$

If $\tilde{y}_t \equiv y_{t \wedge \tau_{y_0}}$, then $\tilde{y}_t \in B_\delta(y^s)$,

$$d\tilde{y}_t = h(\tilde{y}_t)dt + \alpha dB_{t \wedge \tau_{y_0}},$$

and

$$h(\tilde{y}_t) = J_s(\tilde{y}_t - y^s)$$

where

$$J_s = \left(\frac{\partial h_i(\tilde{y}_{ij})}{\partial y_j} \right), \quad \tilde{y}_{ij} \in B_\delta(y^s).$$

By (5.24),

$$(\tilde{y}_t - y^s) J_s(\tilde{y}_t - y^s) \leq -\frac{1}{2}\mu |\tilde{y}_t - y^s|^2. \quad (5.29)$$

Using this in the relation

$$\begin{aligned}
\frac{1}{2}d|\tilde{y}_t - y^s|^2 &= (\tilde{y}_t - y^s)d\tilde{y}_t + \frac{1}{2}\alpha^2 d(t \wedge \tau_{y_0}) \\
&= (\tilde{y}_t - y^s)J_s(\tilde{y}_t - y^s) + (\tilde{y}_t - y^s)\alpha dB_{t \wedge \tau_{y_0}} + \frac{1}{2}\alpha^2 d(t \wedge \tau_{y_0}),
\end{aligned}$$

we thus get

$$d(|\tilde{y}_t - y^s|^2 e^{\mu t}) \leq 2e^{\mu t}(\tilde{y}_t - y^s)\alpha dB_{t \wedge \tau_{y_0}} + e^{\mu t}\alpha^2 d(t \wedge \tau_{y_0}). \quad (5.31)$$

Integrating in t and taking expectations we conclude that

$$E|\tilde{y}_t - y^s|^2 \leq E|y_0 - y^s|^2 e^{-\mu t} + \int_0^t e^{-\mu(t-u)}\alpha^2 \Psi_u(y_0, 0) du \quad (5.32)$$

where we have used (5.28). The estimate (5.32) shows that the asymptotic stability of y^s with respect to the stochastic process (5.21) holds for paths that remain within the δ -neighborhood of the steady point y^s but it is degraded by the diffusion term αdB_t . Thus, the Brownian diffusion term destabilizes the stable deterministic state.

Remark 5.4.1 The above considerations hold also for stochastic processes (5.21) with arbitrary matrix α of constant coefficients, $\alpha = (\alpha_{ij})$, provided we define

$$\alpha^2 = \sum_{i,j=1}^3 \alpha_{ij} \alpha_{ji} \quad (5.33)$$

5.5 Example 1: Malaria model with constant diffusion matrix

As our first example, we consider a stochastic system (5.21) with

$$h(y_t) \equiv f(y_t) = \begin{pmatrix} \Lambda - \mu_1 y_1 - \beta y_1 y_3 \\ \beta y_1 y_3 - (\mu_2 + \gamma) y_2 \\ r\gamma y_2 - \mu_3 y_3 - \beta y_1 y_3 \end{pmatrix}. \quad (5.34)$$

Note that $f(y)$ is not uniformly Lipschitz continuous. Nevertheless, one can prove existence and uniqueness of the solution of (5.21) with (5.34) as the drift matrix as in the case of Theorem 5.3.3, using the Lyapunov-type function

$$V(y) = \exp(y_1 + y_2 + \lambda_3 y_3),$$

with λ_3 large enough to show that

$$E[V(y_{T \wedge \tau_\epsilon}^\epsilon)] \leq V_0 e^{MT}$$

$$V_0 = \exp(y_1^0 + y_2^0 + \lambda_3 y_3^0)$$

for some constant M and thus conclude the existence and uniqueness of the solution for any initial value $y^0 \in R^3$. Recall (Remark 5.2.1) that if the initial value lies in R_+^3 and α^2 is small, then the state variables will remain in R_+^3 with high probability. The model (5.21) with drift matrix (5.34) corresponds to the malaria model (5.1) with Brownian noise in the measurement of the state variables. Biologically, it could represent a host who suffers from chronic illnesses that are not related to malaria but have a significant impact on the population of red blood cells, for example, a schistosome patient, but could also represent different responses of the immune system, as will be illustrated in section 5.8.

The deterministic system of (5.20),(5.34), possesses a parasite-free steady state, $E_0 = \left(\frac{\Lambda}{\mu_r}, 0, 0 \right)$, with the basic reproduction number (cf [11])

$$R_{0c} = \frac{\Lambda \beta ((r-1)\gamma - \mu_2)}{\mu_1(\mu_2 + \gamma)\mu_3}. \quad (5.35)$$

If $R_{0c} < 1$ then E_0 is stable with respect to the process (5.20), but the stability with respect to (5.21)-(5.34) is to be understood only in the sense of (5.32). If $R_{0c} > 1$,

then there exists a parasite-present steady state given by

$$y_{10}^s = \frac{(\mu_2 + \gamma)\mu_3}{\beta((r-1)\gamma - \mu_2)}, \quad y_{20}^s = \frac{\mu_1\mu_3}{\beta((r-1)\gamma - \mu_2)}(R_{0c} - 1), \quad y_{30}^s = \frac{\mu_1}{\beta}(R_{0c} - 1).$$

This steady state is stable with respect to the process (5.23) [23], but again, its stability with respect to the stochastic system (5.21) is degraded by the diffusion term αdB_t .

Remark 5.5.1 If the noises $B_{t,1}, B_{t,2}$ and $B_{t,3}$ are correlated, then in the stochastic process (5.21) α is no longer a diagonal matrix. For example, if

$$\alpha = \begin{pmatrix} \alpha_1 & 0 & 0 \\ \alpha_{12} & \alpha_2 & 0 \\ \alpha_{13} & 0 & \alpha_3 \end{pmatrix},$$

where α_{12} and α_{13} can be viewed as correlation coefficients. This describes an environment in which the processes of infection of susceptible red blood cells and the bursting of infected red blood cells are correlated or synchronized [3] which is a strategy used by the parasite to invade the immune response. Since synchronization increases α^2 (see 5.33) by virtue of (5.32), this results in weakened stability for the steady state of (5.21).

5.6 Example 2: Malaria model with linear diffusion matrix

In this example, we consider the stochastic system (5.3) with drift and diffusion matrices given by (5.4) and (5.5), respectively, and make a change of variable $y_j = -\log x_j$. Setting $g_j(y) = (1/x_j)f_j(x)$, we get

$$dy_t = g_t(y)dt + \sigma dB_t. \quad (5.36)$$

The transformed stochastic system (5.36) has constant diffusion coefficients and in component form (dropping the subindex t) it is given by:

$$dy_1 = \frac{1}{y_1} \left(\left(\mu_1 + \frac{1}{2}\sigma_1^2 \right) y_1 - \Lambda + \beta y_1 y_3 \right) dt + \sigma_1 dB_1, \quad (5.37)$$

$$dy_2 = \frac{1}{y_2} \left(\left(\mu_2 + \gamma + \frac{1}{2}\sigma_2^2 \right) y_2 - \beta y_1 y_3 \right) dt + \sigma_2 dB_2, \quad (5.38)$$

$$dy_3 = \frac{1}{y_3} \left(\left(\mu_3 + \frac{1}{2}\sigma_3^2 \right) y_3 - r\gamma y_2 + \beta y_1 y_3 \right) dt + \sigma_3 dB_3. \quad (5.39)$$

From the form of the functions $g_j(y)$, we can see that the system (5.36) possesses only a parasite-present state $y^s = (y_1^s, y_2^s, y_3^s)$, which is obtained by solving the equations $g_j(y) = 0$ ($j = 1, 2, 3$):

$$\left(\mu_1 + \frac{1}{2}\sigma_1^2 \right) y_1^s + \beta y_1^s y_3^s = \Lambda, \quad (5.40)$$

$$\beta y_1^s y_3^s - \left(\mu_2 + \gamma + \frac{1}{2}\sigma_2^2 \right) y_2^s = 0, \quad (5.41)$$

$$-r\gamma y_2^s + \beta y_1^s y_3^s + \left(\mu_3 + \frac{1}{2}\sigma_3^2 \right) y_3^s = 0. \quad (5.42)$$

Eliminating the quadratic terms from (5.41) we obtain

$$\left(\mu_1 + \frac{1}{2}\sigma_1^2\right) y_1^s + \left(\mu_2 + \gamma + \frac{1}{2}\sigma_2^2\right) y_2^s = \Lambda, \quad (5.43)$$

$$\left((1-r)\gamma + \mu_2 + \frac{1}{2}\sigma_2^2\right) y_2^s + \left(\mu_3 + \frac{1}{2}\sigma_3^2\right) y_3^s = 0. \quad (5.44)$$

Solving (5.43)-(5.44) using the relation (5.41) gives the parasite-present steady state:

$$y_1^s = \frac{\left(\gamma + \left(\mu_2 + \frac{1}{2}\sigma_2^2\right)\right) \left(\mu_3 + \frac{1}{2}\sigma_3^2\right)}{\beta \left((r-1)\gamma - \left(\mu_2 + \frac{1}{2}\sigma_2^2\right)\right)}, \quad (5.45)$$

$$y_2^s = \frac{\left(\mu_1 + \frac{1}{2}\sigma_1^2\right) \left(\mu_3 + \frac{1}{2}\sigma_3^2\right)}{\beta \left((r-1)\gamma - \left(\mu_2 + \frac{1}{2}\sigma_2^2\right)\right)} (R_0 - 1), \quad (5.46)$$

$$y_3^s = \frac{\left(\mu_1 + \frac{1}{2}\sigma_1^2\right)}{\beta} (R_0 - 1), \quad (5.47)$$

where

$$R_0 = \frac{\beta \Lambda \left((r-1)\gamma - \left(\mu_2 + \frac{1}{2}\sigma_2^2\right)\right)}{\left(\mu_1 + \frac{1}{2}\sigma_1^2\right) \left(\gamma + \mu_2 + \frac{1}{2}\sigma_2^2\right) \left(\mu_3 + \frac{1}{2}\sigma_3^2\right)}. \quad (5.48)$$

The solution lies in R_+^3 if and only if $R_0 > 1$. For the system (5.36), we have

$$J_s(y) = \begin{pmatrix} \frac{\Lambda}{y_1^2} & 0 & \beta \\ -\frac{\beta y_3}{y_2} & \frac{\beta y_1 y_3}{y_2^2} & -\frac{\beta y_1}{y_2} \\ \beta & -\frac{r\gamma}{y_3} & \frac{r\gamma y_2}{y_3^2} \end{pmatrix}, \quad (5.49)$$

and the stability of the steady state y^s is determined by the eigenvalues of the transformed Jacobian matrix (5.49) at y^s . The eigenvalue equation of (5.49) is given by

$$a_3\lambda^3 + a_2\lambda^2 + a_1\lambda + a_0 = 0,$$

where

$$\begin{aligned} a_3 &= 1 \\ a_2 &= -\left(\frac{\Lambda}{y_1^s} + \frac{\beta y_1^s y_3^s}{y_2^{s2}} + \frac{r\gamma y_2^s}{y_3^{s2}}\right), \\ a_1 &= \frac{\beta\Lambda y_1^s y_3^s}{y_1^{s2} y_2^{s2}} + \frac{r\gamma\Lambda y_2^s}{y_1^{s2} y_3^{s2}} - \beta^2, \\ a_0 &= \frac{\beta^3 y_1^s y_3^s}{y_2^{s2}} - \frac{r\gamma\beta^2}{y_2^s}. \end{aligned} \tag{5.50}$$

Since $a_2 < 0$, by the Routh-Hurwitz criteria the steady state is unstable.

Remark 5.6.1 *From (5.46)-(5.47) we see that a parasite-present steady states exists if and only if $R_0 > 1$, and from (5.35) and (5.48) we see that $R_0 < R_{0c}$.*

These observations suggest the following:

- The deterministic model overestimates the severity of the disease, compared to the stochastic model with linear diffusion matrix.
- With no parasite-free steady state for the model with linear diffusion matrix, any infection with initial parasite load develops into a clinical case.

Thus, even if one can reduce R_0 as close to 1 as possible, by direct treatment or by bolstering the immune effector cells, there will always be a residue of malaria parasites within the host.

Remark 5.6.2 *The malaria in the parasite-present steady state is more severe in the constant diffusion case than in the linear diffusion case, that is, $y_1^s > y_{10}^s, y_2^s < y_{20}^s, y_3^s < y_{30}^s$.*

The remark can be proved as shown in the following proof.

Proof It is easy to see that y_1^s decreases if σ_1^2, σ_2^2 and σ_3^2 decrease, so that $y_1^s > y_{10}^s$.

Next,

$$\begin{aligned}
y_2^s &= \frac{(\mu_1 + (1/2)\sigma_1^2)(\mu_3 + (1/2)\sigma_3^2)}{\beta((r-1)\gamma - (\mu_2 + (1/2)\sigma_2^2))}(R_0 - 1) \\
&= \frac{\Lambda}{(\gamma + \mu_2 + (1/2)\sigma_2^2)} - \frac{(\mu_1 + (1/2)\sigma_1^2)(\mu_3 + (1/2)\sigma_3^2)}{\beta((r-1)\gamma - (\mu_2 + (1/2)\sigma_2^2))} \\
&< \frac{\Lambda}{(\gamma + \mu_2 + (1/2)\sigma_2^2)} - \frac{\mu_1\mu_3}{\beta((r-1)\gamma - (\mu_2 + (1/2)\sigma_2^2))} \\
&= \frac{\mu_1\mu_3}{\beta((r-1)\gamma - (\mu_2 + (1/2)\sigma_2^2))} \left(\frac{\Lambda\beta((r-1)\gamma - (\mu_2 + (1/2)\sigma_2^2))}{\mu_1(\gamma + \mu_2 + (1/2)\sigma_2^2)\mu_3} - 1 \right) \\
&< \frac{\mu_1\mu_3}{\beta((r-1)\gamma - \mu_2)}(R_0 - 1) = y_{20}^s.
\end{aligned}$$

Finally,

$$\begin{aligned}
y_3^s &= \frac{(\mu_1 + (1/2)\sigma_1^2)}{\beta}(R_0 - 1) \\
&= \frac{\Lambda((r-1)\gamma - (\mu_2 + (1/2)\sigma_2^2))}{(\gamma + \mu_2 + (1/2)\sigma_2^2)(\mu_3 + (1/2)\sigma_3^2)} - \frac{(\mu_1 + (1/2)\sigma_1^2)}{\beta} \\
&< \frac{\Lambda((r-1)\gamma - \mu_2)}{(\gamma + \mu_2)\mu_3} - \frac{\mu_1}{\beta} \\
&= \frac{\mu_1}{\beta}(R_{0c} - 1) = y_{30}^s.
\end{aligned}$$

5.7 Numerical simulations

Figures (5.1)-(5.3) shows how a linear diffusion matrix (model (5.2))introduces a much higher instability into the original deterministic system given in Chapter 3. For parameter values used see [11].

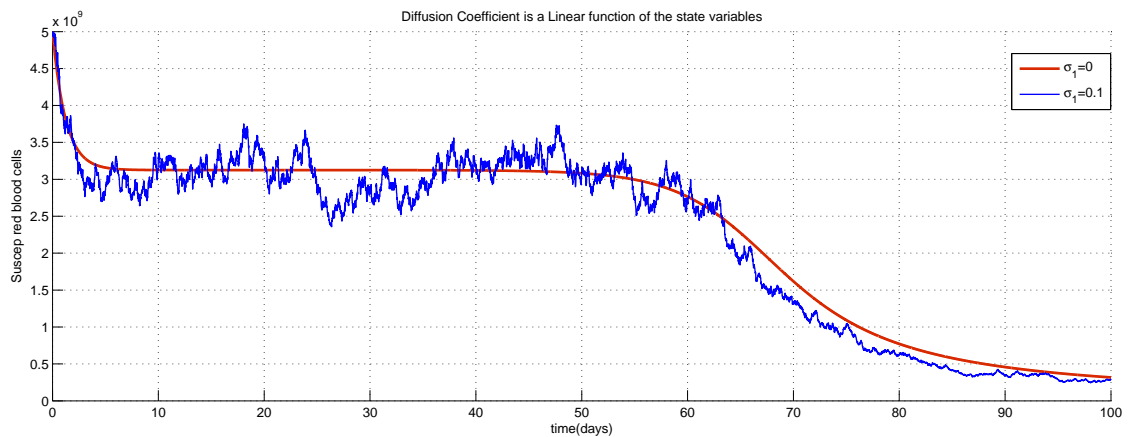


Figure 5.1: A deterministic ($\sigma_1 = 0$) and stochastic graph with linear diffusion coefficient ($\sigma_1 = 0.1$) for the RBCs density over time. Parameter values used: $\Lambda = 2.5 \times 10^9, \mu_r = 0.8, \beta = 2 \times 10^{-11.3}, \mu_i = 0.5, \mu_p = 0, r = 12$, with initial conditions $R(0) = 5 \times 10^9, R_i(0) = 10, P(0) = 2 \times 10^4$.

5.8 Interpretation of patients data

Plasmodium falciparum infections are erythrocytic and are maintained by asexual replication of the parasite during the red blood stage [10]. A study by Hoshen et al [3] formulated a model of within-host dynamics of *P.falciparum* malaria which showed that synchronicity of malaria pathogenesis processes is an inherent feature for this

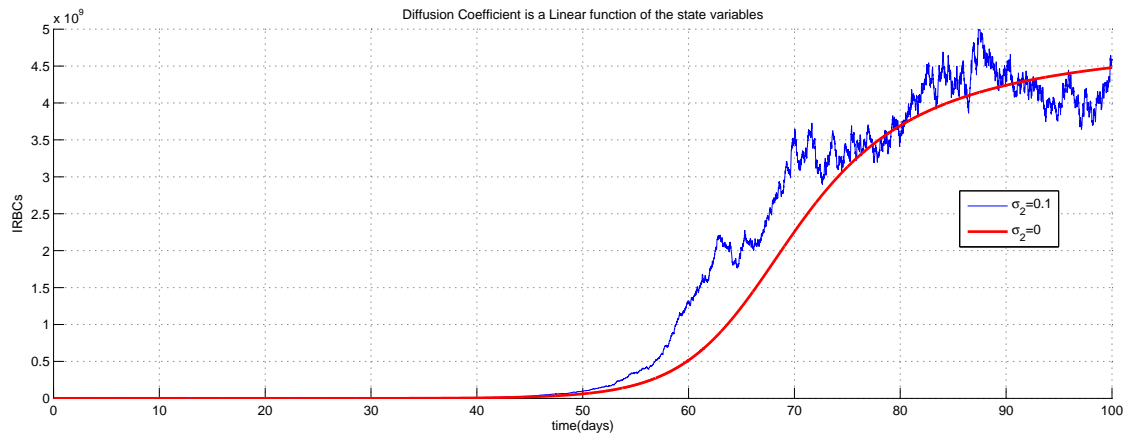


Figure 5.2: A deterministic ($\sigma_1 = 0$) and stochastic graph with linear diffusion coefficient ($\sigma_1 = 0.1$) for the IRBCs density over time. Parameter values used: $\Lambda = 2.5 \times 10^9$, $\mu_r = 0.8$, $\beta = 2 \times 10^{-11.3}$, $\mu_i = 0.5$, $\mu_p = 0$, $r = 12$, with initial conditions $R(0) = 5 \times 10^9$, $R_i(0) = 10$, $P(0) = 2 \times 10^4$.

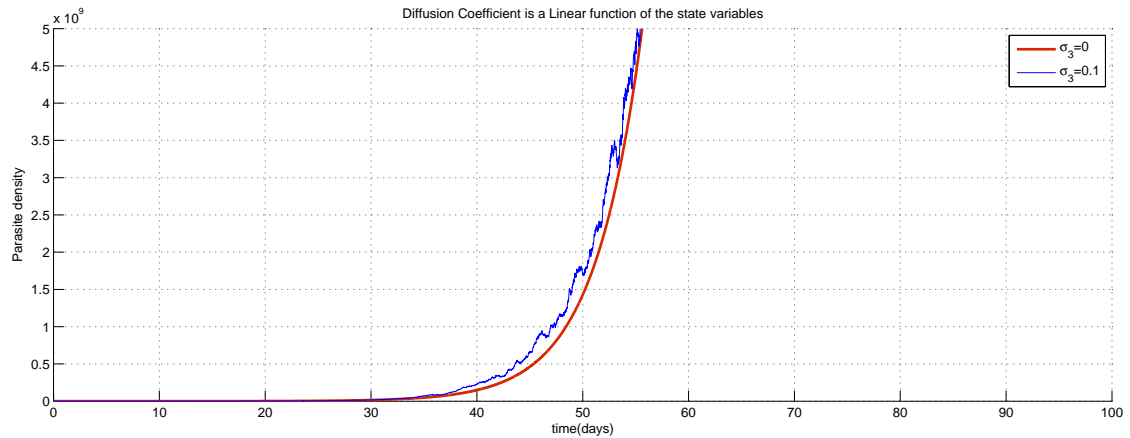


Figure 5.3: A deterministic ($\sigma_1 = 0$) and stochastic graph with linear diffusion coefficient ($\sigma_1 = 0.1$) for the parasite density over time. Parameter values used: $\Lambda = 2.5 \times 10^9$, $\mu_r = 0.8$, $\beta = 2 \times 10^{-11.3}$, $\mu_i = 0.5$, $\mu_p = 0$, $r = 12$, with initial conditions $R(0) = 5 \times 10^9$, $R_i(0) = 10$, $P(0) = 2 \times 10^4$.

parasite. Another clinical study of individuals infected with *P.vivax* malaria reported in White [21] has shown that *P.vivax* infections exhibit disease relapse tendencies, that are maintained by parasite release from the liver stage.

To characterize these two manifestations in malaria infections, we have formulated two stochastic models, one with constant diffusion matrix and another with linear diffusion matrix. The models with constant diffusion coefficients describes a process possessing both parasite-free and parasite-present states. The stability behavior of its deterministic system is such that if $R_{0c} < 1$, then the parasite-free steady state is globally asymptotically stable and if $R_{0c} > 1$, then the parasite-present steady is asymptotically stable. The stochastic model (5.21) (with 5.34) shows that the stability of the parasite-present steady state would degrade with time, but treatment with effective drugs that reduce R_{0c} to levels below 1 could clear the infection. The study by Hoshen *et al* [3] has described plasmodium falciparum infections as synchronized processes. That study [3] was subsequently followed by many authors (see [56] and the references therein) who tried to include synchronization as a clinical feature of infection by formulating deterministic models with periodic coefficients to compensate for the lack of synchronicity in the Anderson *et al* [10] model. The model (5.21) (with 5.34) achieves the same goal without imposing the artificial periodic behavior on the coefficients. We have found out that the model (5.21), (5.23) with a matrix of constant coefficients, $\alpha = (\alpha_{ij})$, as depicted in Remark 5.4.1, describes a malaria disease in which the infection processes are synchronized by the structure of the Brownian diffusion matrix, and it can be used to explain malaria infections that are curable, such as p. falciparum. Furthermore, we have found that the effect of synchronized

Brownian diffusion is to re-inforce the parasite-present state. As we have suggested, this is a strategy used by the parasite to evade the immune response; eventually, however, the Brownian noise destabilizes the steady state.

The stochastic model with linear diffusion matrix (5.4) possesses only a parasite-present steady state. In this case the threshold parameter, R_0 , can be reduced (by treatment) as close to 1 as possible but it still remains above 1, so full recovery is not possible. The stability analysis of the steady state shows that it is always unstable. Our conclusions seem to fit with results reported in a clinical study by White [21] which describes a group of patients in treatment for *p. vivax* malaria whose infection was never cleared by treatment and whose infection exhibited relapse tendencies.

The two stochastic models (5.21) (with 5.34) and (5.4) can be used to study diseases with equilibria exhibiting changes in stability. We illustrate this using clinical records of individuals who were infected with a single mosquito bite with the Chesson strain of *P.vivax* [21]. We have chosen six individuals from that study, identified as S-205, S-197, S-196, S-209, S-198 and S-208, each individual representing a group of volunteers exhibiting a similar response. The trajectories of the disease are shown in Figures 5.4 to 5.9. Three volunteers S-196, S-197, and S-205 (with profiles in Figure 5.4, 5.8, 5.9) were infected with a single mosquito bite at time $t = 1day$, and re-infected twice at times $t = 200days$ and $t = 400days$. The other three volunteers S-198, S-208, and S-209 (with profiles in Figures 5.5, 5.6, 5.7) were infected with a single mosquito bite at time $t = 1day$ but were never re-infected during the remaining period of the study. From the disease progression profiles of the six volunteers, we can classify the immune responses in terms of the diffusion structure as follows: (i) those whose im-

immune response can be explained by the linear diffusion matrix only, (ii) those whose immune response can be explained by the constant diffusion matrix only, and (iii) those whose disease progression pattern switched from the constant diffusion to linear type. Our analysis of the patient data in White [21] will assume that in the constant diffusion case if $R_{0c} < 1$, then the parasite-free steady state is maintained by the patient's strong immunity. However, once the patient's immunity is compromised, that is, if R_{0c} increases above 1, then a patient's prognosis can change to the parasite-present treatable case. For the linear diffusion case, the patient maintains an unstable parasite-present untreatable steady state with a reproduction number always greater than 1.

Figures 5.4 and 5.5 show two contrasting responses both explained by the linear diffusion matrix. Figure 5.4 gives the disease profile of a patient (S-197) whose response to infection and re-infection shows a relapse pattern with arbitrary relapse periods after each re-infection. Each infection was characterized by disease relapse (unstable parasite-present states). This volunteer possessed an unstable parasite-present untreatable state with a reproduction number which remained above 1 during the entire period of infection. Figure 5.5 describes an infection profile for patient S-198 who was infected once at day 1. The patient tested negative for the malaria parasite after treatment, and remained asymptomatic until day 500 when there was a malaria disease relapse, which suggests that some parasites remained but pathogenesis was controlled by the immune system, which kept the reproduction close but just above 1. This immunity was gradually compromised at day 500.

Figure 5.6 (volunteer S-208) and 5.7 (volunteer S-209) show two disease patterns that

can be explained by the constant diffusion matrix. Figure 5.6 shows an immune response which had to overcome parasite escape. The patient suffered two disease relapses after the primary infection before recovering fully. Figure 5.7 shows a different immune response that easily overcome the pathogen resulting in a patient recovering fully after treatment.

Figure 5.8 (volunteer S-205) shows a switching type response to infection; from constant diffusion type to linear diffusion type. Indeed the volunteer S-205 developed clinical symptoms of malaria following the primary infection. The primary infection was successfully treated (model (5.21)), and this individual's baseline resistance to infection remained strong for some time, but repeated re-infection weakened this resistance as S-205 progressed to a permanent unstable parasite-present untreatable status with arbitrary relapse periods.

Figure 5.9 shows a more complicated response for S-196 which seems to mimic a switch from linear diffusion as in the progression pattern similar to Figure 5.4 to the constant diffusion as in a disease pattern similar to Figure 5.6. However, from the considerations in section 5.6 we see that if the primary and first re-infection had resulted into an infection explained by linear diffusion matrix then complete recovery was not possible whereas this patient did recover. Hence, the patient's disease progression can only be explained using the model with constant diffusion matrix (model (5.21)). This patient's clinical condition was characterized by a long period of active disease as in Figure 5.4, which turned out to be a stable parasite-present treatable state. The patient responded positively to treatment at $t = 300$ days and recovered with strong immunity that resisted the second re-infection at $t = 400$ days.

The disease progression pattern for S-196 is an example of how complicated malaria diagnosis can be.

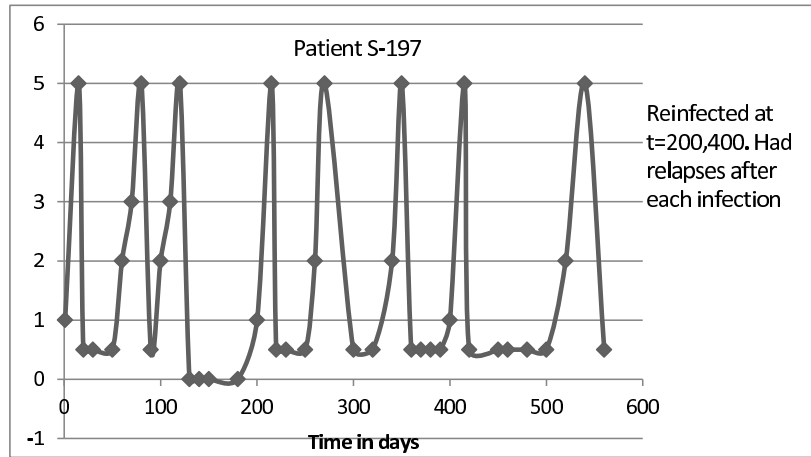


Figure 5.4: Patient s-197 immune response explained by linear diffusion matrix. This describes an unstable parasite-present state

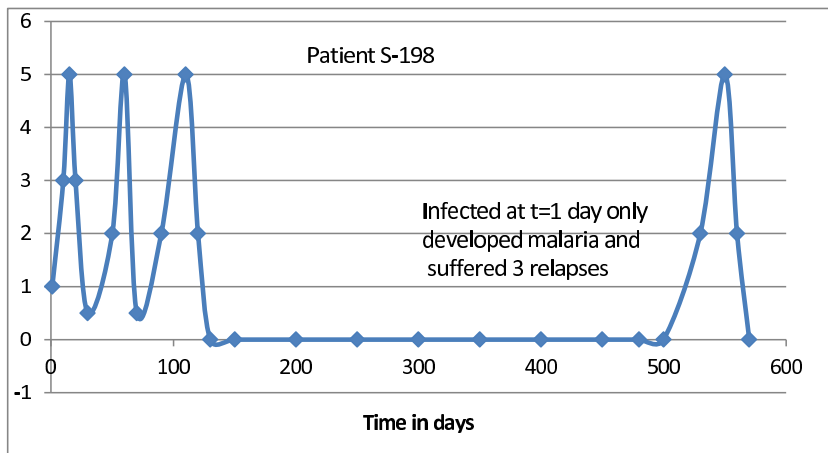


Figure 5.5: Patient's immune response explained by a linear diffusion matrix. This describes symptomatic state which is followed by an asymptomatic state and again by a symptomatic state

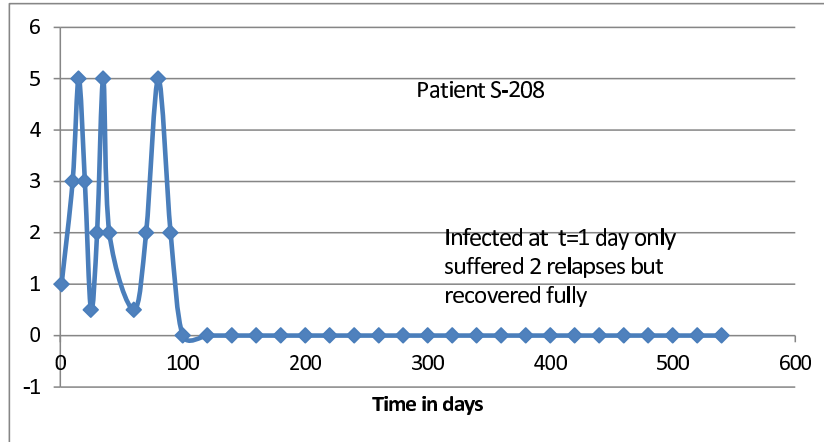


Figure 5.6: Patient’s immune response explained by a constant diffusion matrix. This represents a stable parasite-present treatable state

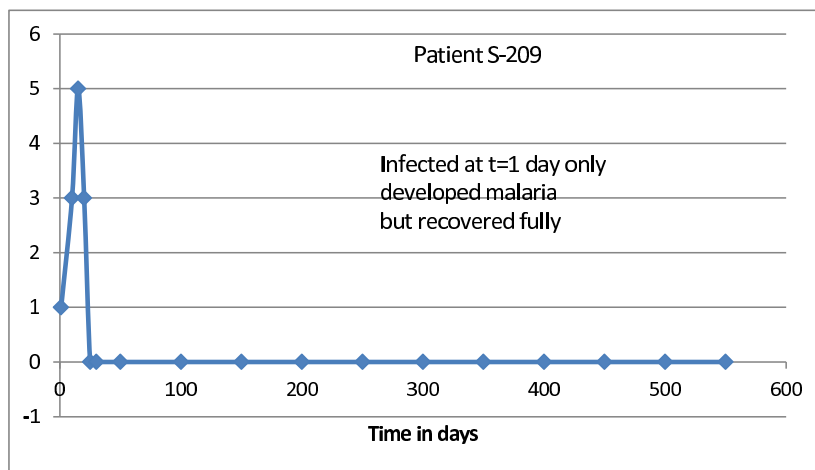


Figure 5.7: Patient’s immune response explained by a constant diffusion matrix. This represents a stable parasite-present treatable state

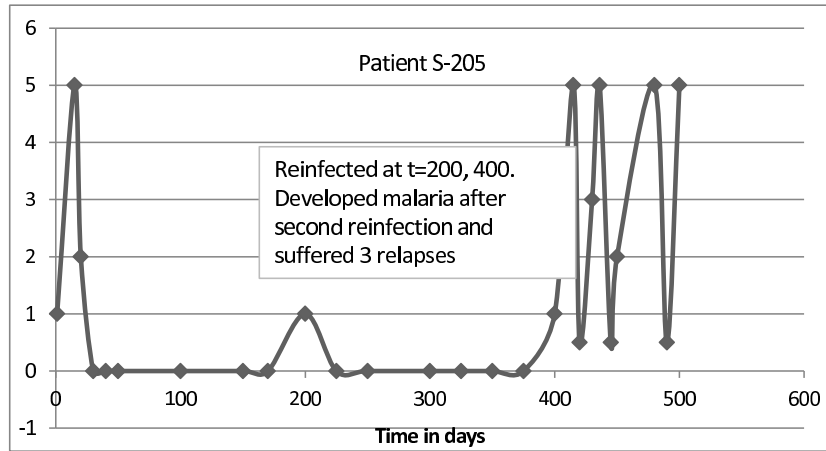


Figure 5.8: Patient’s immune response explained by linear diffusion matrix. This shows an unstable asymptomatic parasite-present state which degraded into a symptomatic unstable parasite-present state

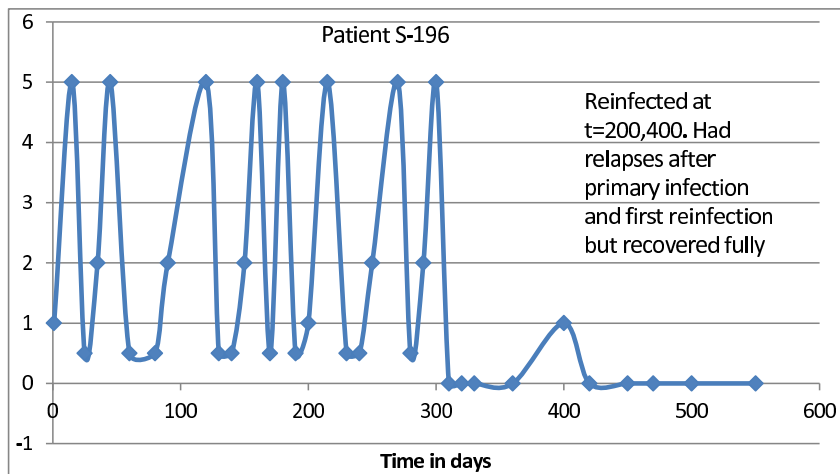


Figure 5.9: Patient’s immune response explained by linear diffusion matrix. This represents an unstable parasite-present treatable state

Chapter 6

Conclusions and Discussions

An inhost treatment model for plasmodium falciparum infection was developed in Chapter 3, based on the earlier work of Anderson *et al*, and others thereafter. In this chapter, we explored the drug therapy benefits, following treatment with antimalarial drugs. Using numerical simulations of the model, it is shown that infection can be eradicated within the host if the drug efficacy level exceeds a threshold value of approximately 0.9532. It will persist if the efficacy is below this threshold value.

Despite the public health importance of placental malaria, its impact on pregnancy outcome in sub-Saharan Africa has not been comprehensively reviewed [77]. The quantification of the contribution of malaria and its treatment to maternal morbidity and mortality will help provide the evidence necessary to improve the effectiveness of advocacy to incorporate malaria prevention strategies in Safe Motherhood Programs (SMP) [77].

In chapter 4 we provide, just but, an insight into the possible public health outcomes in the case management of malaria in pregnant mothers with reduced harm to the

foetus. The model without delay, (4.8)-(4.13), is shown to possess three infected states, that is, an infected state where the erythrocytic infection in the host is active but latent in the foetus that is locally stable for $R_{0at} > 1$ and $R_{0ft} < 1$, a state where the erythrocytic infections are active in both the mother and the foetus which is locally stable for $R_{0at} > 1$ and $R_{0ft} > 1$, and lastly, a state where the erythrocytic infections are under control in the mother but active in the foetus which exist for for $R_{0at} < 1$ and $R_{0ft} > 1$.

Numerical simulations have shown that administering antimalarial drugs with a drug efficacy level between 0.982 and 0.983 at an estimated placental drug transfer permeability coefficient of at least $\eta = 0.97$, we will be able to completely wipe out the disease from both the mother and foetus. Because of the changes in the permeability properties of the placenta during pregnancy, administering a drug with efficacy of 0.95 might not help in clearing the infection in the mother at any stage of pregnancy and a drug efficacy level of 0.983 will completely clear the malaria parasite in both the mother and foetus irrespective of the stage of pregnancy.

In the presence of intracellular delay, we determined a critical delay parameter τ_0 where delay might cause instability to the endemic state as τ passes through the critical value (see figure 4.5), though our model is not exhibiting that for the parameter values given in table (4.1), at the drug efficacy level of $\epsilon_1 = 0.983$ (see 4.6).

Due to White N. J. [21]'s review on a clinical study for patients infected with vivax malaria; while some recovered others suffered relapses even after treatment. These findings motivated the birth of the stochastic analysis of malaria inhost dynamics in

Chapter 5. It is well known that responses to disease infection and treatment can be highly personalized, often depending on the patient's immune system. Mathematical models of disease progression and treatment are almost always described by a system of deterministic differential equations. The variability in patients response to the same treatment is then explained by varying some of the parameters of the equations; these parameters are viewed as "personalized" parameters which depend on the patient's immune system(see, for example, [72, 73]). In chapter 5 we have developed, in the case of a simple malaria model, a new approach that can explain such personalized responses. We have introduced a stochastic model with constant or linear diffusion matrix and demonstrate, using actual data, how varied patients response can be explained by the model. We believe that this new stochastic approach should be applicable to many other disease models, including for example HIV/AIDS, and that it could also be useful in developing prognosis tools.

Bibliography

- [1] World Malaria Report,2012. <http://who.int/malaria/publications/worldmalaria-report2012/report/en/index.html>. Accessed Feb. 2013.

- [2] Rodriguez M. et al, 2007. Malaria Infection through Multiorgan Donation: An Update from Spain. *Liver transplantation* 13,1302-1304.

- [3] Hoshen M. B., Heinrich R., W. D. Stein W.D., Ginsburg H.,2000. Mathematical modelling of the within-host dynamics of *Plasmodium falciparum*, *Parasitology*,121,227-235.

- [4] Trape J.F.,1987. Malaria and urbanisation in Central Africa, the examples of Brazzaville. Part IV. Parasitological and serological surveys in urban and surrounding rural areas. *Trans. Roy. Soc. Trop. Med. Hyg. Supp* 2 81:26-33.

- [5] Trape J.F., Rogier C.,1996. Combating Malaria Morbidity and Mortality by

Reducing Transmission. *Parasitology Today*, 12(6):236-40.

- [6] Fenton Hall B.F., Anthony S. Fauci A.N.,2009. Malaria Control, Elimination, and Eradication: The Role of the Evolving Biomedical Research Agenda, Perspective. *JID* 2009:200(1 December),1639.
- [7] Riedel S.,2005. Edward Jenner and the history of smallpox and vaccination. *Proc(Bayl Univ. Med. Cent.)*, 18(1):21-5.
- [8] McQueen P.G., McKenzie F. E,2004. Age-structured red blood cell susceptibility and the dynamics of malaria infections . *PNAS* 101(24),9161-9166.
- [9] Herbert W. Hethcote H. W.,2000. The Mathematics of infectious diseases. *Society for Industrial and Applied Mathematics SIAM Review* 42(4), 599-653.
- [10] Anderson et al, 1989. Non-linear phenomena in host-parasite interactions. *Parasitology*,99,S59-S79.
- [11] Avner Friedman A.,Lungu E.,2013. Can malaria parasite pathogenesis be prevented by treatment with Tumour Necrosis Factor-Alpha?. *Math. Biosci.*

and Eng, Vol. 10, No. 3.

- [12] Francis EG Cox F.E. G.,2010. History of the discovery of the malaria parasites and their vectors. *Parasites and Vectors* , 3:5, <http://www.parasitesandvectors.com/content/3/1/5>.
- [13] Brandy,2001. Malaria parasite exit from the host erythrocytic: A two-step process requiring exoerythrocytic proteolysis. *PNAS* 98(1), 271-276.
- [14] <http://apps.who.int/gho/data/view.main.14120?/en>. Accessed: April 2014.
- [15] Mahdal M.. Malaria Mechanisms: <http://www.news-medical.net/Malaria-Mechanism.aspx>. Accessed Nov. 2013.
- [16] Pradhan P.,2009. Malaria anaemia and nitric oxide induced megaloblastic anaemia: a review on the causes of malarial anaemia. *J. Vector Borne Dis.* 46.
- [17] Louis H. Miller L.H.,1997. Hypothesis on the mechanism of erythrocytic invasion by malaria merozoites. *Bul. of the World Health Org.*, 55(2-3):157-162.

- [18] Chiyaka C. et al,2008. Modelling immune response and drug therapy in human malaria infection. *Comp. and Math. Methods in Med.* , 9(2), ,143-163.
- [19] Yilong Li Y.,2011. The within -host dynamics of Malaria infection with immune response. *Math. Biosc. and Eng.* 8(4),999-1018.
- [20] Saul A.,1998. Models for the in-host dynamics of malaria revisited: errors in some basic models lead to large over-estimates of growth rates. *Parasitology* , 117, 405-407.
- [21] White N. J.,2011. Determinants of relapse periodicity in *Plasmodium vivax* malaria. *Malaria Journal*, 10:297.
- [22] Gravenor M. B., Lloyd A. L.,1998. Reply to: Models for the in-host dynamics of malaria revisited: errors in some basic models lead to large overestimates of growth rate. *Parasitology* , 117, 409-410.
- [23] Niger A.M., Gumel A.B,2011. Immune Response and Imperfect Vaccine in Malaria Dynamics. *Math. Pop. Studies*, 18:55-86.
- [24] Alphose O. et al,2012. Transplacental transmission of *Plasmodium falciparum*

in a highly malaria endemic area of Burkina Faso. *J. of Trop. Med.*, Vol 2012(ID 10975) 7 pages.

- [25] Uneke C. J.,2007. Impact of placental *Plasmodium falciparum* malaria on pregnancy and perinatal outcome in Sub-Saharan Africa: Introduction to placental malaria. *Yale Journal of Bio. and Med.*, 80(2), 39-50.
- [26] Uneke C. J.,2007. Impact of placental *Plasmodium falciparum* malaria on pregnancy and perinatal outcome in Sub-Saharan Africa II. Effects of placental malaria on perinatal outcome; Malaria and HIV. *Yale Journal of Bio. and Med.*, 80, 95-103.
- [27] Malhotra I., Mungai P., Muchiri E., Kwiek J. J., Meshnick S. R., King C. L.,2006. Umbilical cord-blood infections with *Plasmodium falciparum* malaria are acquired antenatally in Kenya. *J. of Infect. Dis.*;194:176-83.
- [28] Dellicour S., Tatem A.J., Guerra C. A., Snow R.W., Ter Kuile F.O.,2010. Quantifying the Number of Pregnancies at risk of Malaria in 2007: A Demographic Study. *Plos Med.* 2010.DOI:10.1371/journal.pmed.1000221.
- [29] Poesporprodjo J. R., Itasanuddiu A., Fobia W., Sugiarto P., Kenongalem

- E., Lampah D.A., Tjitra E., Price R. N., Anstey N. M.,2010. Case Report: Severe Congenital Malaria Acquired in utero. *American J. Trop. Med. Hyg.*, 82(4),563-565.
- [30] Schantz-Dun J., Nour N.M., 2009: Malaria and Pregnancy: A Global Health Perspective, Vol 2 No. 3. *Reviews in Obstetrics and Gynecology*.
- [31] WHO/AFRO . A strategic framework for malaria prevention and control during pregnancy in the African region. Brazzaville: WHO Regional Office for Africa,2004. Accessed: June 2013.
- [32] Mwaniki M. K. et al,2010. Congenital and neonatal malaria in a rural Kenyan district hospital: An eight-year analysis. *Malaria Journal*, 9: 313.
- [33] Uneke C. J.,2011. Congenital malaria: an overview. *Tanzania J. of Health Research*. 13(3):1-17..
- [34] Jimenet J. G. et al,2011. Congenital malaria in Uraba, Colombia. *Malaria Journal*,10:239.
- [35] Autino et al,2012. Pathogenesis of Malaria in Tissues and Blood. *Mediterr. J.*

Hematol. Infect. Dis.;4.

- [36] Rogerson et al,2007. Malaria in pregnancy: pathogenesis and immunity. *Lancet Infect. Dis*, 7:105-117.
- [37] Greenwood B. et al,2007. Malaria in pregnancy: priorities for research. *Lancet Infect Dis*, 7: 169-74.
- [38] Graves P. M. , Gelband H.,2009. Vaccines for preventing malaria (SPF66) (Review). *The Cochrane Collaboration*, Issue 2.
- [39] Nostum F. et al,2006. Antimalarial Drugs in Pregnancy: A Review. *Current Drug Safety*,1,1-15.
- [40] Aguirre P.,1991. On two families of Stochastic Predation Models with Allee Effect. *Mathematics Subject Classification* 92D25,34F05,37C10,34Cxx.
- [41] Viet Ton T.A., Yagi A.,2011. Dynamics of a Stochastic Predator-Prey Model with the Beddington-DeAngelis Functional Response. *Communications on Stochastic Analysis*, 5(2), 371-386.

- [42] Molineaux L., Dietz K.,1999. Review of intra-host models of malaria. *Parasitologia* 41, 221-231.
- [43] Diekmann, O., Hesterbeek, J.A.P., Metz J.A.J.,1990. On the definition and computation of the basic reproduction ratio R_0 in models for infectious disease in heterogeneous population. *J. Math. Biol.*, 28:365-382.
- [44] Chima R. I. et al,2003. The economic impact of malaria in Africa: a Critical review of the evidence: *Health Policy* 63, 17-36.
- [45] WHO:World Malaria report 2008'WHO/HMT/GMP/2008.1'ISBN9789241563697. Accessed 2013.
- [46] WHO Guidelines for the treatment of Malaria,2nd ed. , 2010. Accessed 2013.
- [47] UNICEF/WHO: The Prescriber: Promoting Rational Use of Drugs and Correct Case Management in Basic Health Services, Jan. 2000.
- [48] Straton L. et al, 2008. The persistent problem of malaria: Addressing the fundamental causes of a global killer. *J. Social Science and Medicine* 67, 854-862.

- [49] Plowe V. S., 2009. The evolution of drug-resistant malaria., *Trans. of the R. Soc. of Trop. Med. and Hyg*, 103s, s11-s14.
- [50] UNICEF/WHO: The Prescriber: Promoting rational use of drugs and correct case management in basic health services, Jan. 2000. Accessed 2012
- [51] Thomas J. C. et al, 2004. Mixed picture for changes in stable malaria distribution with future climate in Africa. *Trends in Parasitology* 20(5).
- [52] Van Den Driessche P., Watmough J., 2002. Reproduction numbers and sub-threshold endemic equilibria for compartmental models of disease transmission, *Math. Biosci.* 180, 29-48.
- [53] Castillo-Chavez C., Baojun Song B., 2004. Dynamical Models Of Tuberculosis And Their Applications pp.361-404, *Math. Biosci. and Eng*, 1(2).
- [54] Boyd, M. F., Kitchen, S. F., 1937. On the infectiousness of patients infected with *Plasmodium vivax* and *Plasmodium falciparum*. *American Journal of Tropical Medicine.* 75, 253-62.
- [55] Cheng, Q., Lawrence, G., Reed, C., Towers, A., Ranford-Cartwright, L., Creasey, A., Carter, R., Saul, A. 1997. Measurement of *Plasmodium falciparum* growth

- rates in vivo: a test of malaria vaccines. *American Journal of Tropical Medicine and Hygiene*, 57, 495–500.
- [56] Su, Y., Ruan, S., Wei, J., 2011. Periodicity and synchronization in blood-stage malaria infection. *J. Math Biol.* 63(3), 557–74.
- [57] Chirove F., Lungu E., 2013. Effects of replicative fitness on competing HIV strains. *BioSystems*. 113, 28–36.
- [58] Dalal, N., Greenhalgh, D., Mao, X. R., 2007. A stochastic model of AIDS and condom use. *Journal of Mathematical Analysis and Applications*. 325, 36–53.
- [59] Punta V.D., Gulletta M., Matteelli A., Spinoni V., Regazzoli A., Castelli F., 2010. Congenital *Plasmodium vivax* malaria mimicking neonatal sepsis: a case report. *Malaria J.*, 9: 63.
- [60] Opare P., 2010. Congenital malaria in new born twins. *Ghana Med. J.*, 44(2), 76–78.
- [61] Ferri, F. F., 2009. Protozoal infections. *Ferri's color atlas and text of clinical medicine*. Elsevier Health Sciences. Chapter 332, 1159.
- [62] Friedman, A., 2006. *Stochastic Differential Equations and Applications*. Chapter 5, 98–25.

- [63] Gravenor, M. B., Kwiatkowski, 1998a. An analysis of the temperature effects of fever on the intra-host population dynamics of *Plasmodium falciparum*. *Parasitology*, 117, 97–05.
- [64] Ji, C. Y., Jiang, D. Q., Shi, N. Z., 2009. Analysis of a predator-prey model with modified Leslie-Gower and Holling-type II schemes with stochastic perturbation. *Journal of mathematical Analysis and Applications*. 359, 482–98.
- [65] Chunyan J., Jiang D., Qingshan Y, Ningzhong S., 2012. Dynamics of a multi-group SIR model with stochastic perturbation. *Automatica*. 48, 121–31.
- [66] Lungu, E. M., Oksendal, B., 1997. Optimal harvesting from a population in a stochastic crowded environment. *Mathematical Biosciences*. 145, 47–75.
- [67] Mideo, N., Day, T., Read, A. F. 2008. Modelling malaria pathogenesis. *Cellular Microbiology*. 10 (10), 1947–55.
- [68] Shoji Isao and Ozaki Tohru, 1995. A local linearization method for multivariate stochastic processes. Research Memo 586, Institute of Statistical Mathematics.
- [69] Southgate, V. R., Rollinson, D., Tchuem Tchuente, L. A., Hagan, P., 2005. Towards control of schistosomiasis in sub-Saharan Africa. *Journal of Helminthology*. 79 (3), 181–5.
- [70] White, N. J., Chapman, D., Watt, C. 1992. The effects of multiplication and synchronicity on the vascular distribution of parasites in *falciparum* malaria. *Transactions of the Royal Society of Tropical Medicine and Hygiene*, 86, 590–97.

- [71] Wikipedia, 2013. The free encyclopedia. www.wikipedia.org/wiki/Malaria. Tech. rep.
- [72] Budu-Grajdeanu, P. Schugart, R., Friedman, A., Birmingham, D. J., Rovin, B. H. 2010. Mathematical framework for human SLE Nephritis: disease dynamics and urine biomarkers. *Theoretical Biology and Medical Modeling*, 7(14), 1-20.
- [73] Jain, H., Clinton, S., Bhinder, A., Friedman, A., 2011. Modeling mutation acquisition in prostate cancer undergoing androgen ablation therapy. *PNAS*, 108,19701-06.
- [74] Enrique M. O. Jr, Silvestre M.A., Jacinto Blas Mantaring III, 2004. Drugs that affect the fetus and newborn infant via the placenta or breast milk, *Pediatr. Clin. N. Am.* 51, 539-579.
- [75] Li Q. and Peter J. Weina P.J., 2010. Severe Embryotoxicity of Artemisinin Derivatives in Experimental Animals, but Possibly Safe in Pregnant Women. *Molecules*, 15, 40-57; doi: 10.3390/molecules15010040.
- [76] Dellicour S., HALL S., Chandramohan D., Green B., 2007. The safety of artemisinin during pregnancy: a pressing question, *Malaria Journal*, 6,15.
- [77] Uneke C.J., 2007. Malaria on Pregnancy and Perinatal Outcome in Sub-Saharan Africa. *Yale Journal of Biology and Medicine* 80, 39-50.
- [78] Fox H., 1991. A contemporary view of the human placenta. *Midwifery*; 7(1):31.

- [79] Boyd P. D., Hamilton W. H.,1967. Development and structure of the human placenta from the end of the 3rd month of gestation. J. Obstet. Gynecol. Br. Commonw. 1967; 74:161.
- [80] Culshaw R. V., Ruan S.,2000. A delay differential equation model for HIV infection of $CD4^+$ T cells. Math. Biosc. 165, 27-39.
- [81] Wang H., Wang R., Hu Z., Liao F.,2013. Stability Analysis of an In-Host Viral Model with Cure of Infected Cells and Humoral Immunity. J. of App. Math., Article ID102757, 5 pages.
- [82] Wang H.,Wang R., Hu Z., Liao F.,2013. Stability analysis of an In-Host viral with cure of infected cells and humoral immunity. J. App. Math.
- [83] Ping B., Ruan S.,2013. Birfucations in delay differential equations and applications to tumor and immune system interaction Models. SIAM J. App. Dyn. Sys. 12(4),1847-1888.

Chapter 7

Appendices

7.1 Appendix

Proof The Jacobian matrix of the system 4.8-4.13 evaluated at x_o is given by:

$$J_{x_o} = \begin{pmatrix} -\mu_r & 0 & -\beta_a \frac{\Pi_a}{\mu_r} & 0 & 0 & 0 \\ 0 & -(\alpha + \delta) & \beta_a \frac{\Pi_a}{\mu_r} & 0 & 0 & 0 \\ 0 & \alpha r & -(\mu_p + \beta_a \frac{\Pi_a}{\mu_r}) & 0 & 0 & 0 \\ 0 & 0 & 0 & -\mu_f & 0 & -\beta_f(\delta) \frac{\Pi_f}{\mu_f} \\ 0 & \delta & 0 & 0 & -\alpha_f & \beta_f(\delta) \frac{\Pi_f}{\mu_f} \\ 0 & \delta r & 0 & 0 & \alpha_f r & -(\mu_{pf} + \beta_f(\delta) \frac{\Pi_f}{\mu_f}) \end{pmatrix}.$$

The eigenvalues of J_{x_o} arranged as foetus and adult host specific are given as follows:

For the Foetus:

$$\lambda_1 = -\mu_f,$$

$$\lambda_2 = \frac{-(\alpha_f + (\mu_{pf} + \beta_f(\delta) \frac{\Pi_f}{\mu_f})) - \sqrt{(\alpha_f + (\mu_{pf} + \beta_f(\delta) \frac{\Pi_f}{\mu_f}))^2 + 4\alpha_f(\mu_{pf} + \beta_f(\delta) \frac{\Pi_f}{\mu_f})(R_{of}^2 - 1)}}{2}$$

$$\lambda_3 = \frac{-(\alpha_f + (\mu_{pf} + \beta_f(\delta)\frac{\Pi_f}{\mu_f})) + \sqrt{(\alpha_f + (\mu_{pf} + \beta_f(\delta)\frac{\Pi_f}{\mu_f}))^2 + 4\alpha_f(\mu_{pf} + \beta_f(\delta)\frac{\Pi_f}{\mu_f})(R_{of}^2 - 1)}}{2}$$

For the Adult host:

$$\lambda_4 = -\mu_r,$$

$$\lambda_5 = \frac{-(\alpha + \delta + \mu_p + \beta_a\frac{\Pi_a}{u_r}) - \sqrt{(\alpha + \delta + \mu_p + \beta_a\frac{\Pi_a}{u_r})^2 + 4(\alpha + \delta)(\mu_p + \beta_a\frac{\Pi_a}{u_r})(R_{oa}^2 - 1)}}{2}$$

$$\lambda_6 = \frac{-(\alpha + \delta + \mu_p + \beta_a\frac{\Pi_a}{u_r}) + \sqrt{(\alpha + \delta + \mu_p + \beta_a\frac{\Pi_a}{u_r})^2 + 4(\alpha + \delta)(\mu_p + \beta_a\frac{\Pi_a}{u_r})(R_{oa}^2 - 1)}}{2}.$$

7.2 Matlab Codes

ANDERSON.m

```
function dydt=ANDERSON(t,y) dydt=zeros(size(y)); pia=41664;mur=0.8;betaa=8E-
4;alpha=0.5;r=16;mup=3;e=0.996;mu=0.8; R=y(1); RI=y(2); P=y(3); dydt(1)=pia-
mur*R-(1-e)*betaa*R*P; dydt(2)=(1-e)*betaa*R*P-(alpha)*RI; dydt(3)=alpha*r*RI-
mup*P-(1-e)*betaa*R*P; R1=r*(1-e)*betaa*pia; R2=mur*mup+(1-e)*betaa*pia; R3=R1/R2
ecrt=((r-1)*betaa*pia-mur*mup)/((r-1)*betaa*pia)
```

ANDERSONSOL.m

```
clc;
```

```
global pia mur betaa alpha r mup e subplot(1,1,1) hold on [t,y]=ode45('ANDERSON',[0
```

```
20],[20000,20000,35000]); plot(t,y(:,3),'b','LineWidth',2) title('Concentration of IR-
BCs') xlabel('Time t (in days)') ylabel('Ri') hold off
```

No time delay

```
function ddex12 global p1 u1 b1 a1 r u2 d k u4 a2 p2 u3 d1 e1 e2 n
```

```
sol = dde23(@ddex1de,[1],@ddex1hist,[0, 270]); figure(1) subplot(1,1,1) hold on plot(sol.x,sol.y(4,:), 'black', 'r')
title('Vertical Transmission With Delay'); xlabel('time t'); ylabel('solution y'); hold
off function s = ddex1hist(t) s = [5*10(9);0;55 * 10; 5 * 10(9);0;0]; function dydt =
ddex1de(t, y, Z) p1 = 2.5 * 10(9); u1 = 0.022; b1 = 2 * 10(- 11.3); a1 = 0.4; r =
12; u2 = 0.0208; d = 1; k = 2 * 10(- 11.3); u4 = 0.0208; a2 = 0.4; p2 = 2.5 * 10(9); u3 =
0.022; e1 = 0.0; n = 0.4; e2 = n * e1; t = 12; d1 = d * 10(- 1); ylag1 = Z(:, 1); dy1dt =
p1 - u1 * y(1) - b1 * (1 - e1) * y(1) * y(3); dy2dt = b1 * (1 - e1) * y(1) * y(3) - (a1 + d) *
y(2); dy3dt = a1 * r * y(2) - u2 * y(3) - b1 * (1 - e1) * y(1) * y(3); dy4dt = p2 - u3 * y(4) -
k * d * (1 - e2) * y(4) * ylag1(1); dy5dt = k * d * (1 - e2) * y(4) * ylag2(6) - a2 * y(5); dy6dt =
a2 * r * ylag1(5) + d * r * y(2) - u4 * ylag1(6) - k * d * (1 - e2) * y(4) * ylag1(6); dydt =
[dy1dt; dy2dt; dy3dt; dy4dt; dy5dt; dy6dt]
```

With Time delay

```
function ddex12 global p1 u1 b1 a1 r u2 d k u4 a2 p2 u3 d1 e1 e2 n
```

```
sol = dde23(@ddex1de,[7],@ddex1hist,[0, 270]); figure(1) subplot(1,1,1) hold on plot(sol.x,sol.y(5,:), 'black', 'r')
title('Vertical Transmission With Delay'); xlabel('time t'); ylabel('solution y'); hold
off function s = ddex1hist(t) s = [5*10(9);0;55 * 10; 5 * 10(9);0;0]; function dydt =
```

$ddex1de(t, y, Z)p1 = 2.5 * 10^{(9)}$; $u1 = 0.022$; $b1 = 2 * 10^{(- 11.3)}$; $a1 = 1$; $r = 12$; $u2 = 0.022$; $d = 1$; $k = 2 * 10^{(- 11.3)}$; $u4 = 0.022$; $a2 = 1$; $p2 = 2.5 * 10^{(9)}$; $u3 = 0.022$; $e1 = 0.998$; $n = 0.92$; $e2 = n * e1$; $d1 = d * 10^{(- 1)}$; $ylag1 = Z(:, 1)$; $dy1dt = p1 - u1 * y(1) - b1 * (1 - e1) * y(1) * y(3)$; $dy2dt = b1 * (1 - e1) * y(1) * y(3) - (a1 + d) * y(2)$; $dy3dt = a1 * r * y(2) - u2 * y(3) - b1 * (1 - e1) * y(1) * y(3)$; $dy4dt = p2 - u3 * y(4) - k * d * (1 - e2) * y(4) * ylag1(1)$; $dy5dt = k * d * (1 - e2) * y(4) * ylag1(6) - a2 * y(5)$; $dy6dt = a2 * r * y(5) + d * r * y(2) - u4 * ylag1(6) - k * d * (1 - e2) * y(4) * ylag1(6)$; $dydt = [dy1dt; dy2dt; dy3dt; dy4dt; dy5dt; dy6dt]$

stochastic model code

hold on subplot(1,1,1) N=10000; T=100; omega=2.5*10⁹; mur = 0.8; beta = 2 * 10^(- 11.3); mu1 = 0.5; mu2 = 0; r = 12; rho = 0.12; h = T/N; t = (0 : h : T); x = zeros(size(t)); y = zeros(size(t)); z = zeros(size(t)); x(1) = 5 * 10⁽⁹⁾; y(1) = 10; z(1) = 2 * 10⁽⁴⁾; sigma = 0.1; for i = 1 : Nx(i + 1) = x(i) + (omega - mur * x(i) - beta * x(i) * z(i)) * h - sigma * x(i) * randn * sqrt(h); y(i + 1) = y(i) + (beta * x(i) * z(i) - mu1 * y(i)) * h - sigma * y(i) * randn * sqrt(h); z(i + 1) = z(i) + (r * mu1 * y(i) - mu2 * z(i) - beta * x(i) * z(i)) * h - sigma * z(i) * randn * sqrt(h); end; plot(t,z); axis([0 100 0 5*10⁹]); grid on; title('Diffusion Coefficient is a Linear function of the state variable')